Electron microscopy

Introduction to lenses

http://micro.magnet.fsu.edu/primer

Ray diagrams (geometrical optics):

1. The optical axis contains the object focal point and the image focal point.
2. Rays going through the lens optical center (principal rays) are not deflected.
3. Parallel rays diverge from and converge to the focal points.
4. For identical optical media on both sides: $f_{object} = f_{image}$
5. Reversibility principle: swapping the object with the image results in a symmetrical ray diagram.

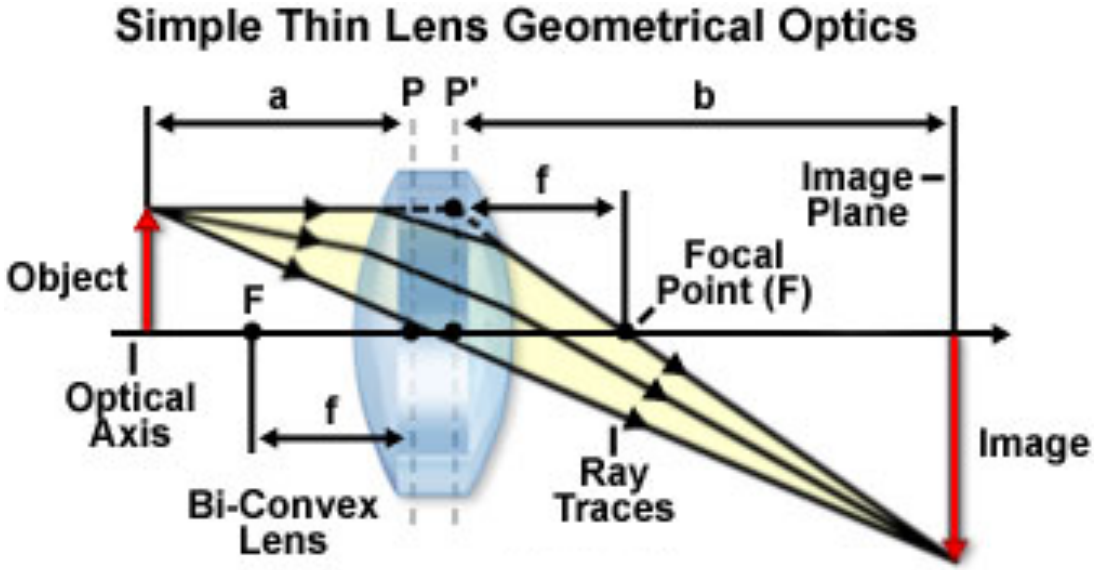

1/a + 1/b = 1/f

M = b/a

(magnification)

Image formation

http://micro.magnet.fsu.edu/primer

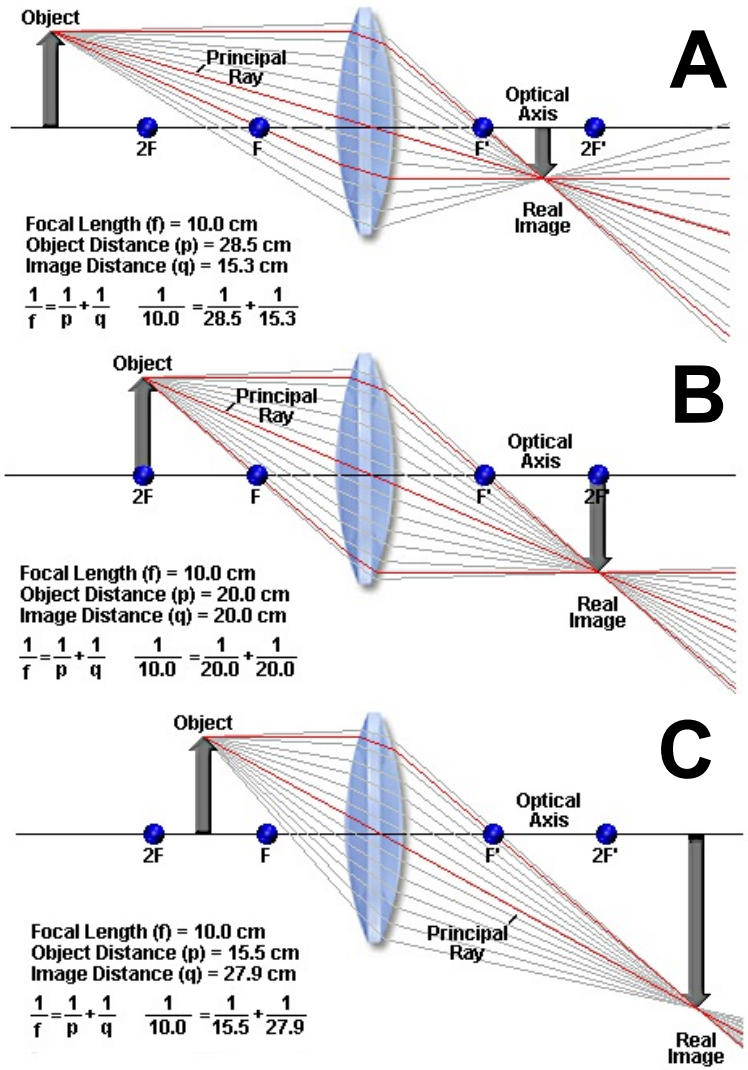

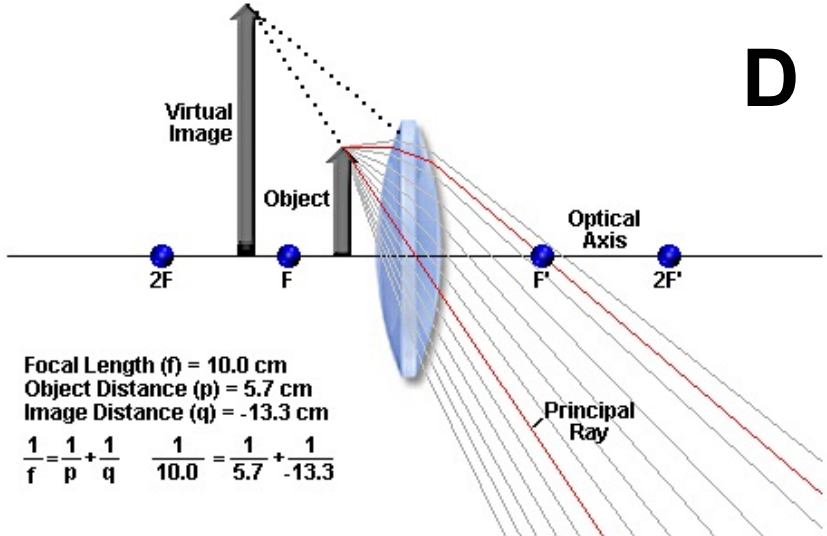

For given lens the path ray shows that the image of an object situated. Before 2F the image is inverted and demagnified (A). As the object comes close to the lens the image becomes larger, with a maximum for the object at the focal point (C). After this point the image is formed at the other side of the lens and is virtual (D). The object and image planes are conjugate planes.

There are mainly three types of lenses. Condensers that prepare the light to illuminate the specimen(A). Objectives which are the imaging forming lens (C). Eyepieces which are in fact magnifying glasses (D).

Compound microscope

http://micro.magnet.fsu.edu/primer

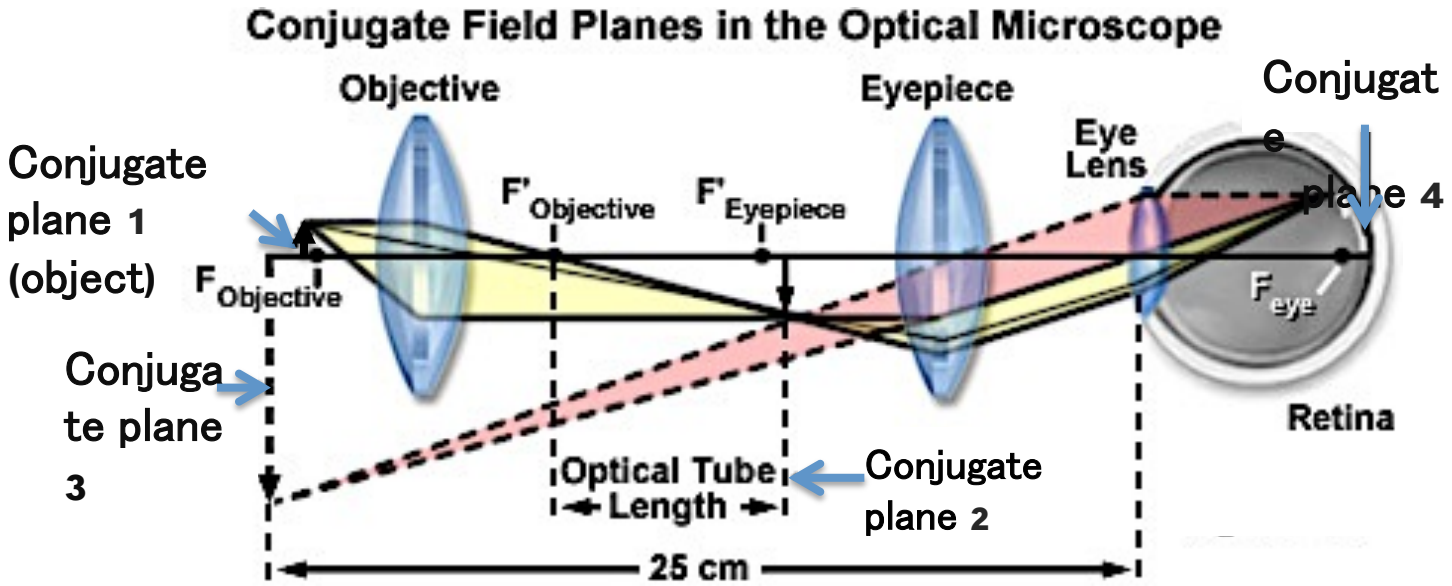

For an object at point (1) the objective forms an image at plane (2) and this image is magnified by the eyepiece which forms a virtual image at plane (3). The virtual image (diverging rays) is then focused by the eye lens on the retina (4).

This scheme is showing to of the important lenses, the objective and the eyepiece but it lacks the condenser lens that illuminates the specimen.

Microscope working principles

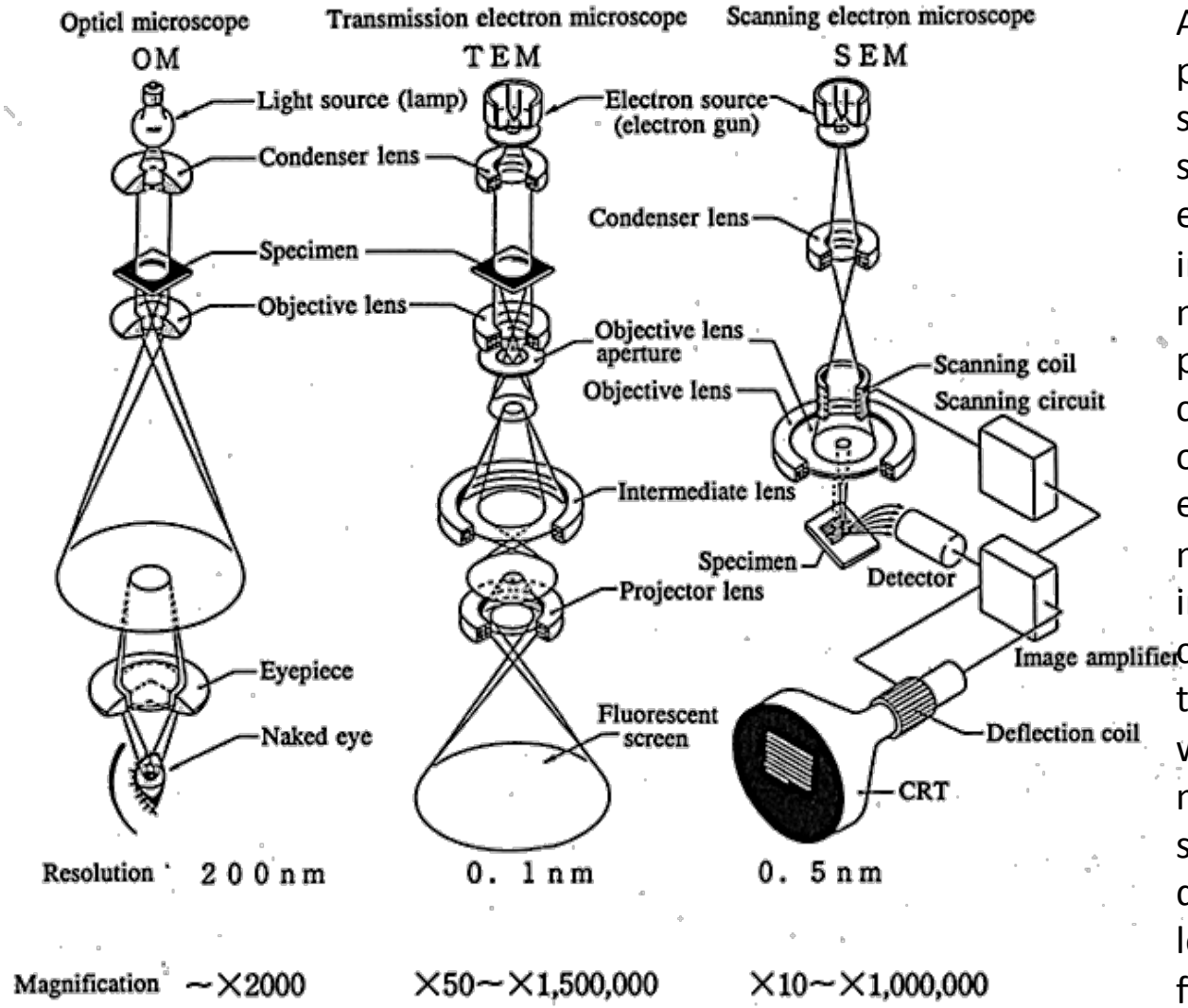

After understanding the working principles of an OM with its light source, the condenser lens, the specimen, the objective lens, the eyepiece and the eye, one can readily infer that the transmission electron microscope has very similar working principles: the electron source, the condenser lens, the specimen, the objective lens, and instead of eyepiece it has other type of magnifying lenses that form the image on a fluorescent screen or CCD camera. When we compare the transmission electron microscope with the scanning electron microscope we see that we have something different. In fact the SEM does not even has an objective… the lens does not form an image but a fine probe.

Image types

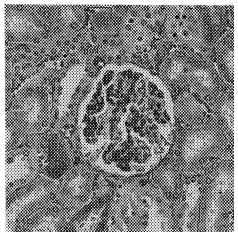

OM image: × 200
Specimen: Rat's glomerulus (section)
HE stained

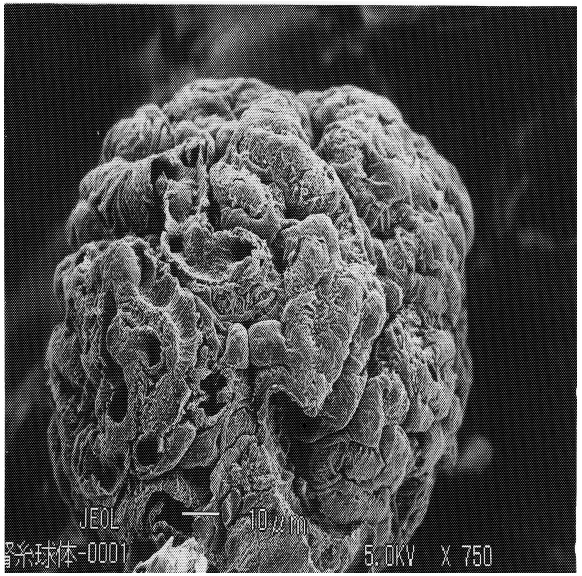

SEM image: × 750 (secondary electron image)
Specimen: Rat's glomerulus
Surface morphology of
the bulk-state specimen is observed.

TEM image: × 750
Specimen: Rat's glomerulus
The internal structure of
a thin section specimen is observed.

So if the OM and TEM images look similar why bother using the TEM? That is, why using electrons to inspect specimens?

Resolution
+ local diffraction
+ local spectroscopy

JEOL

Electron diffraction

Why use electron diffraction

✔ Wavelength of fast moving electrons much smaller than spacing of atomic planes: diffraction from atomic planes (e.g. @200 kV, λ_{e^-}= 0.0025 nm)

✔ Electrons interact very strongly with matter: strong diffraction intensity (patterns in seconds unlike X-ray diffraction)

✔ Spatially-localized information ($\gtrsim$ 200 nm for selected-area diffraction; 2 nm possible with convergent-beam electron diffraction)

✔ Close relationship to diffraction contrast in imaging

✔ Orientation information

✔ Immediate in the TEM!

✖ Diffraction from only selected set of planes in one pattern: Only 2D information

✖ Limited accuracy of measurement: errors = 2-3%

✖ Intensity of reflections difficult to interpret due to dynamical effects

TEM diffraction vs imaging

Abbe's principle of imaging:

Unlike with visible light, due to the small λ, electrons can be coherently scattered by crystalline samples so the diffraction pattern at the back focal plane of the object corresponds to the sample reciprocal lattice.

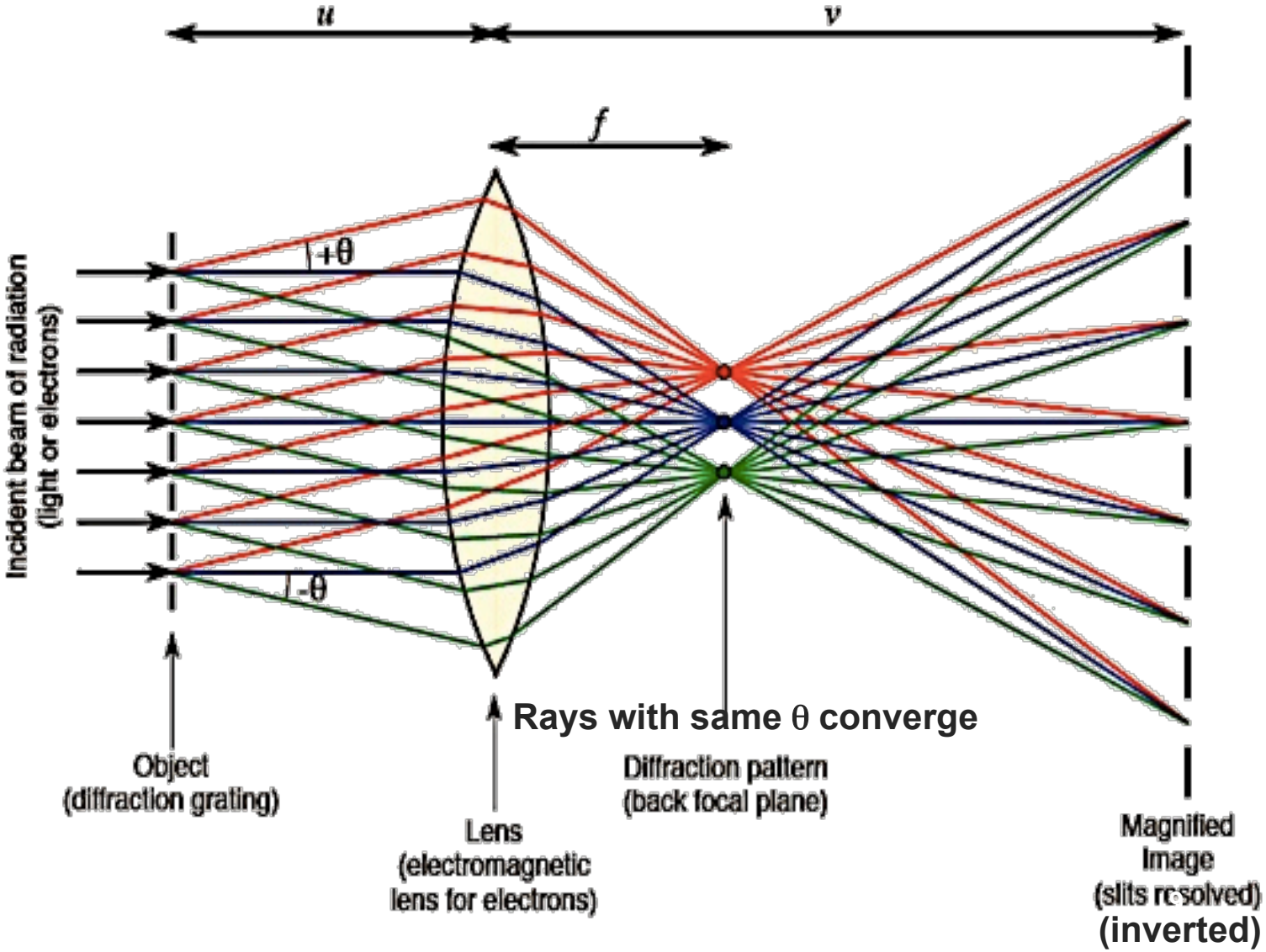

TEM diffraction vs imaging

Rays with same θ converge (color scheme different from previous slide)

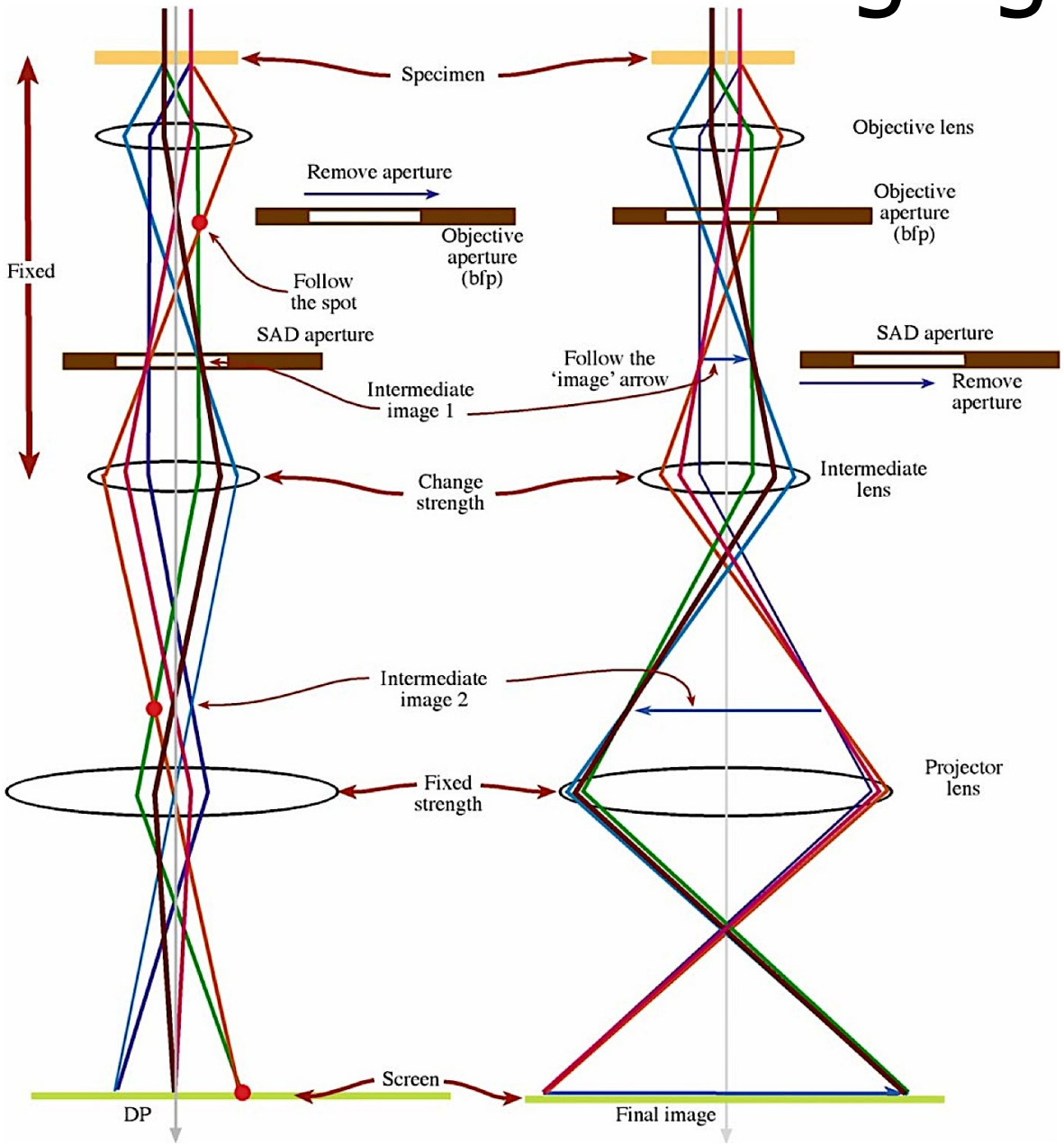

TEM diffraction vs imaging

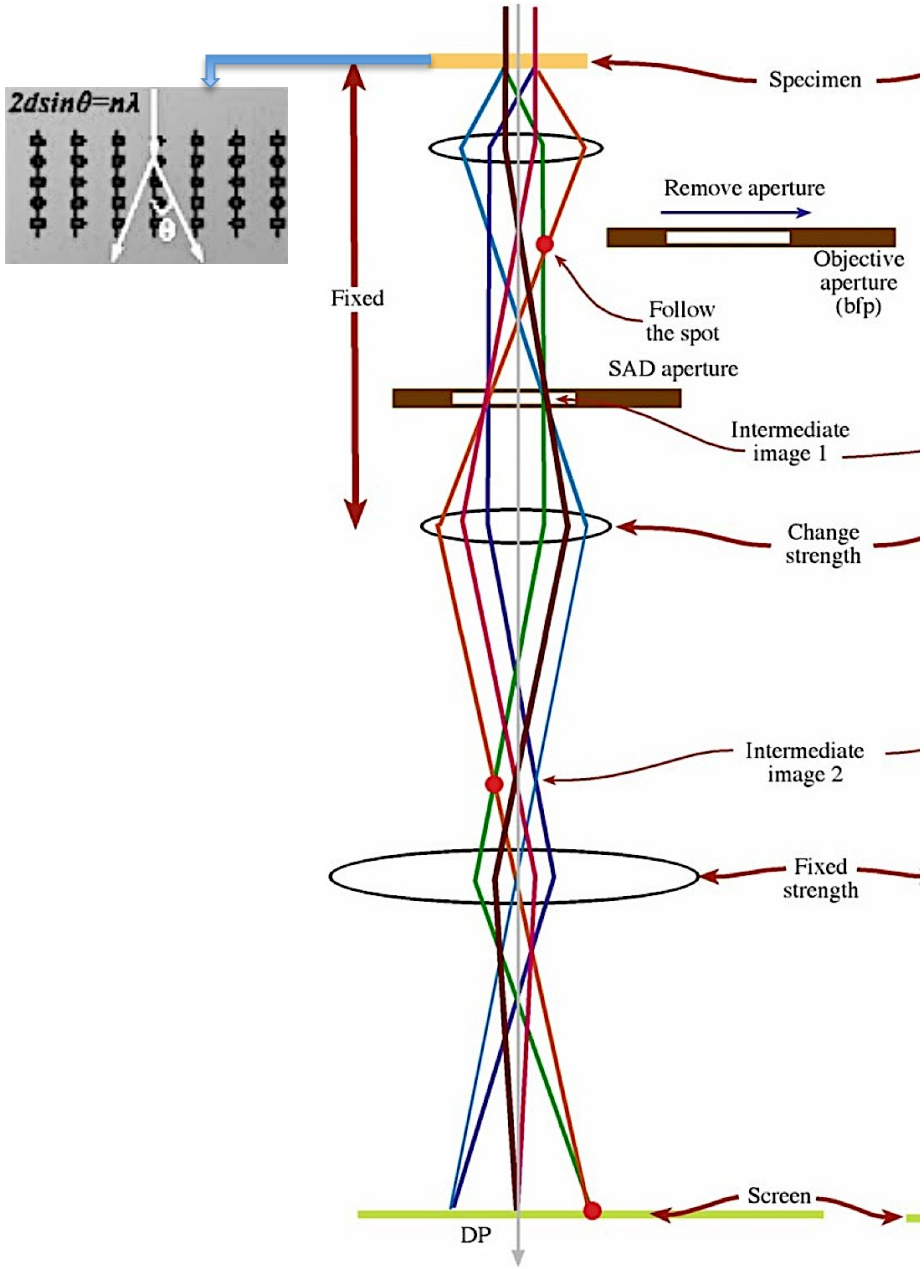

Insert selected area aperture to choose region of interest

Press Diffraction on microscope console

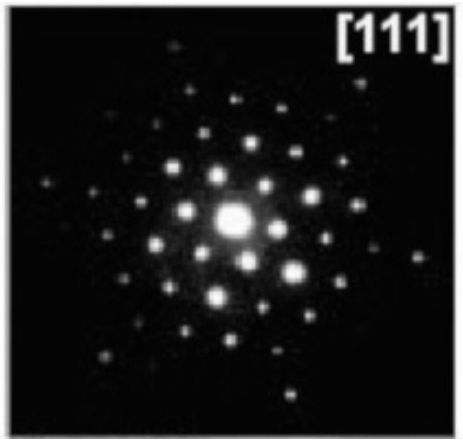

TEM diffraction vs imaging

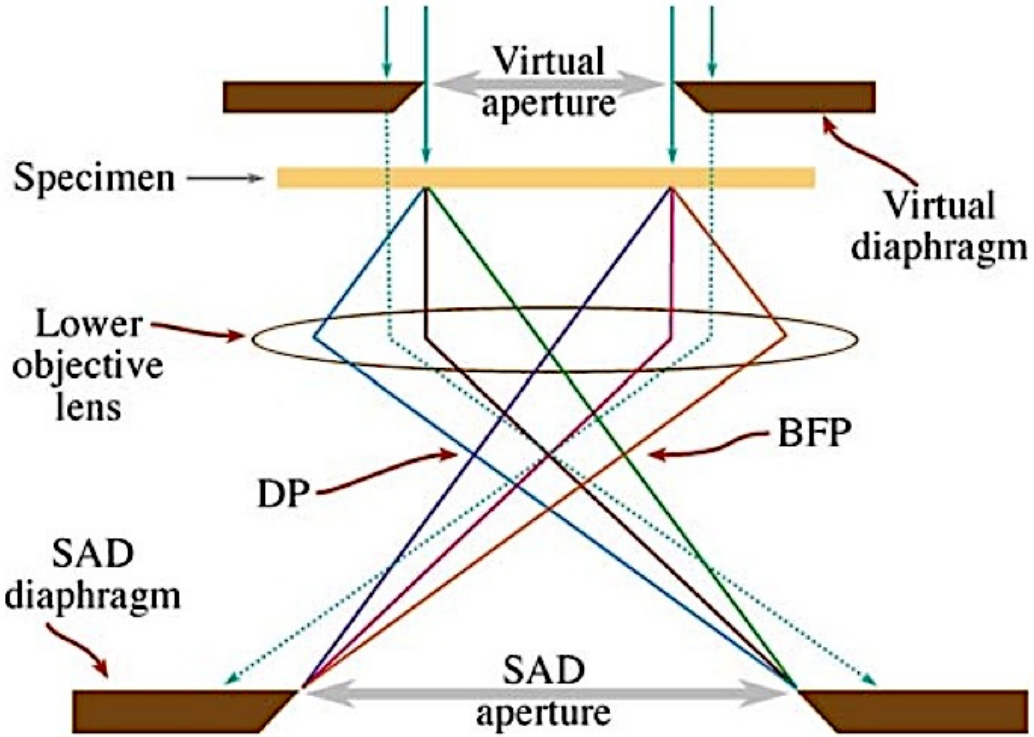

Ray diagram showing SADP formation: the insertion of an aperture in the image plane results in the creation of a virtual aperture in the plane of the specimen (shown here slightly above the specimen plane). Only electrons falling inside the dimensions of the virtual aperture at the entrance surface of the specimen will be allowed through into the imaging system to contribute to the SAD pattern. All other electrons (dotted lines) will hit the SAD diaphragm.

The SAD aperture is inserted at a conjugate plane of the specimen, so it seems that it is **at** the specimen plane

Diffraction concepts

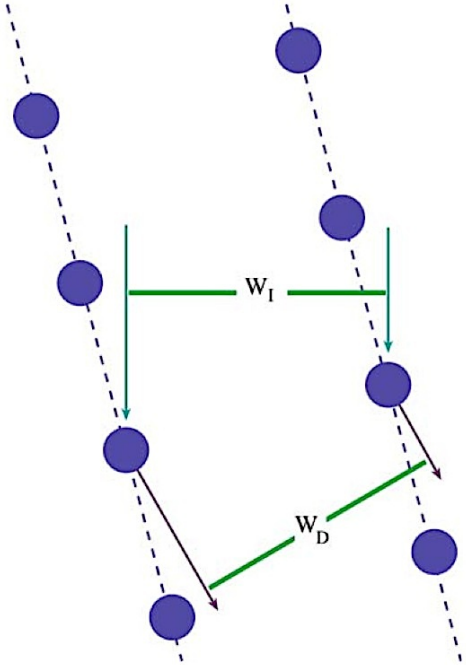

Scattering from two planes of atoms. W_I and W_D are the incident and diffracted wavefronts, respectively.

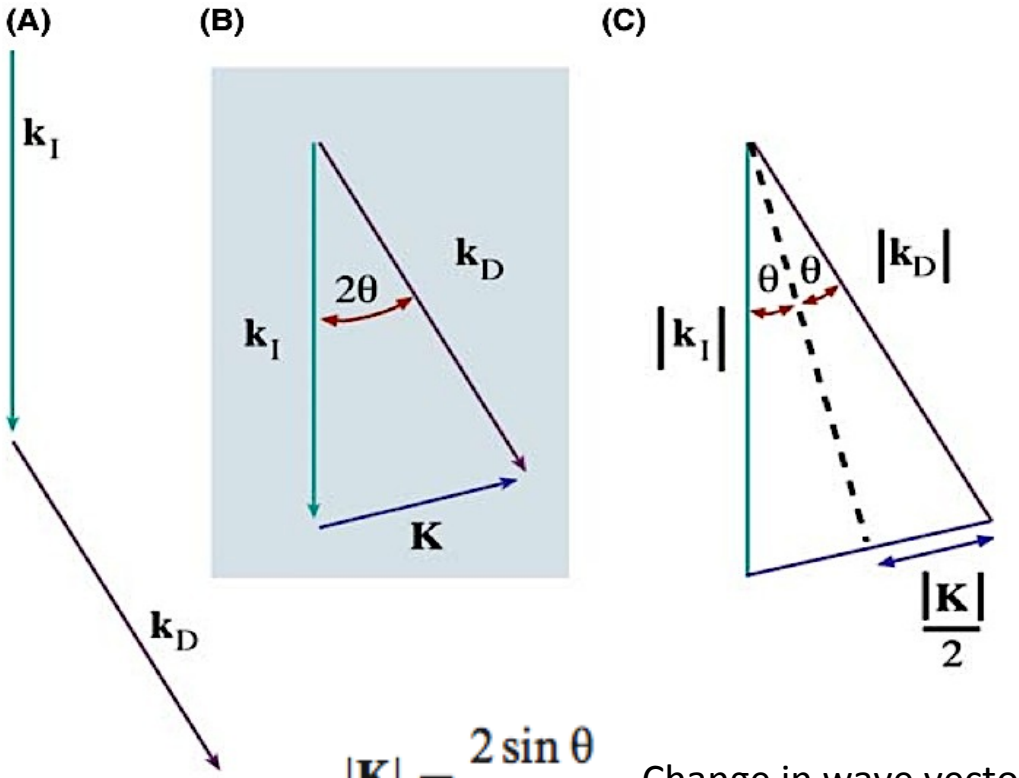

$$|\mathbf{K}| = \frac{2\sin\theta}{\lambda}$$

Change in wave vector

Nomenclature may change yet the concepts are the same as in diffraction gratings…

Diffraction concepts

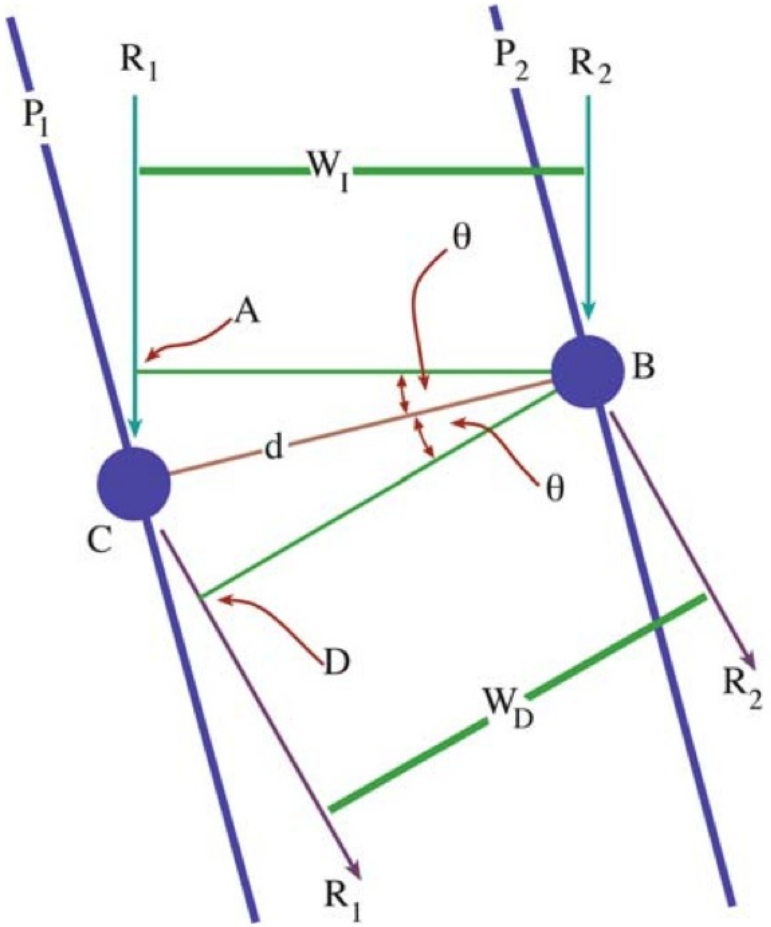

Path differences…

Diffraction concepts

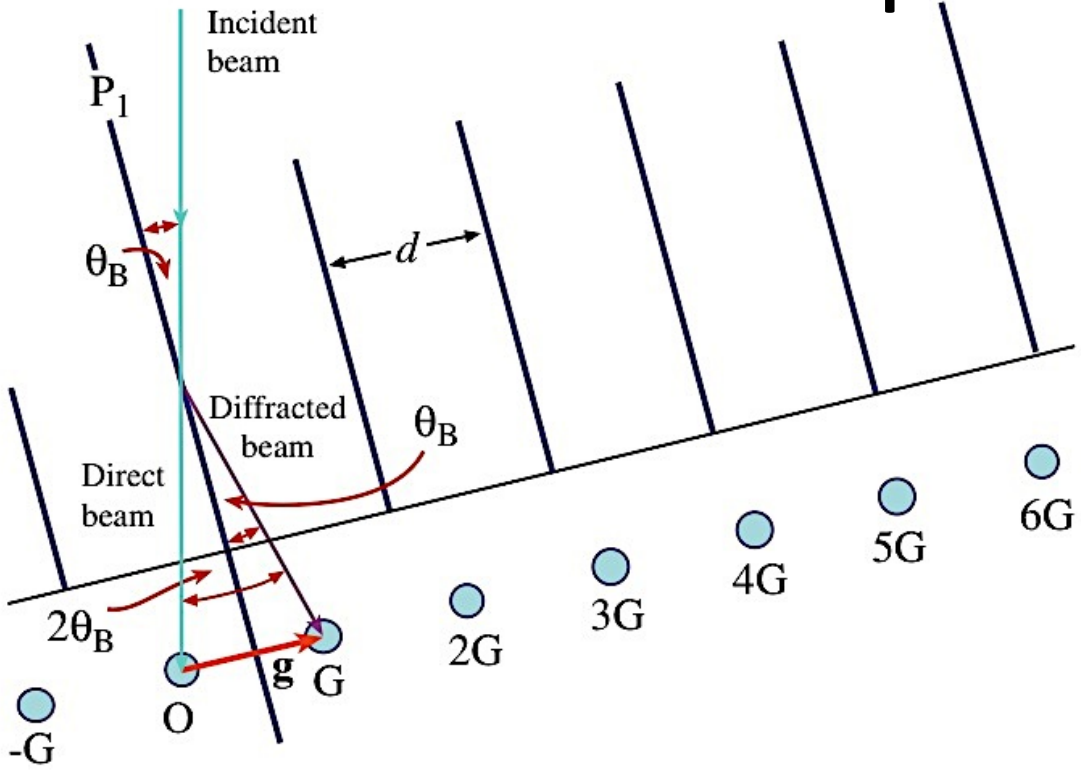

Diffraction from a set of planes a distance d apart. The planes have been oriented to be in the Bragg diffracting condition (θ_B is the incident angle). The resultant diffraction **spots** (reciprocal-lattice points) are labeled G, 2G, etc. The **vector g** from the origin (O) to the first diffraction spot G is normal to the diffracting planes.

Systematic row: the Fourier transform encodes sharp **square-wave type features** as the sum of a series of smooth sinusoids. A perfect sinusoidal function requires only one frequency, i.e., if the atomic planes could be described by 1 sinusoid function then there would be only G and –G (this mirroring comes from the mathematical properties of the Fourier transform).

Diffraction concepts

Why do electron diffraction patterns have many spots?

- Typically in X-ray or neutron diffraction only one reciprocal lattice point is on the surface of the Ewald sphere at one time.
- In electron diffraction the Ewald sphere is not highly curved due to the very short wavelength electrons used. This almost flat Ewald sphere intersects with many reciprocal point (relps) at the same time (in fact, because they have non-zero height).

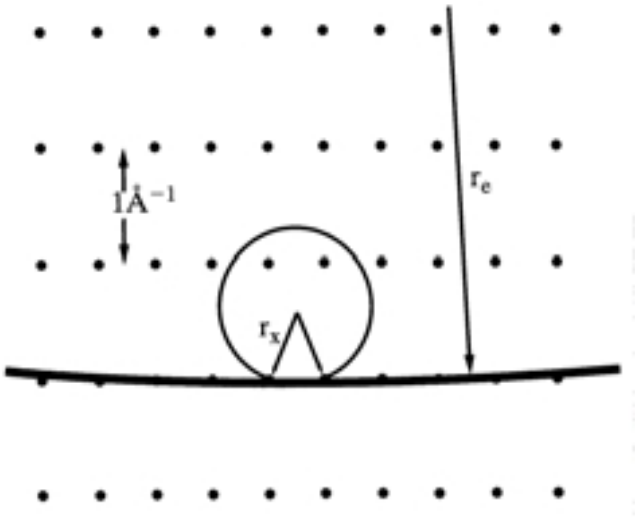

Ewald sphere for Cu radiation is much more curved than that for electrons in an electron diffraction experiment

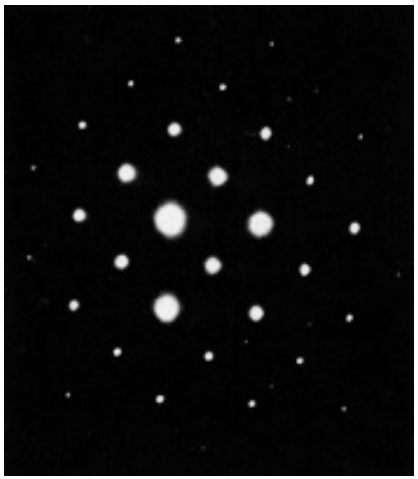

Electron diffraction pattern from NiAl

Ewald sphere in multi-beam condition

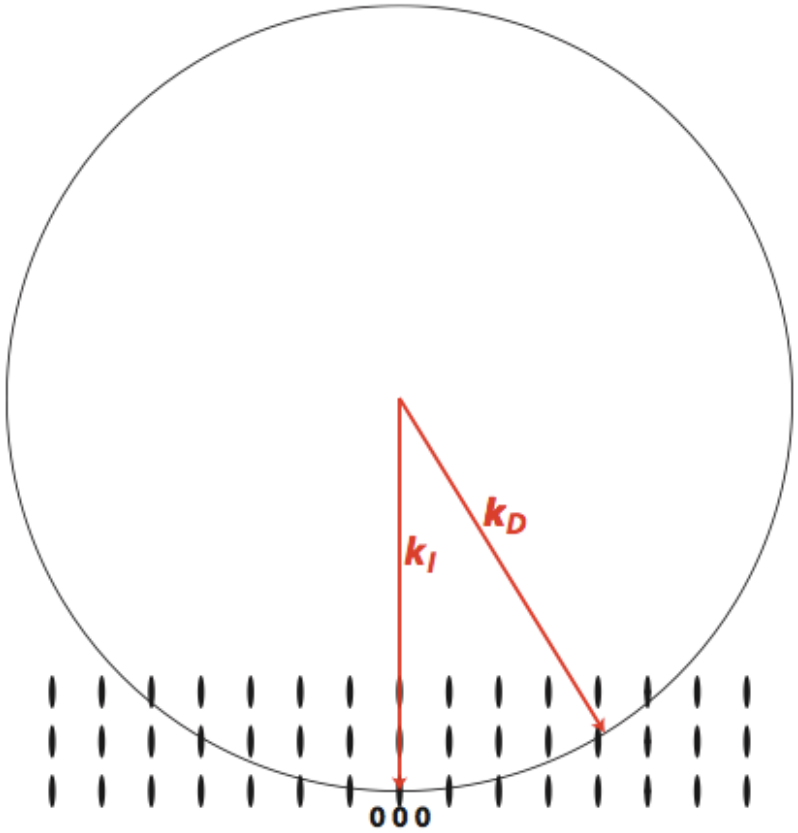

Reciprocal lattice rods (relrods)

- For reciprocal lattice points (infinitely small): even with the crystal oriented along low-index zone axis the intersection at the Zero Order Laue Zone would be impossible for relps other than the origin…
- The strong diffraction from many planes in this condition occurs because relps have size and shape!

Multi-beam scattering condition

Electron beam parallel to low-index crystal orientation [U V W] = zone axis

Crystal "viewed down" zone axis is like diffraction grating with planes parallel to e-beam

In diffraction pattern obtain spots perpendicular to plane orientation

Example: primitive cubic with e-beam parallel to [0 0 1] zone axis

2 x 2 unit cells

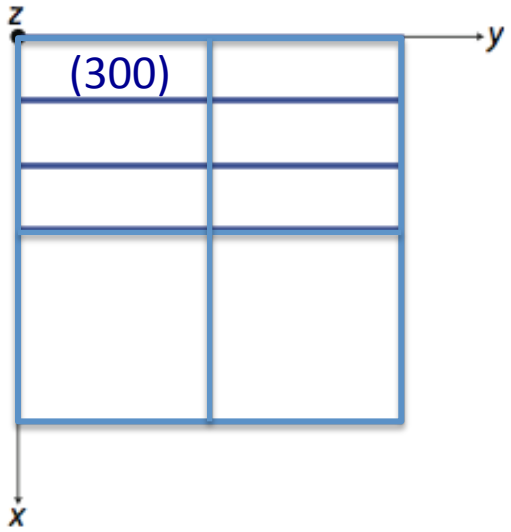

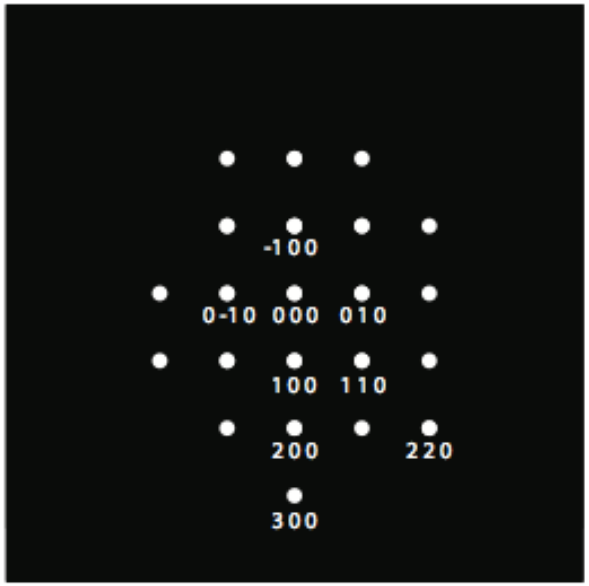

Note reciprocal relationship: smaller plane spacing => larger indices (*h k l*)
& greater scattering angle on diffraction pattern from (0 0 0) direct beam

Also note Weiss Zone Law obeyed in indexing ($hU + kV + lW = 0$)

Scattering from non-orthogonal crystals

With scattering from the cubic crystal we can note that the diffracted beam for plane (1 0 0) is parallel to the lattice vector [1 0 0]; makes life easy

However, not true in non-orthogonal systems - e.g. hexagonal:

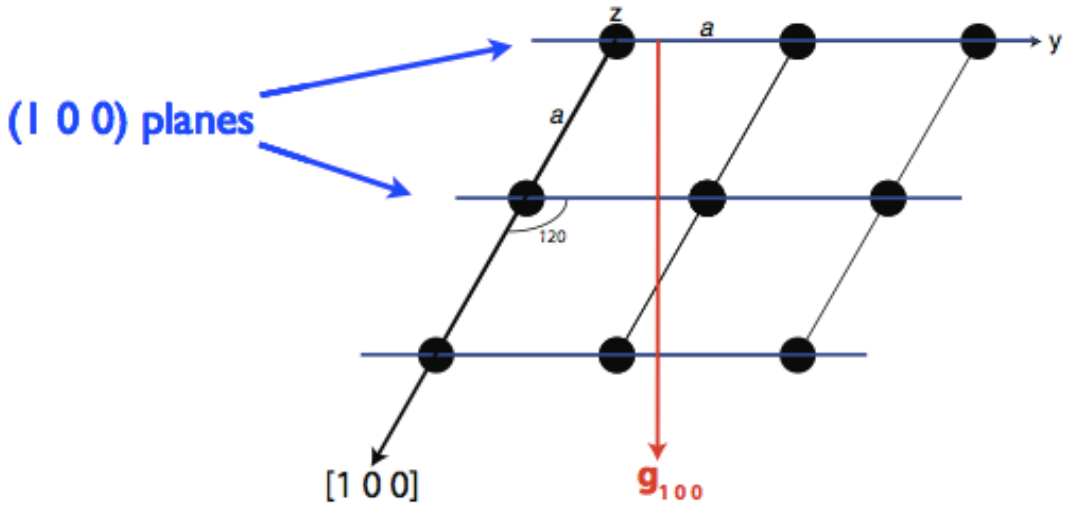

=> care must be taken in reciprocal space!

Ewald sphere in 2-beam condition

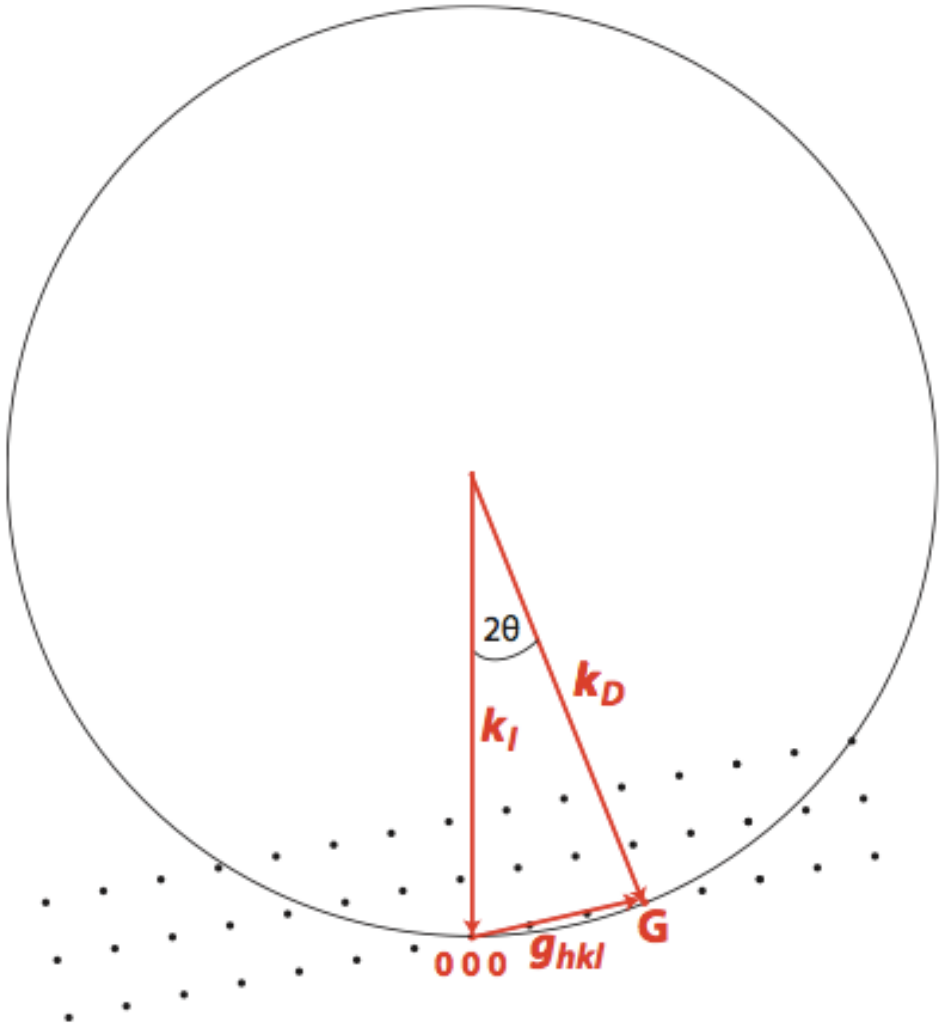

Only **one** strong Bragg reflection corresponds to strong scattering from a single set of planes

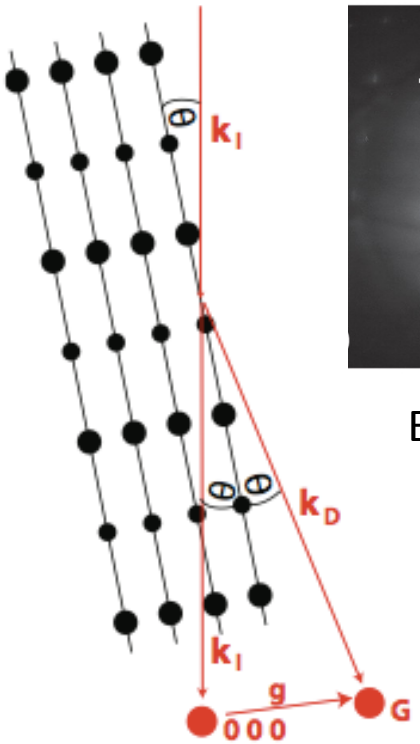

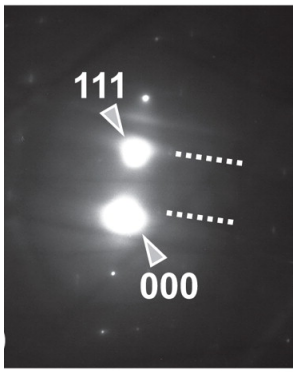

Example

2-beam condition with one strong Bragg reflection corresponds to Ewald sphere intersecting one reciprocal lattice point

How to obtain a 2-beam condition

Tilting the specimen from one low-index zone axis to another: in between we find 2-beam conditions, i.e., only one set of planes fulfill the Bragg condition, unlike in multi-beam diffraction where many beams are at (or close to) Bragg condition.

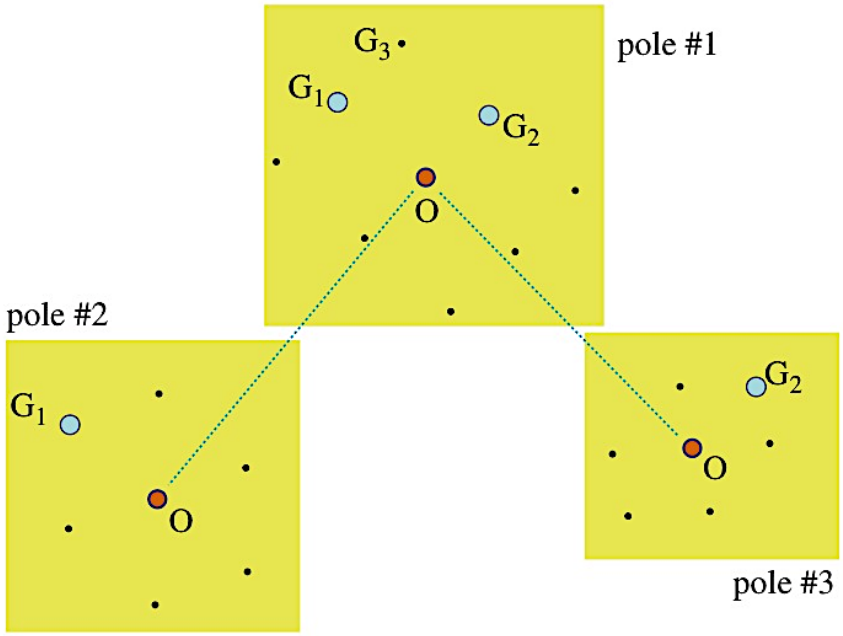

Tilting the specimen: first keeping G1 excited, then keeping G2 excited

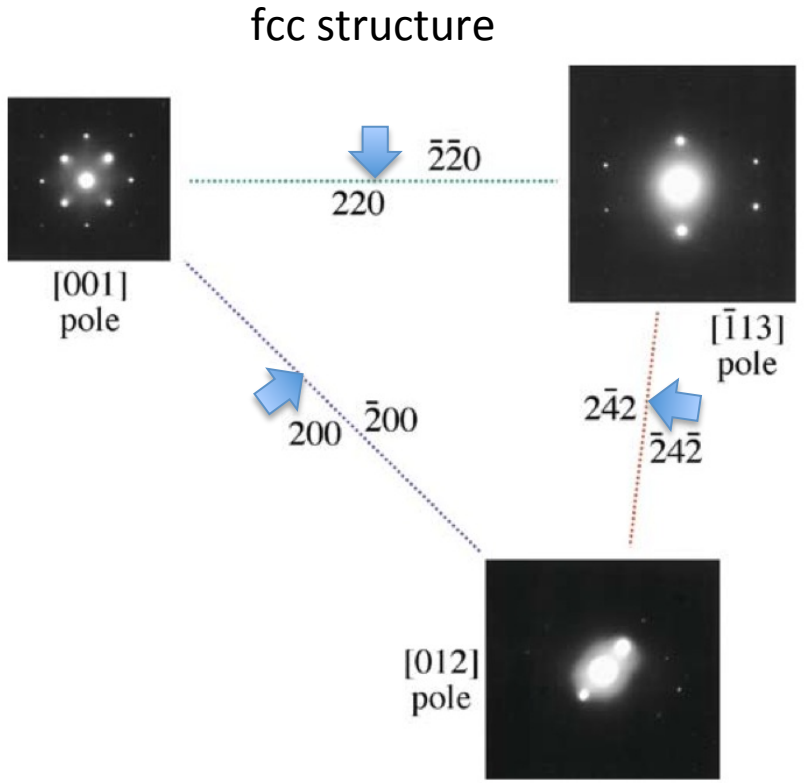

Relrod shape

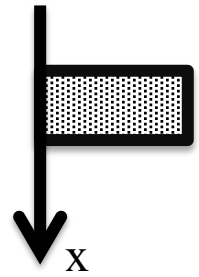

Shape (e.g. thickness) of sample is like a "top-hat" function

Therefore shape of Relrod is: sin(x)/x

Can compare to single-slit diffraction pattern with intensity: $I \propto \left(\frac{\sin x}{x}\right)^2$

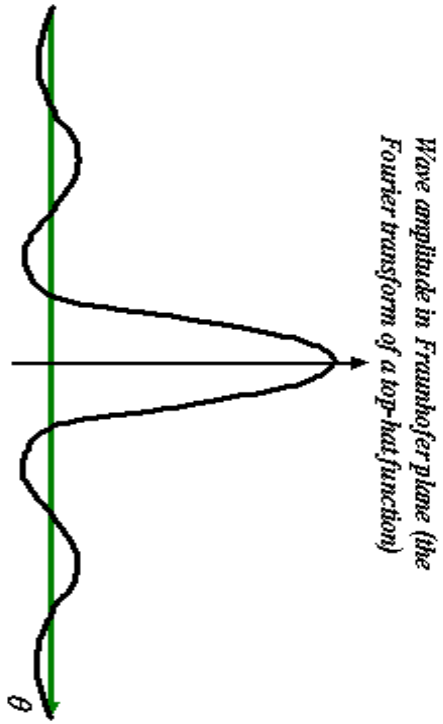

Relrod shape

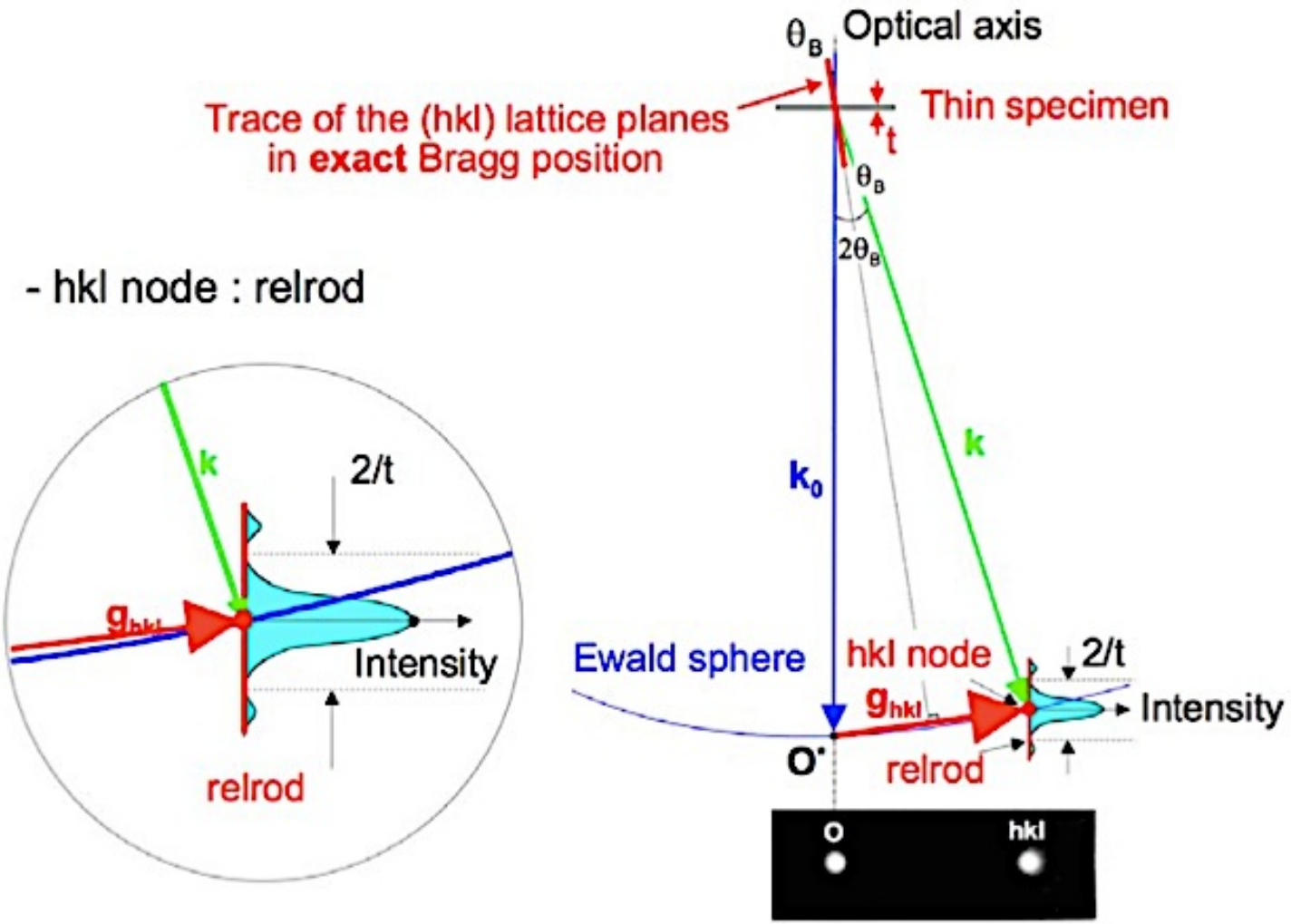

Excitation error or deviation parameter

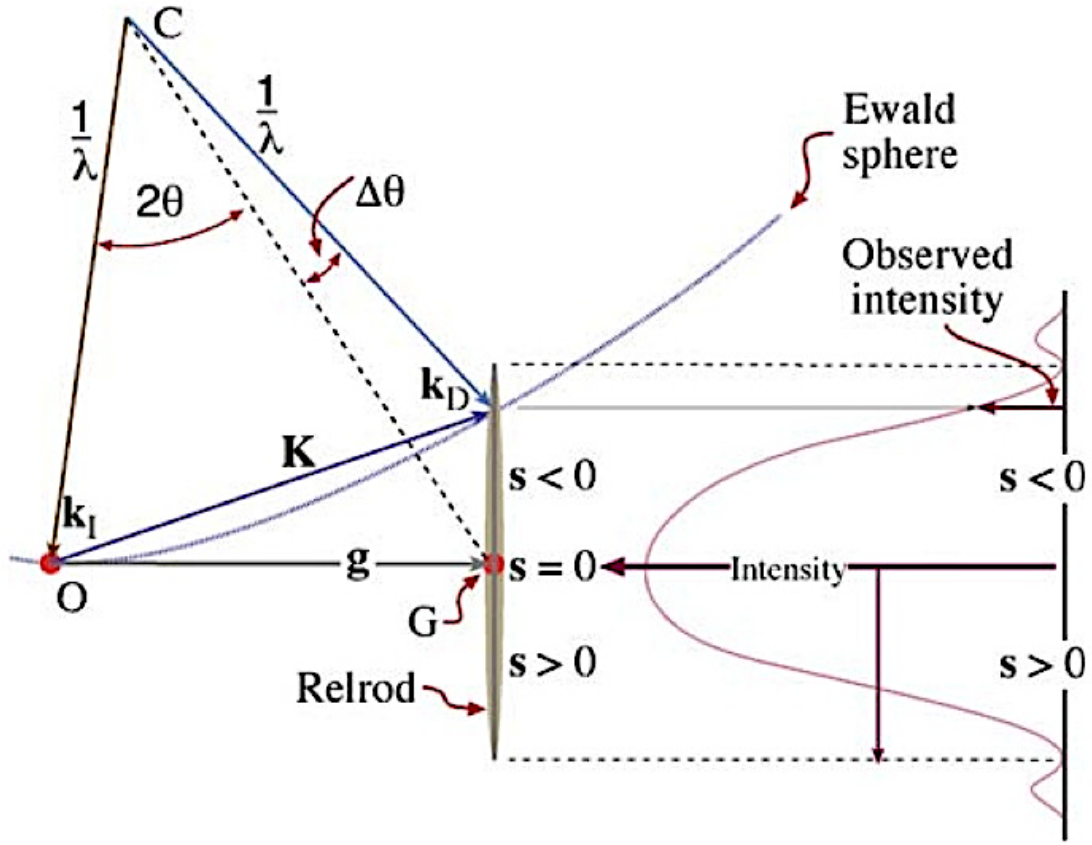

The relrod at $\mathbf{g}_{hkl}$ when the beam is Δθ away from the exact Bragg condition. The Ewald sphere intercepts the relrod at a negative value of **s** which defines the vector $\mathbf{K} = \mathbf{g} + \mathbf{s}$. The intensity of the diffracted beam as a function of where the Ewald sphere cuts the relrod is shown on the right of the diagram. In this case the intensity has fallen to almost zero.

Other notation (Williams and Carter):
$\mathbf{K}=\mathbf{k}_D-\mathbf{k}_I=\mathbf{g}+\mathbf{s}$

Excitation error or deviation parameter

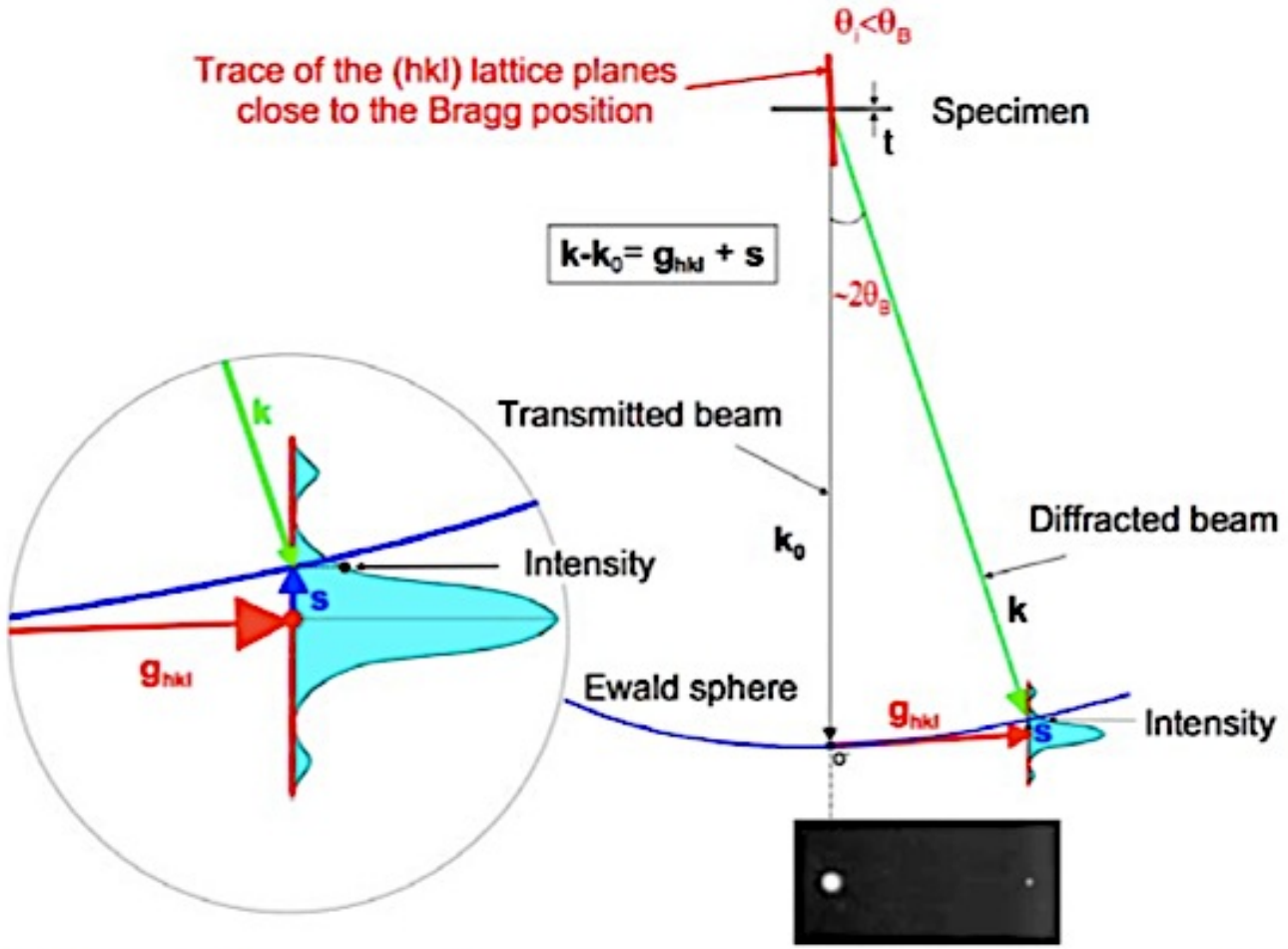

Tilted slightly off Bragg condition, intensity of diffraction spot much lower

Introduce new vector **s** - "*the excitation error*" that measures deviation from exact Bragg condition

Excitation error or deviation parameter

Excitation vector s
Conventions

negative when G is outside the Ewald sphere
positive when G is inside the Ewald sphere.

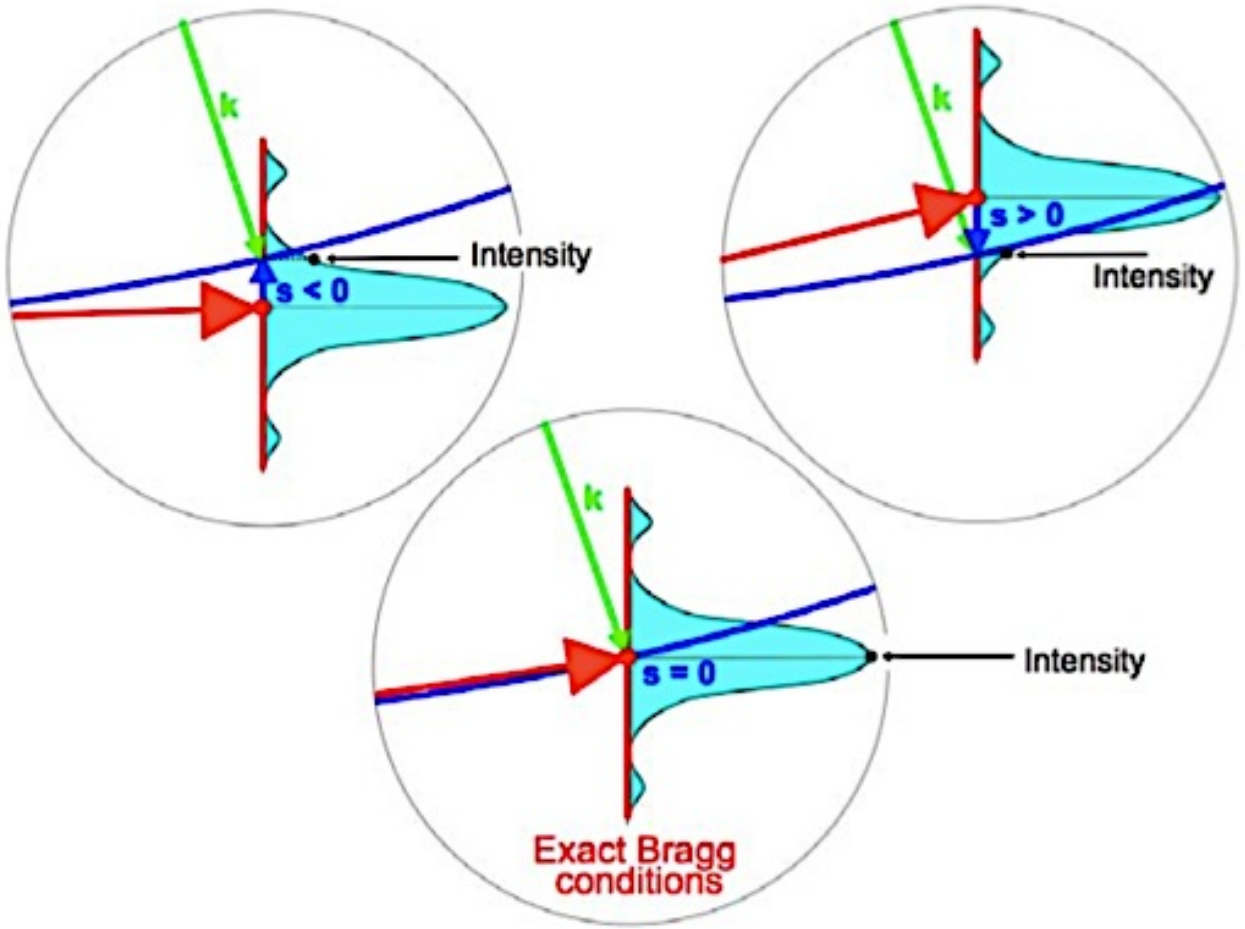

2-beam scattering condition

Dynamical theory as a system of differential equations (Howie-Whelan formulation)

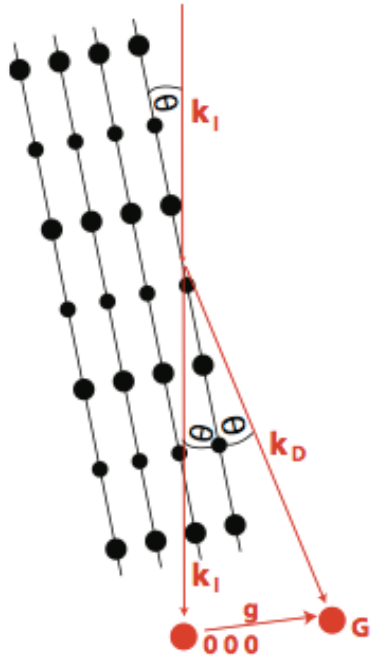

$$\frac{d\Psi_0}{dz} = \frac{i\pi}{\xi_0}\Psi_0 + \frac{i\pi}{\xi_g}\Psi_g \exp\left(2\pi i s_g z\right)$$

$$\frac{d\Psi_g}{dz} = \frac{i\pi}{\xi_0}\Psi_g + \frac{i\pi}{\xi_g}\Psi_0 \exp\left(-2\pi i s_g z\right)$$

An incident wave of amplitude Ψ0 and a scattered wave of amplitude Ψ*g* pass through a layer of thickness d*z* inside the crystal. In contrast with the kinematical theory, where the amplitude of the incident beam is taken as a constant, it is assumed that after passing through the layer, the amplitude Ψ0 will have changed by *d*Ψ0 and Ψ*g* by *d*Ψg.

2-beam scattering condition
Dynamical theory as a system of differential equations (Howie-Whelan formulation)

For a 2-beam condition (i.e. strong scattering at Θ_B) it can be derived that:

$$I_{\mathbf{g}} = \left(\frac{\pi t}{\xi_{\mathbf{g}}}\right)^2 \frac{\sin^2(\pi t s_{eff})}{(\pi t s_{eff})^2} \qquad \text{where:} \qquad s_{eff} = \sqrt{s^2 + \frac{1}{\xi_{\mathbf{g}}{}^2}}$$

and $\xi_{\mathbf{g}}$ is the "extinction distance" for the Bragg reflection: $\xi_{\mathbf{g}} = \frac{\pi V_C \cos\theta_B}{\lambda F_{\mathbf{g}}}$

Further: $I_0 = 1 - I_{\mathbf{g}}$

i.e. the intensities of the direct and diffracted beams are complementary, and in anti-phase, to each other. *Both* are periodic in t and s_{eff}

If the excitation distance $s = 0$ (i.e. perfect Bragg condition), then:

$$I_{\mathbf{g}} \propto \sin^2\left(\frac{\pi t}{\xi_{\mathbf{g}}}\right)$$

2-beam scattering condition
Dynamical theory as a system of differential equations (Howie-Whelan formulation)

Solution to the differential equations:

$$I_0(t) = \psi_0 \psi_0^* = \cos^2\left(\pi t/\xi_g\right)$$

$$I_g(t) = \psi_g \psi_g^* = \sin^2\left(\pi t/\xi_g\right)$$

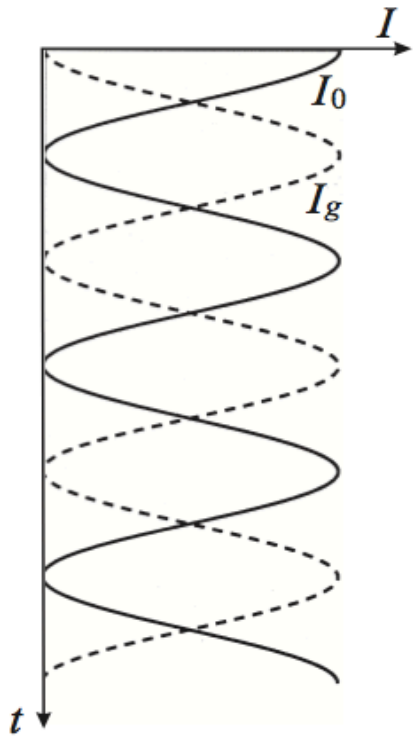

There is an interchange of intensity between the two beams as a function of *tickness (t).* The so-called thickness fringes, which can be observed for a crystal of varying *t* (when imaged with any of the two beams), originate from this effect.

The total intensity is conserved i.e., $\boldsymbol{I_0(t) + I_g(t) = 1}$ and the intensity in the diffracted beam is zero for $t = n\xi_g$ (*n* an integer), hence the term **extinction distance**.

Variation of intensity with thickness for a crystal at a Bragg condition, using the two-beam theory and without including any absorption. ξ*g* is the extinction distance, *i.e.*, the periodicity of the thickness fringes.

Extinction Distance, ξ_g

• The amplitude or intensity of diffracted beams depends on a characteristic length called the extinction distance, ξ_g, which is a dynamic diffraction effect where the intensity from the direct beam is transferred to the diffracted beams, which then transfer the intensity back into the direct beam.

• The extinction distance is thus dependent on Bragg angle, θ_B, and the specific diffracted beam whose characteristics are determined by the structure factor, F_g.

• The extinction distance can be expressed as:

$$\xi_{\mathbf{g}} = \frac{\pi V_c \cos\theta_B}{\lambda F_{\mathbf{g}}}$$

where $F_{\mathbf{g}}$ is the $F(\theta)$ for reflection **g** (i.e., $F_{\mathbf{g}}$ is a special value of $F(\theta)$ when θ is the Bragg angle).

V_c is the volume of the unit cell of the crystal.

Extinction Distance, ξ_g

Examples of Extinction Distances (in nm)*

Material					
hkl =	110	111	200	220	400
Al	–	56.3	68.5	114.4	202.4
Cu	–	28.6	32.6	47.3	76.4
Au	–	18.3	20.2	27.8	43.5
MgO	–	272.6	46.1	66.2	103.3
Fe	28.6	–	41.2	65.8	116.2
W	18.0	–	24.5	35.5	55.6
Diamond		47.6	–	66.5	121.5
Si		60.2	–	75.7	126.8
Ge		43.0	–	45.2	65.9

*For two-beam condition at 100 kV.

The extinction distance is larger for higher order diffracted beams.

Absorption effect

As the thickness increases absorption occurs leading to reduced contrast.

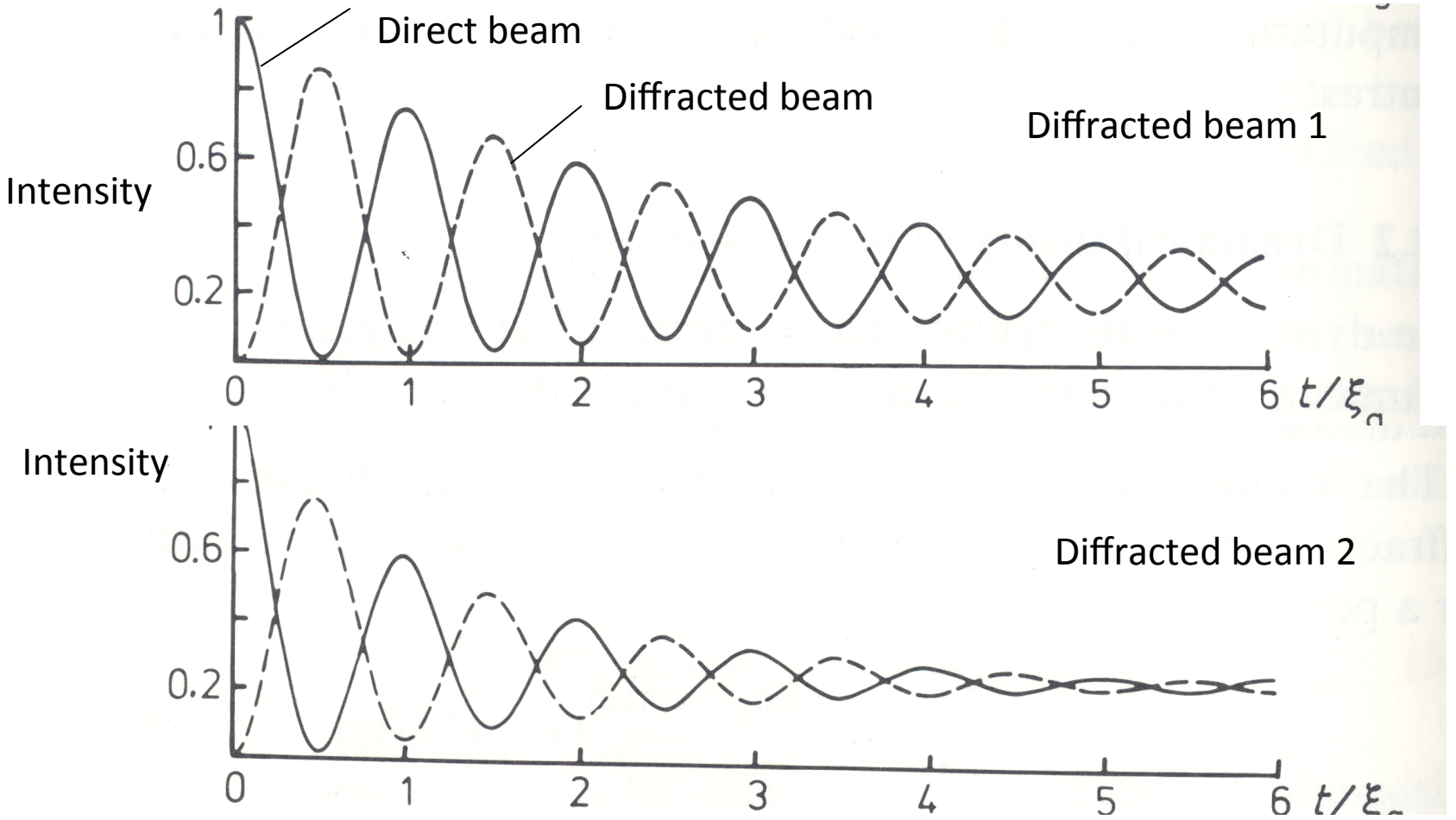

There is also a difference in periodicity (not obvious here).

Dynamical scattering for 2-beam condition

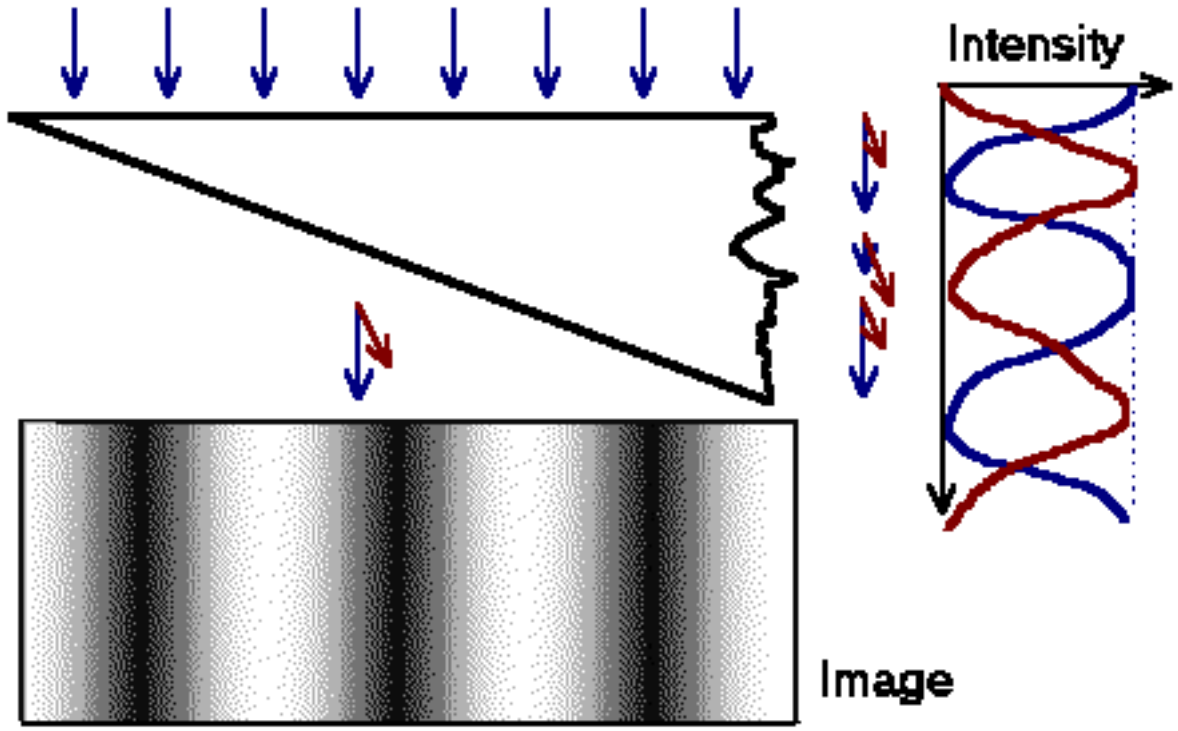

The images of wedged samples present series of so-called thickness fringes.

http://www.tf.uni-kiel.de/

Dynamical scattering for 2-beam condition

The image intensity varies sinusoidally depending on the thickness and on the beam used for imaging.

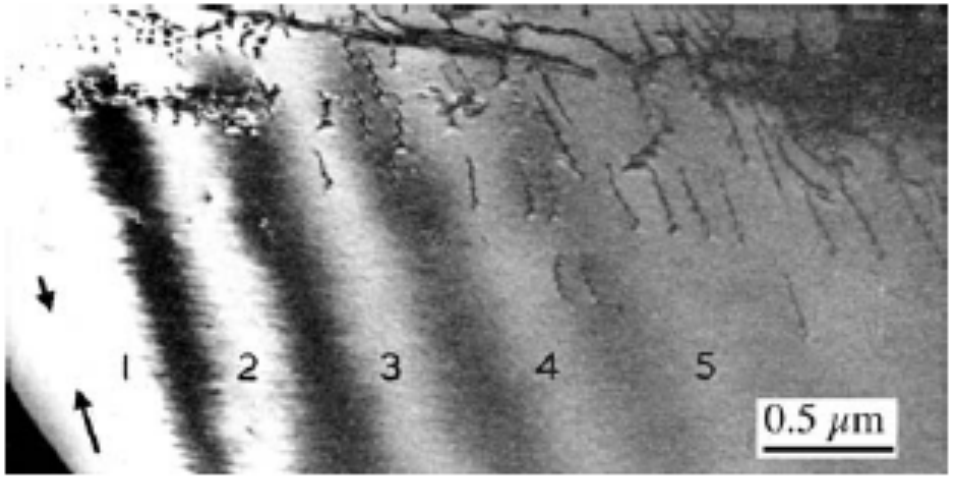

The contrast of thickness fringes in a two-beam BF image decreases when the effect of anomalous absorption is included. Note that the defects are still visible when the fringes have disappeared at a thickness of $-5\,\xi_g$.

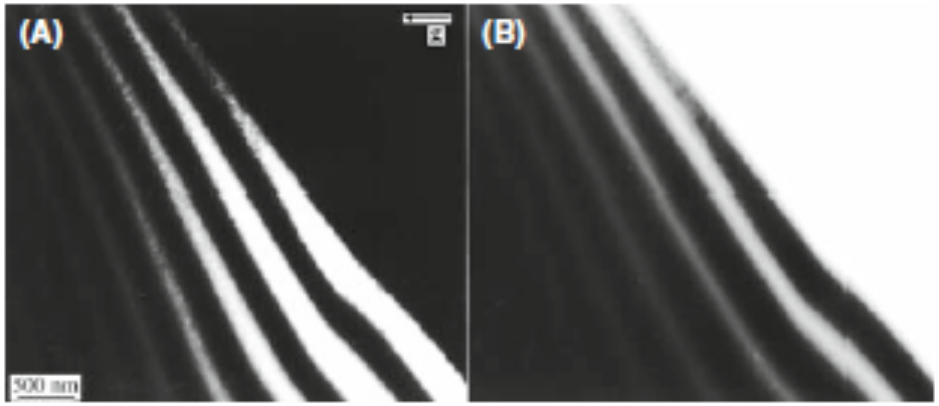

(A) BF and (B) DF images from the same region of a wedge-shaped specimen of Si at 300 kV tilted so that g(220) is strong. The periodicity and contrast of the fringes are similar and complementary in each image.

Reduced contrast as thickness increases due to absorption

2 beam condition
A: image obtained with transmitted beam (Bright field)
B: image obtained with diffracted beam (Dark field)

Selected area diffraction

Symmetry information

Zone axis SADPs have symmetry closely related to symmetry of crystal lattice

Example: FCC aluminium

[0 0 1]

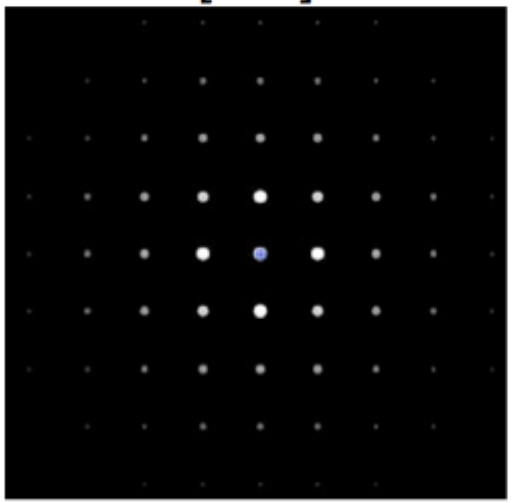

4-fold rotation axis

[1 1 0]

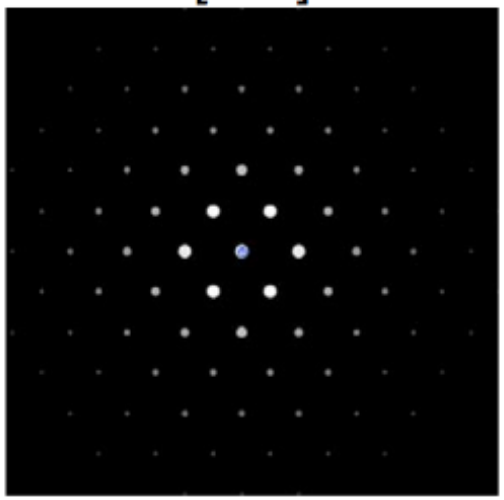

2-fold rotation axis

[1 1 1]

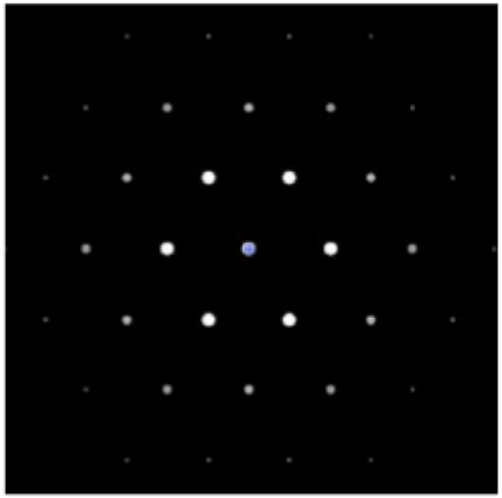

6-fold rotation axis - but [1 1 1] actually 3-fold axis

Need third dimension for true symmetry!

Atomic positions information

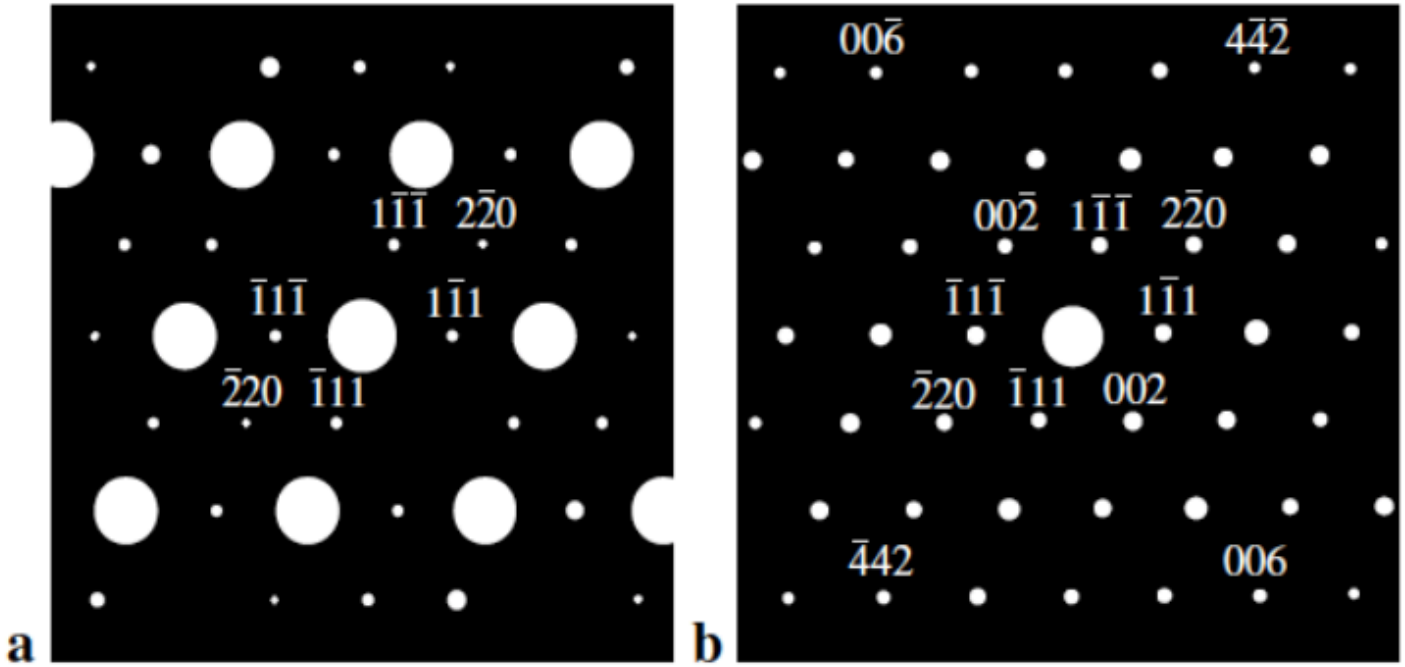

(a) Kinematic simulation and (b) experimental DP of fcc $Nd_2Hf_2O_7$ with the beam parallel to [110] (zone axis = [110]).

Atomic positions information

Forbidden reflections

Consider FCC lattice with lattice point coordinates:
0,0,0; ½,½,0; ½,0,½; 0,½,½

Calculate structure factor for (0 1 0) plane (assume single atom motif):

$$F_{hkl} = \sum_i f_i \, e^{[2\pi i(hx_i + ky_i + lz_i)]}$$

$$F_{010} = f \sum_i e^{[2\pi i(hx_i + ky_i + lz_i)]}$$

$$\Rightarrow \quad F_{010} = f\left[e^0 + e^{\pi i} + e^0 + e^{\pi i}\right] = f[2 - 2] = 0$$

$$F_{020} = f\left[e^0 + e^{2\pi i} + e^0 + e^{2\pi i}\right] = f[2 + 2] = 4f$$

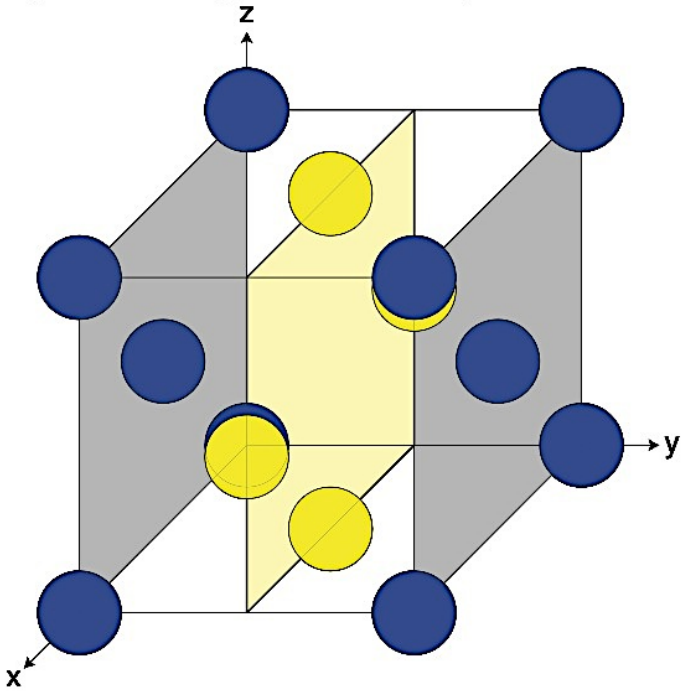

Atomic positions information

Forbidden reflections

Cu_3Au - like FCC Au but with Cu atoms on face-centred sites.

What happens to SADP if we gradually increase Z of Cu sites until that of Au (to obtain FCC Au)?

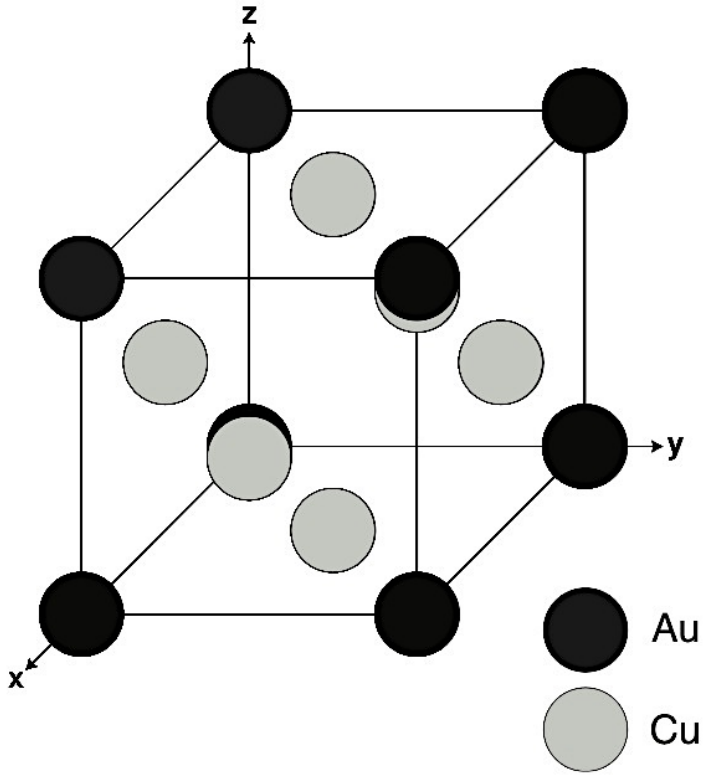

Diffraction pattern on [0 0 1] zone axis:

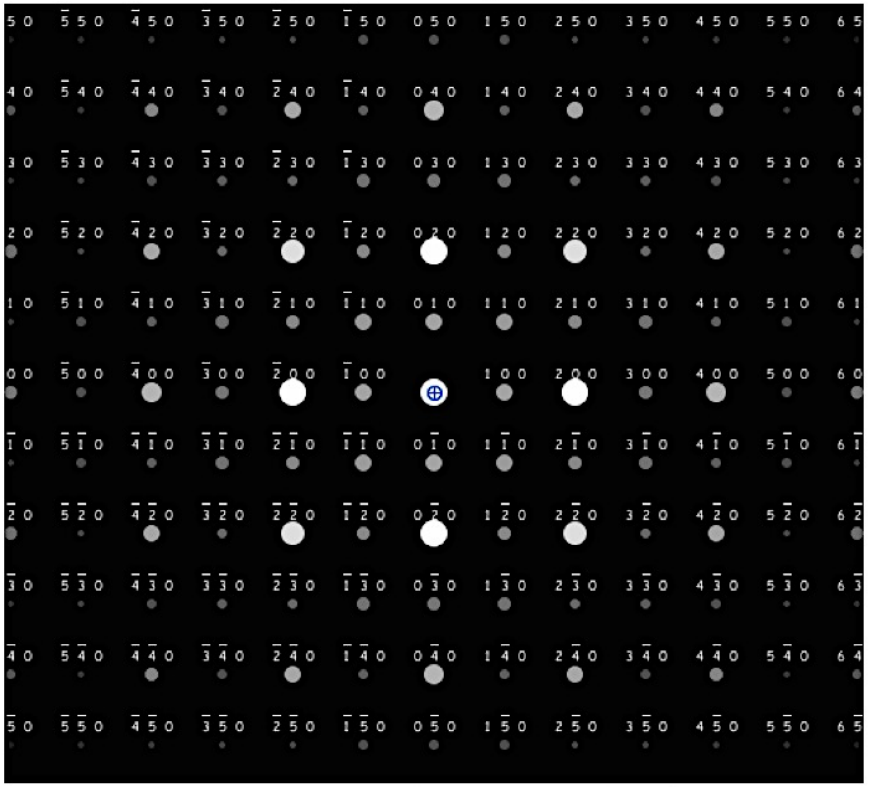

Patterns simulated using JEMS

Atomic positions information

Forbidden reflections

Cu_3Au - like FCC Au but with Cu atoms on face-centred sites.

What happens to SADP if we gradually increase Z of Cu sites until that of Au (to obtain FCC Au)?

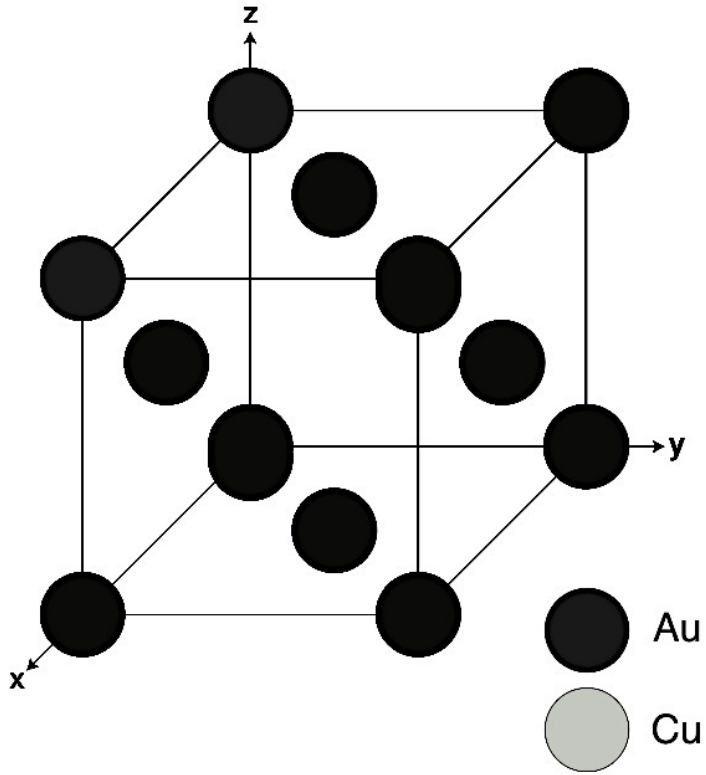

Diffraction pattern on [0 0 1] zone axis:

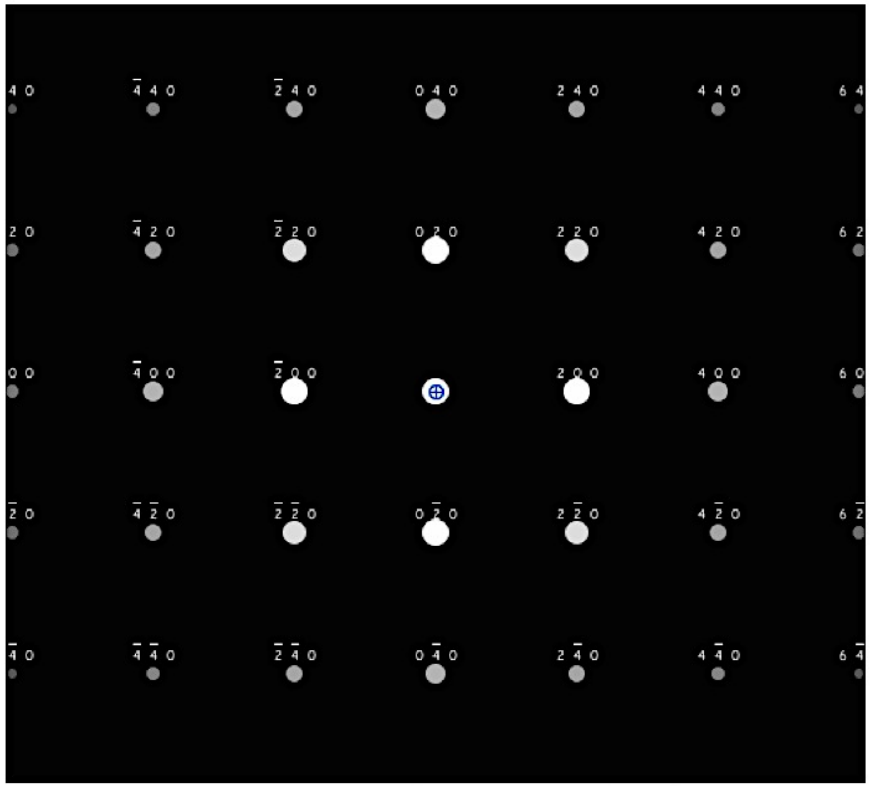

Patterns simulated using JEMS

Orientation relation

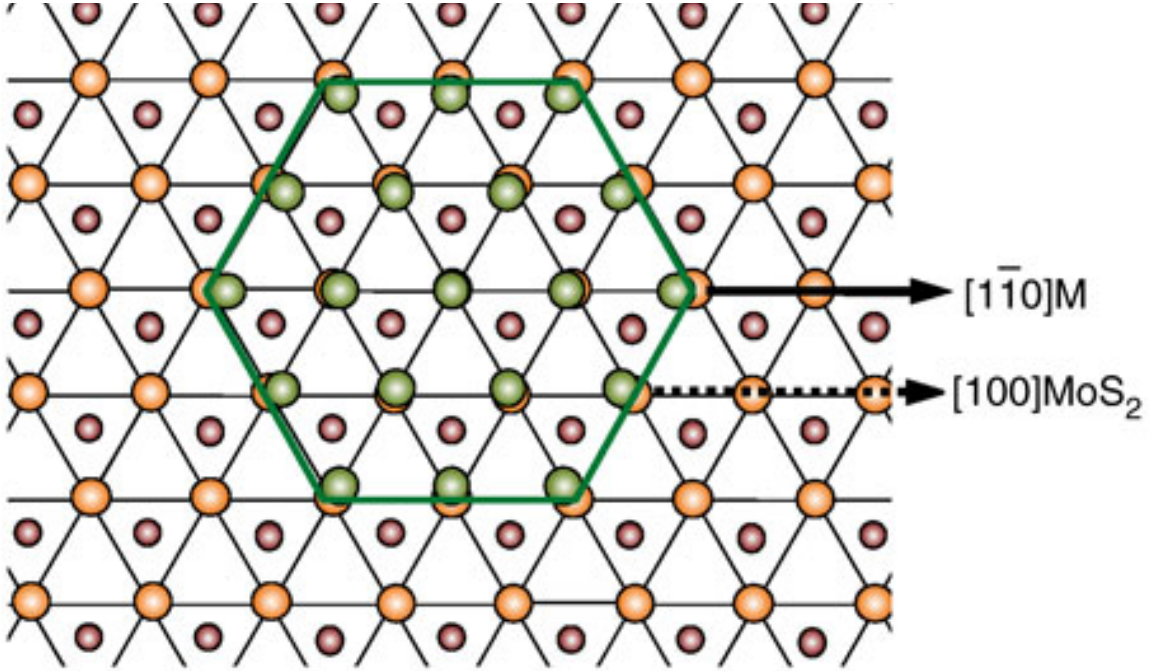

Mo
S
M = Pt, Pd, Ag

$(111)M \parallel (001)MoS_2$

$[1\bar{1}0]M \parallel [100]MoS_2$ (directions must be in the parallel plane)

Huang, Nature communications 2013

Twinning in diffraction

Example: FCC twins

Stacking of close-packed {1 1 1} planes reversed at twin boundary:

A B C A B C A B C A B C

→ A B C A B C B A C B A C

{1 1 1} planes:

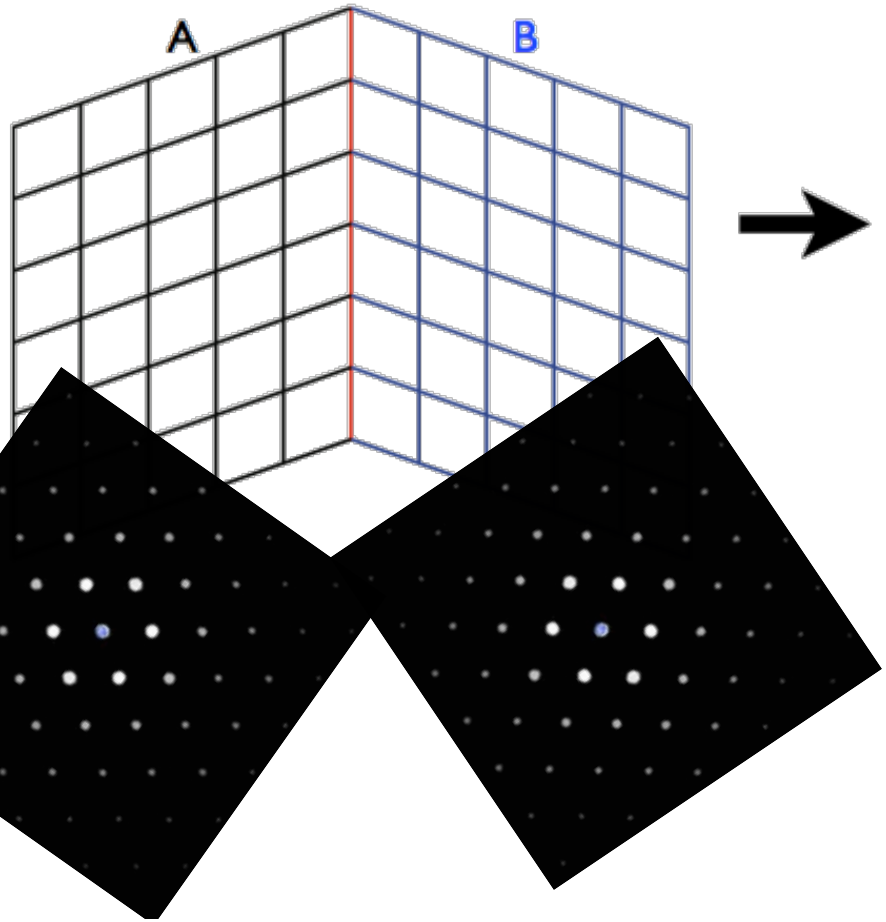

View on [1 1 0] zone axis:

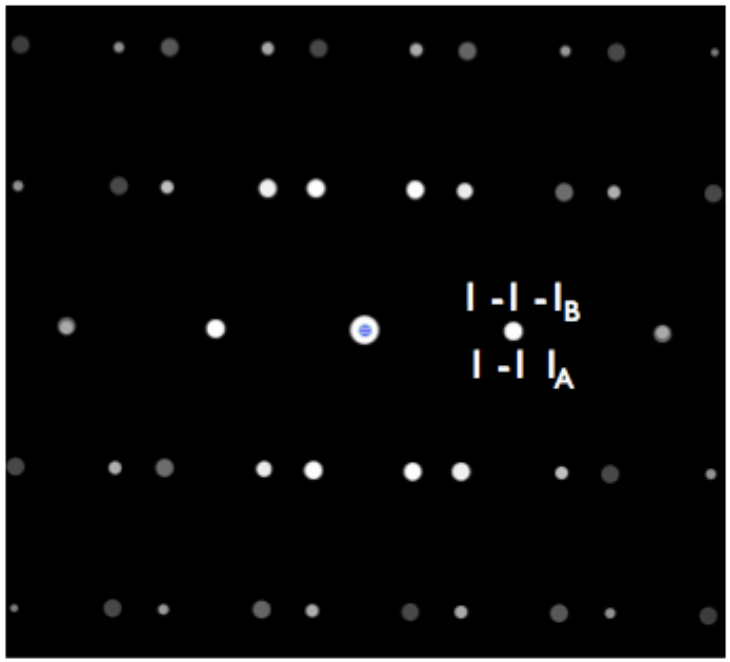

Twinning in diffraction

High nitrogen stainless steel

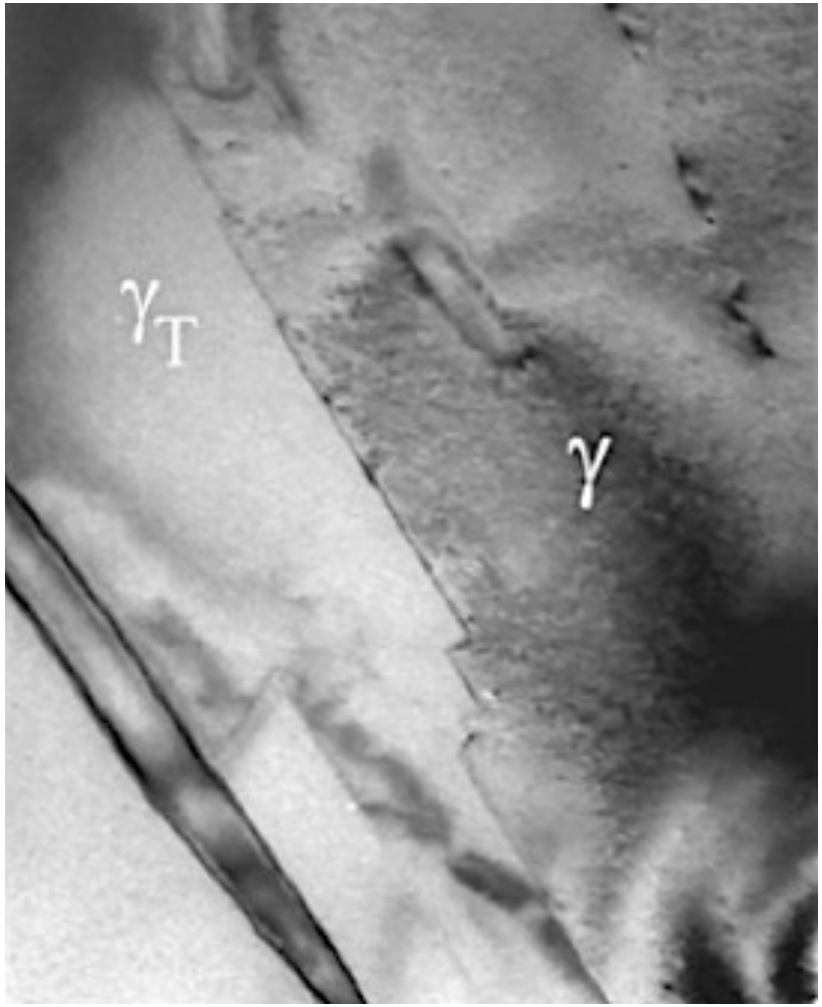

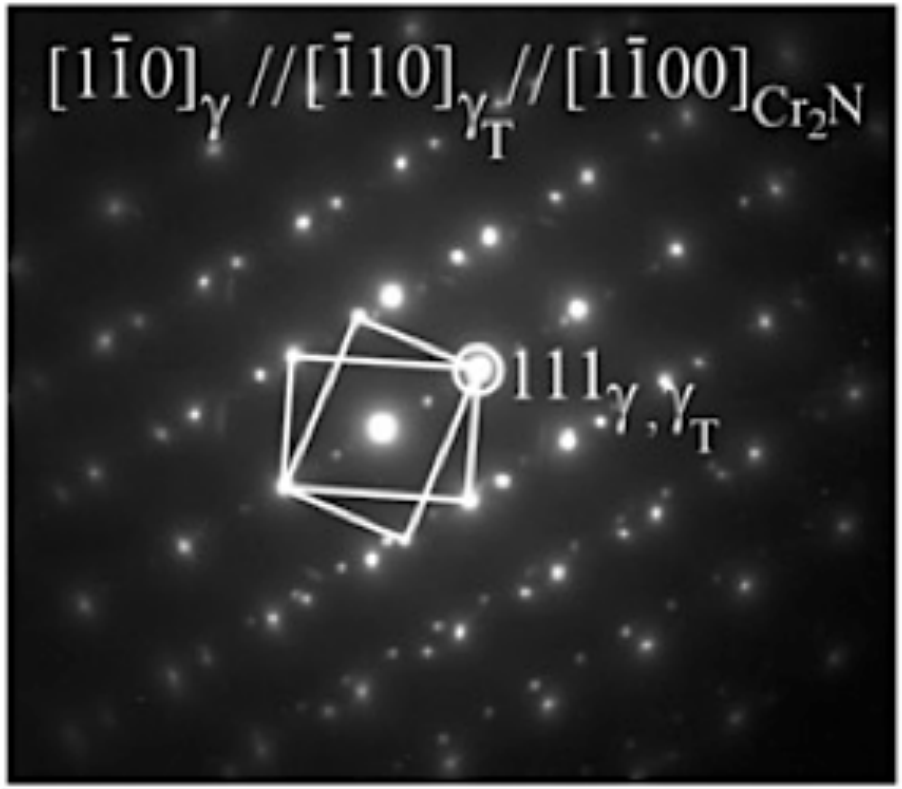

Random distribution of planar defects (Polysynthetic twinning)

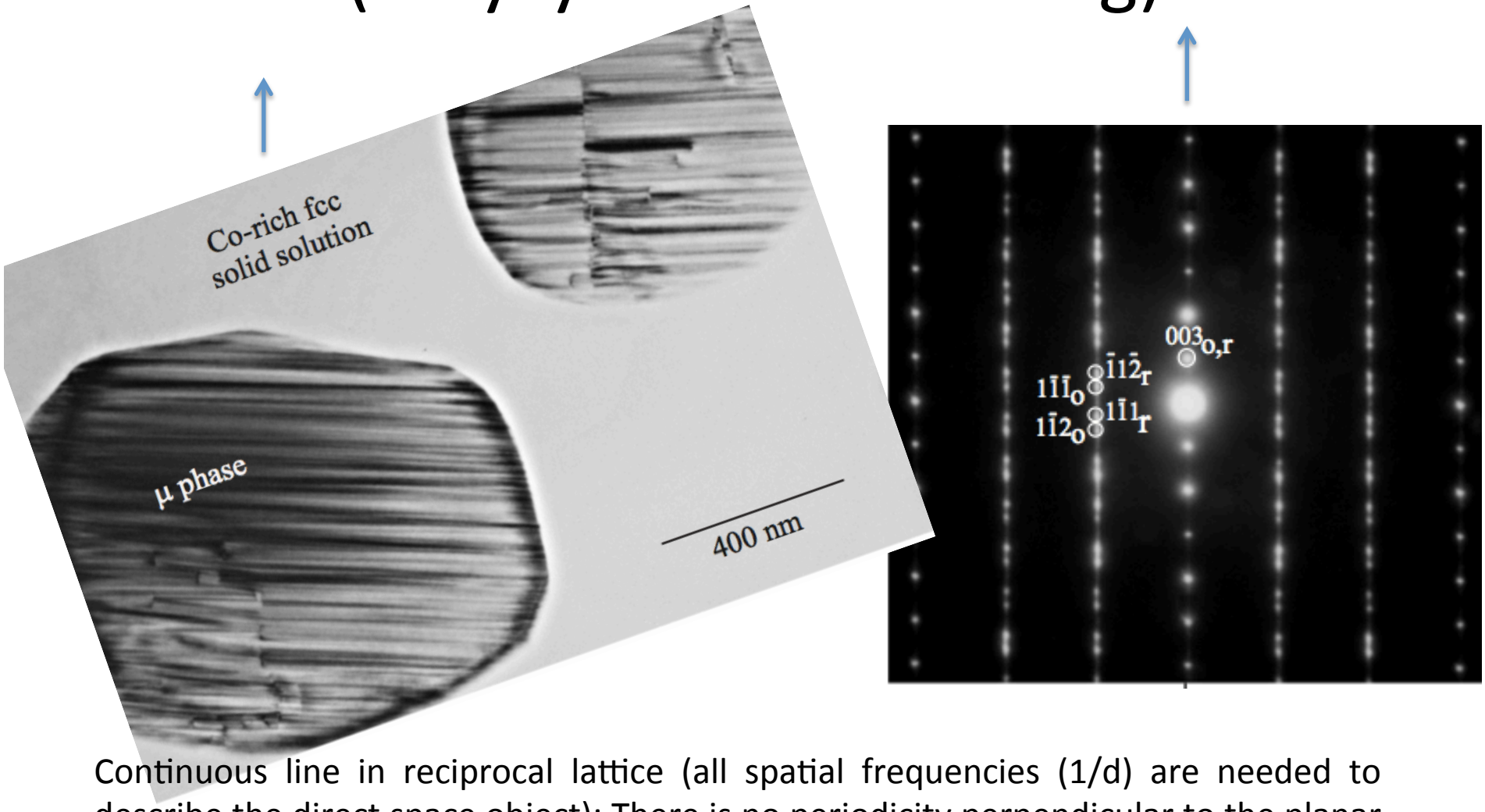

Continuous line in reciprocal lattice (all spatial frequencies (1/d) are needed to describe the direct space object): There is no periodicity perpendicular to the planar defects.

Epitaxy and orientation relations

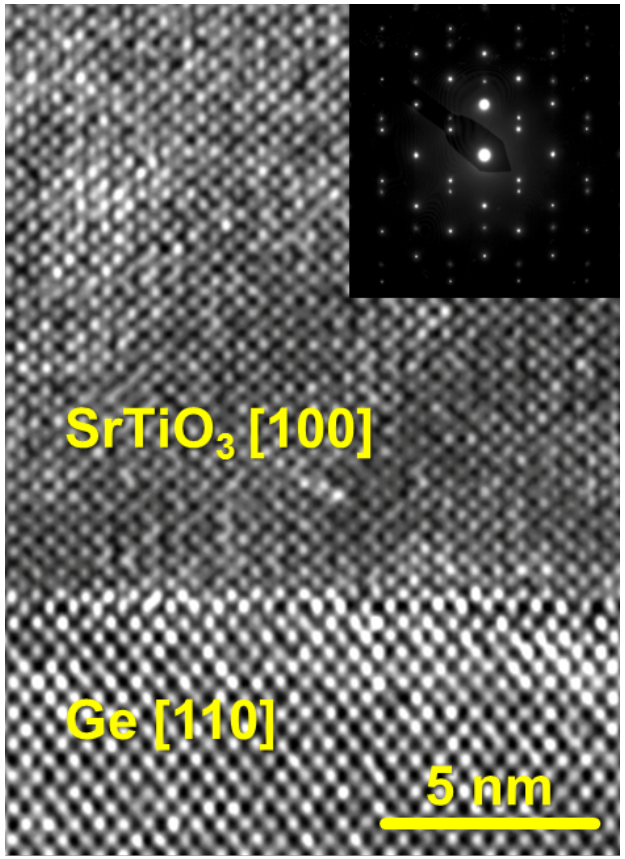

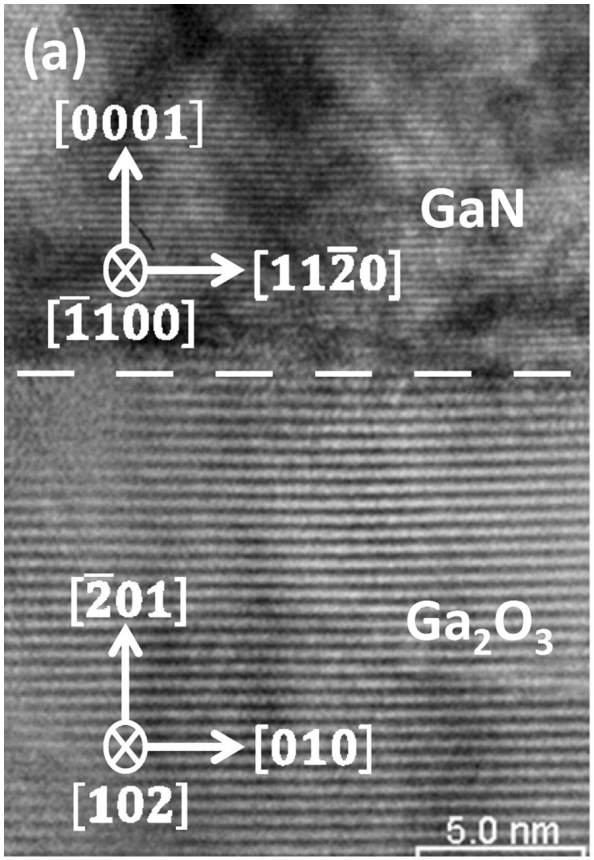

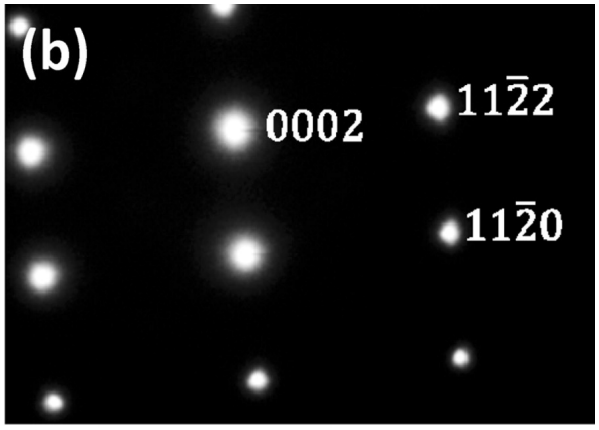

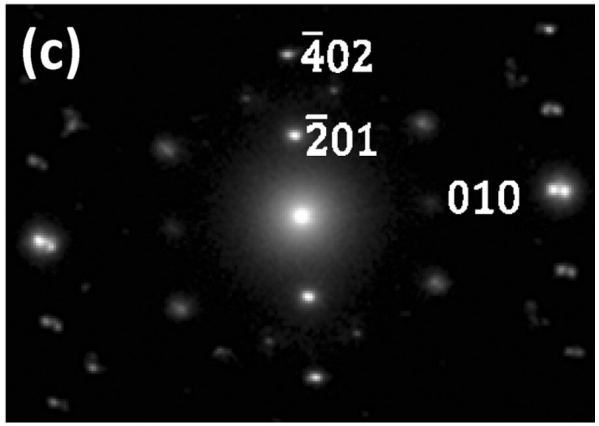

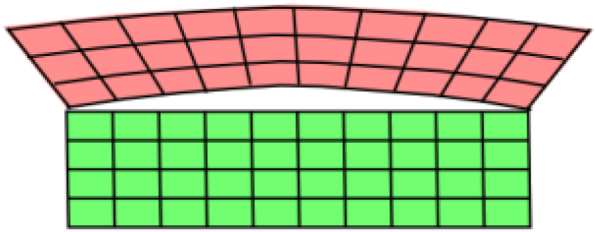

Due to lattice misfit complete coherence is generally impossible: misfit dislocations:

semi-coherent interfaces

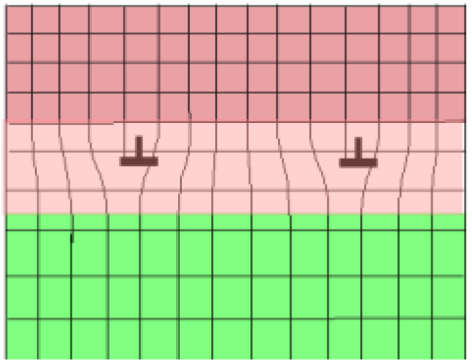

Intergrowth and orientation relations

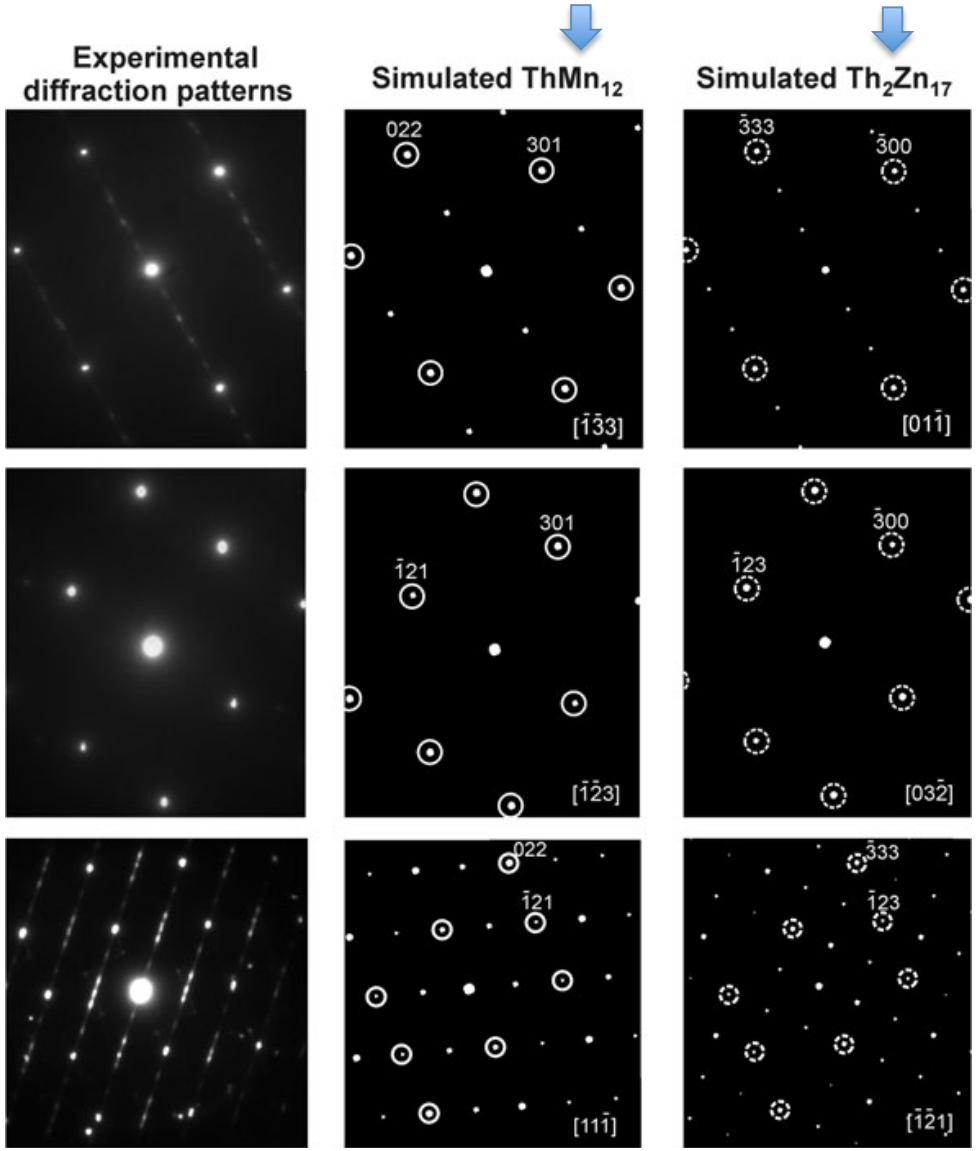

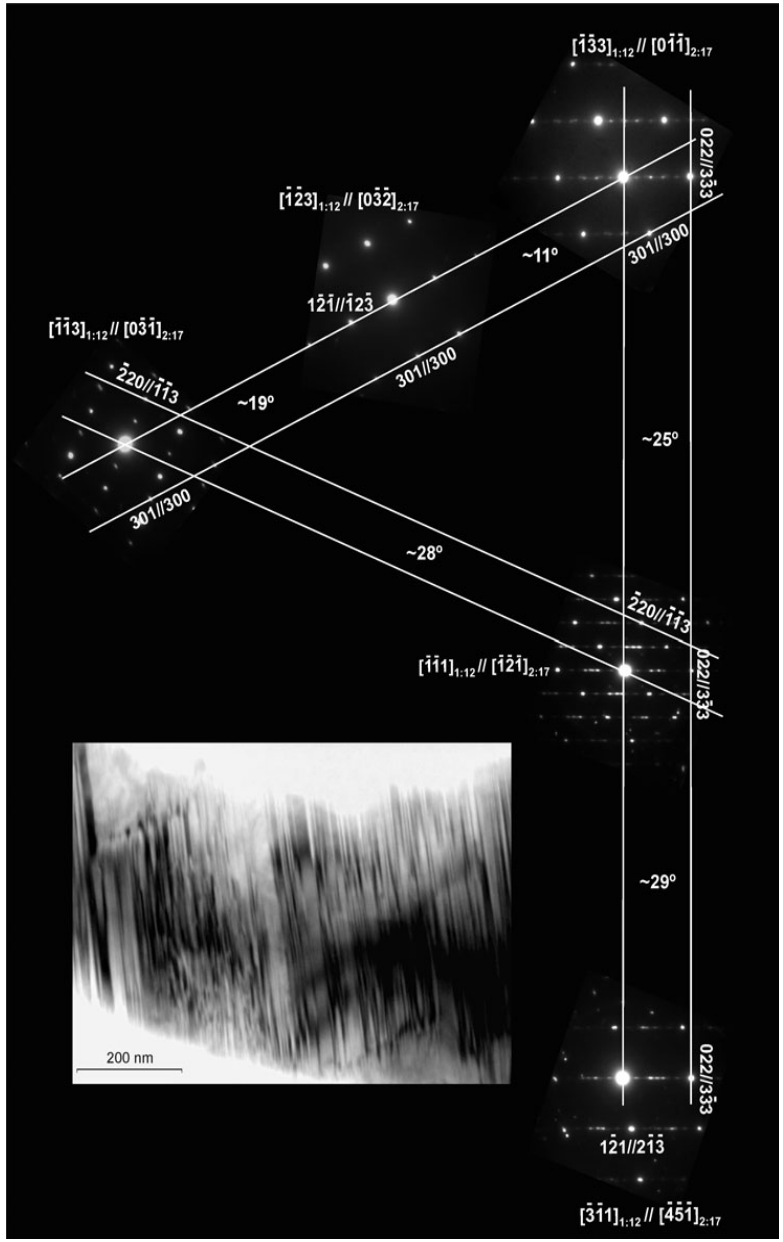

Crystallographic oriented precipitates

Co-Ni-Al shape memory alloy, austenitic with Co-rich precipitates

Bright-field image

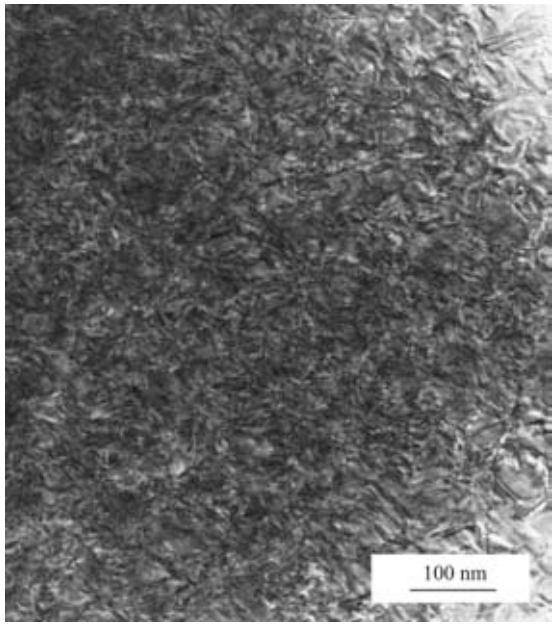

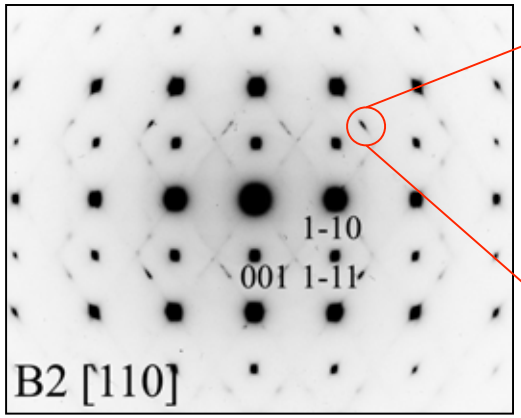

Dark-field image

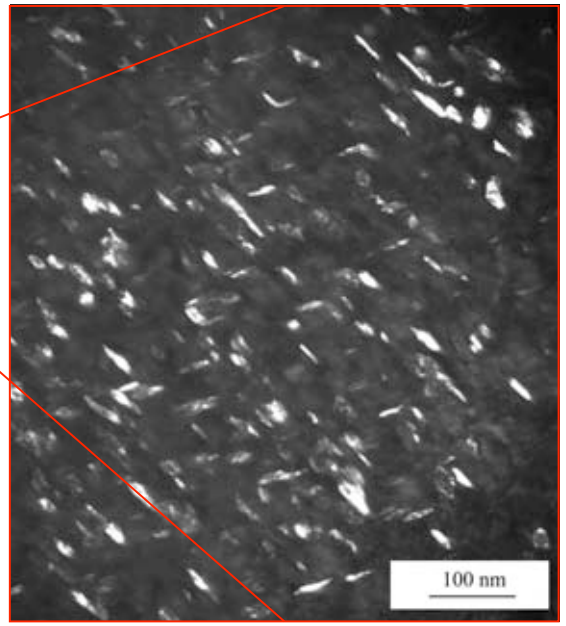

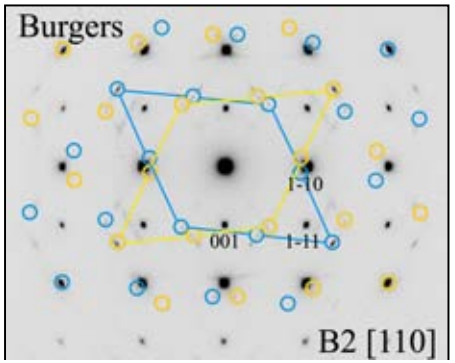

Burgers relationship:

1st variant of *h.c.p. ε-Co* $(110)_{B2}//(001)_{h.c.p.}$; $[-11-1]_{B2}//[110]_{h.c.p.}$

2nd variant of *h.c.p. ε-Co* $(110)_{B2}//(001)_{h.c.p.}$; $[-111]_{B2}//[110]_{h.c.p.}$

Images provided by Barbora Bartová, CIME

Double diffraction: Forbidden reflections

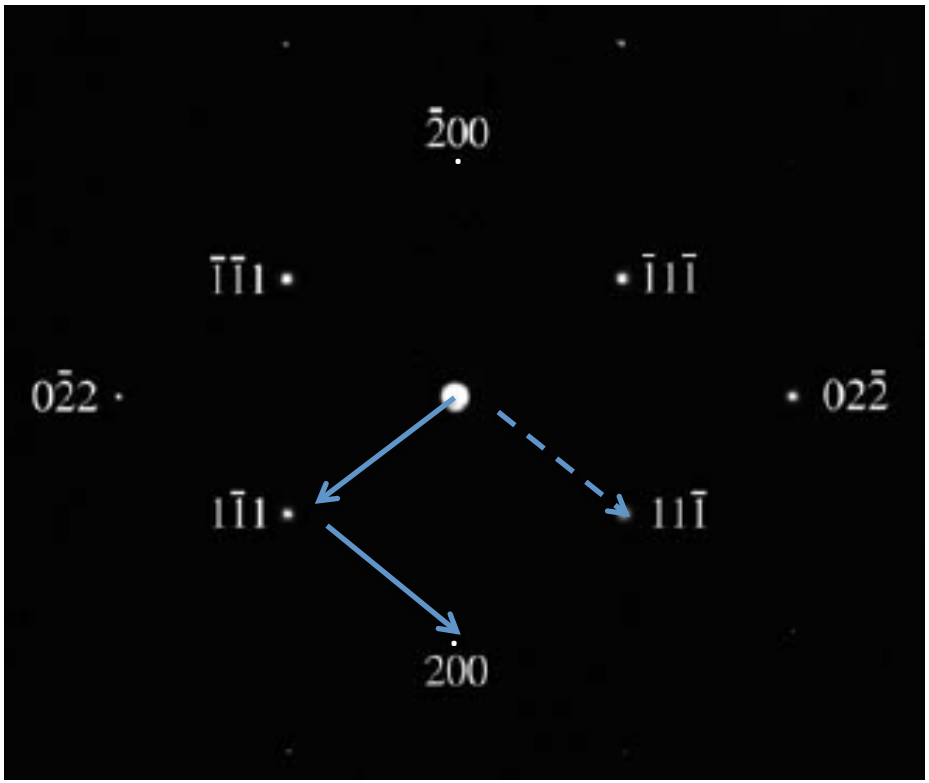

The planes of the (200) form are not diffracting instead, multiple diffractions are occurring at planes of the (111) form.

The [011] DP from Si. The 200 reflection is forbidden, but it is present because the allowed $11\bar{1}$ diffracted beam acts like a new incident beam and is rediffracted by the $(1\bar{1}1)$ plane. The sum of the two allowed reflections $(11\bar{1})$ + $(1\bar{1}1)$ results in a 200 reflection, which is so weak you may not see it.

Double diffraction: Forbidden reflections

Special type of multiple elastic scattering: diffracted beam travelling through a crystal is rediffracted by the same crystal: intensity at forbidden reflections!

Example of silicon; from symmetry of the structure {2 0 0} reflections should be absent

However, normally see them because of double diffraction

Simulate diffraction pattern on [1 1 0] zone axis:

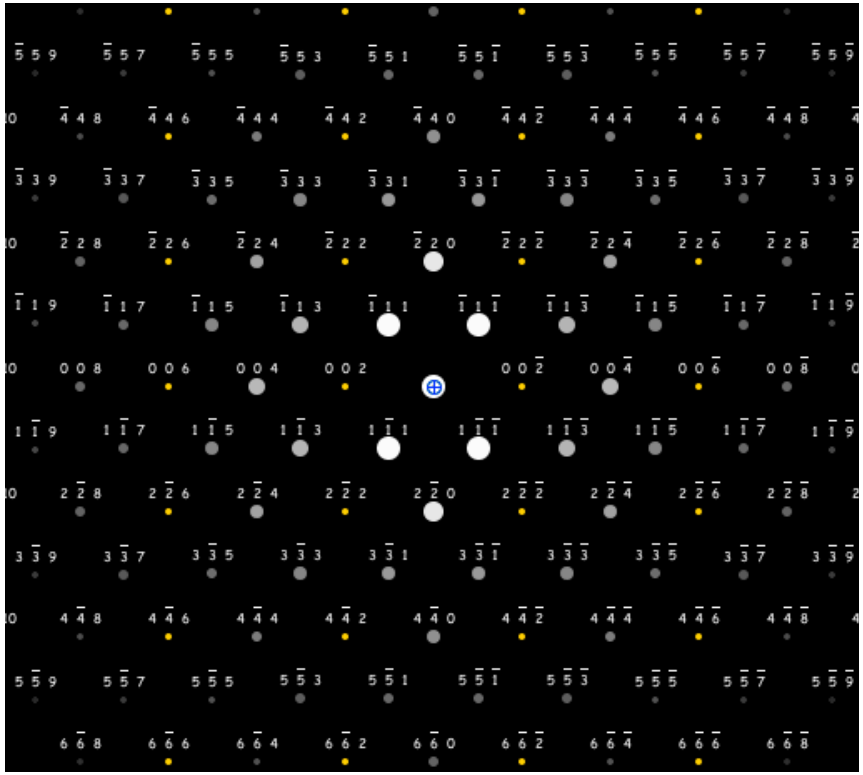

Dynamical simulation JEMS

Double diffraction: Forbidden reflections

Special type of multiple elastic scattering: diffracted beam travelling through a crystal is rediffracted by another crystal

High nitrogen stainless steel

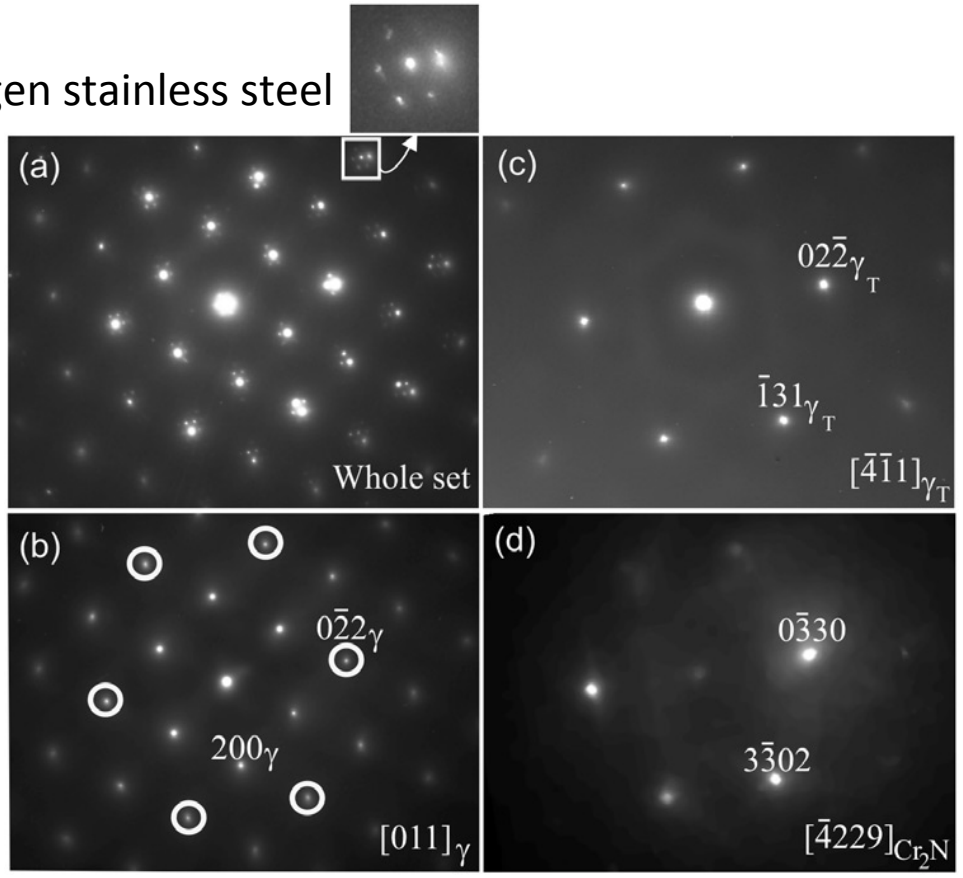

Double-diffraction spots are visible around each of the primary reflections. They also surround the direct beam, although they are hidden by the flare from that beam.

Ring diffraction patterns

- If selected area aperture selects numerous, randomly-oriented nanocrystals, SADP consists of rings sampling all possible diffracting planes: like powder X-ray diffraction
- Larger crystals: “spotty” patterns
- “Texture” - i.e. preferential orientation - is seen as arcs of greater intensity in the diffraction rings

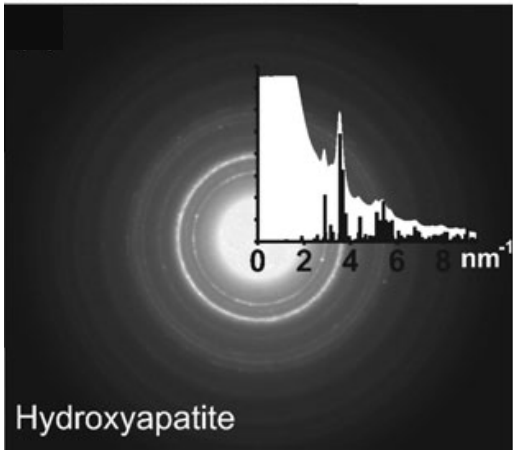

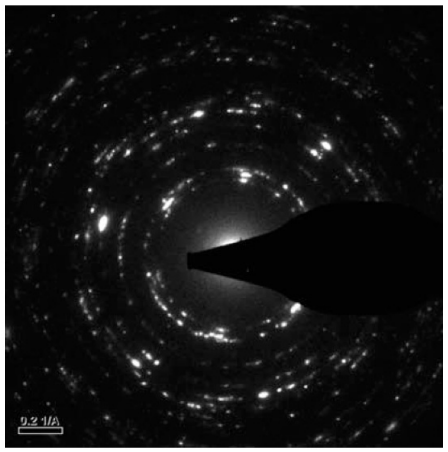
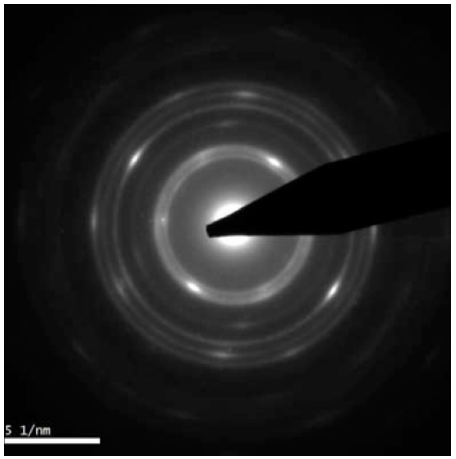

Random distribution of planar defects

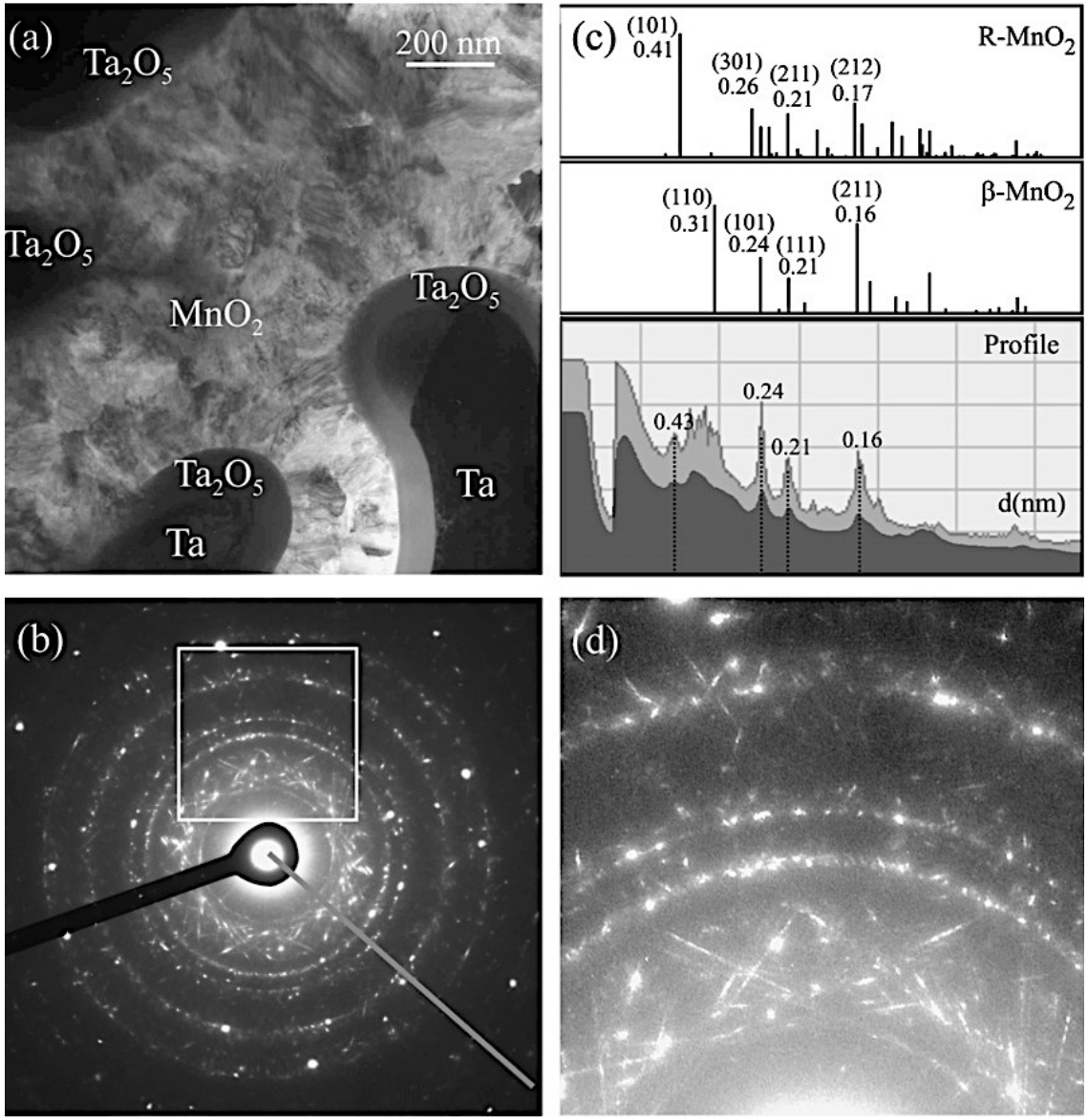

Generate streaks!

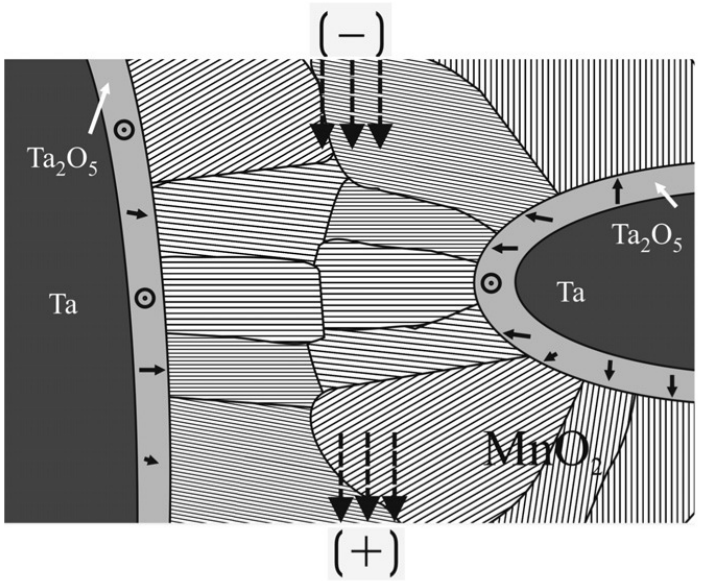

Diffraction patterns of amorphous materials

- Crystals: short-range order *and* long-range order
- Amorphous materials: no long-range order, but do have short-range order (roughly uniform interatomic distances as atoms pack around each other)

Short-range order produces diffuse rings in diffraction pattern

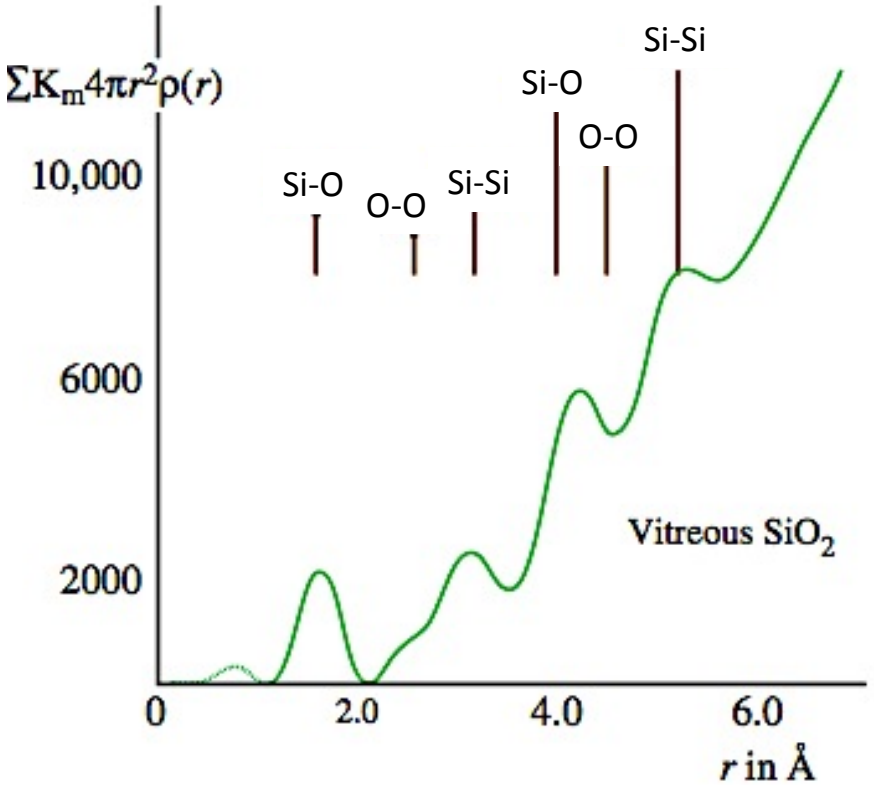

Example:

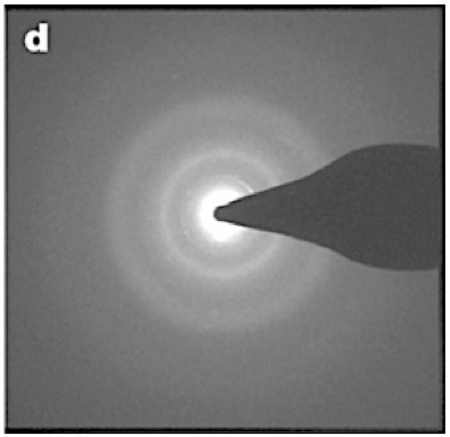

Vitrified germanium
(M. H. Bhat *et al.* Nature **448** 787 (2007)

Phase/orientation mapping

NanoMEGAS ASTAR: phase and orientation mapping in TEM
– similar to EBSD in SEM but e.g. much higher spatial resolution (~5 nm possible)

Record diffraction patterns as electron probe moved across sample

Analyse diffraction patterns by "template matching"
– i.e. correlate to ~2000 patterns simulated at different orientations

Combine with precession and can achieve angular resolution of < 1°

Orientation map for nanocrystalline Cu:

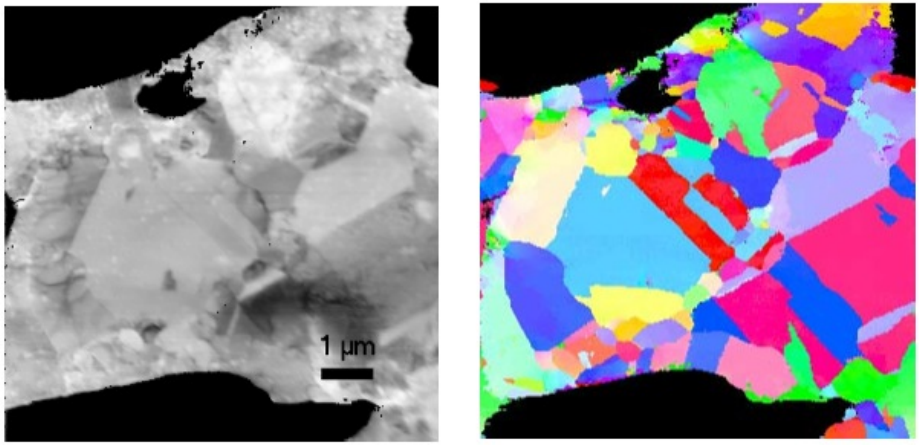

Phase map showing local martensitic structure of steel at stacking faults:

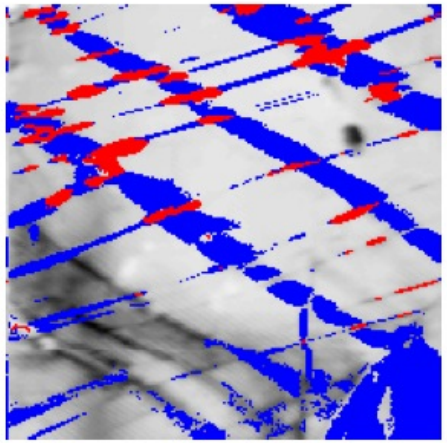

Images from NanoMEGAS company literature

Kikuchi lines

Kikuchi lines

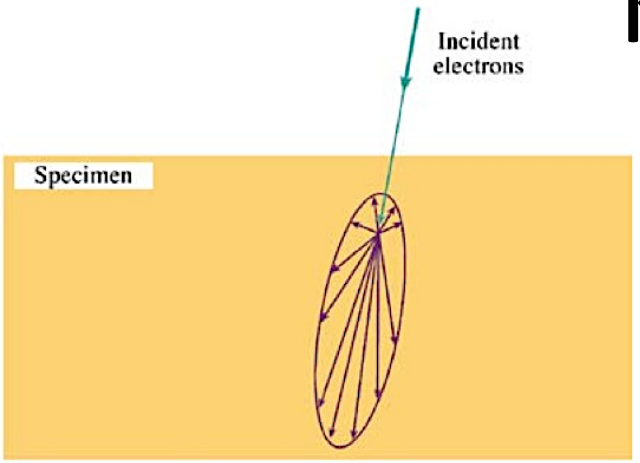

Inelastic scattering: electron in all directions inside crystal. Some scattered electrons in correct orientation for Bragg scattering: cone of scattering

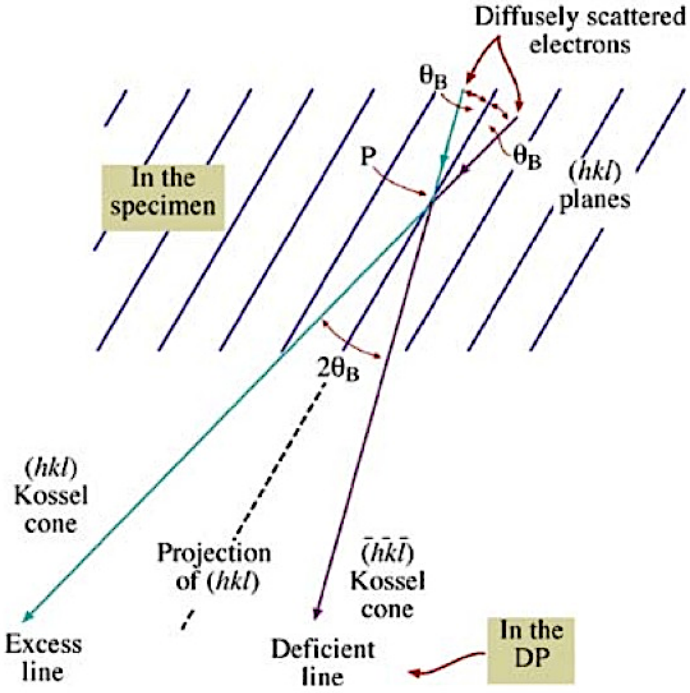

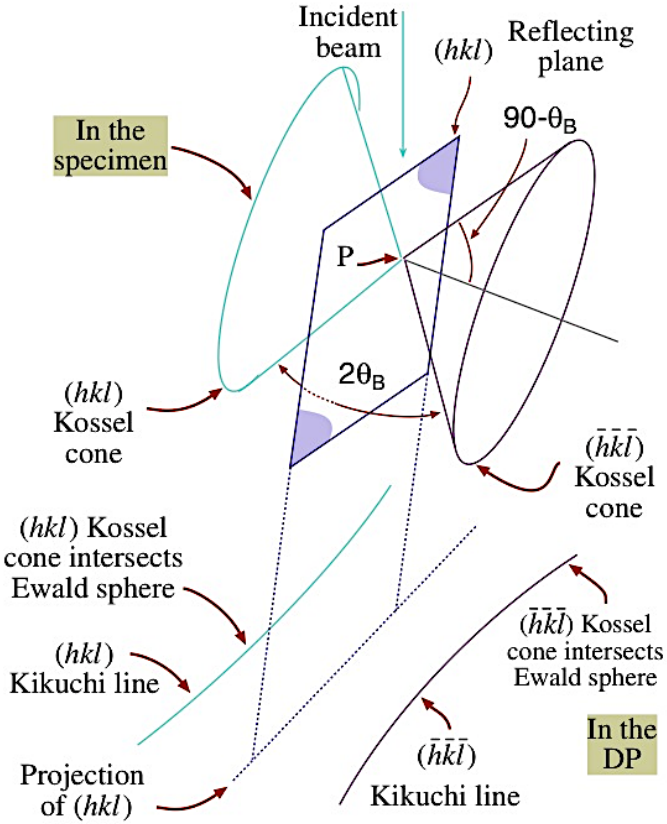

Kikuchi lines

Lower-index lattice planes: narrower pairs of lines

Difficult to see if excess or deficient lines due to intense dynamical scattering

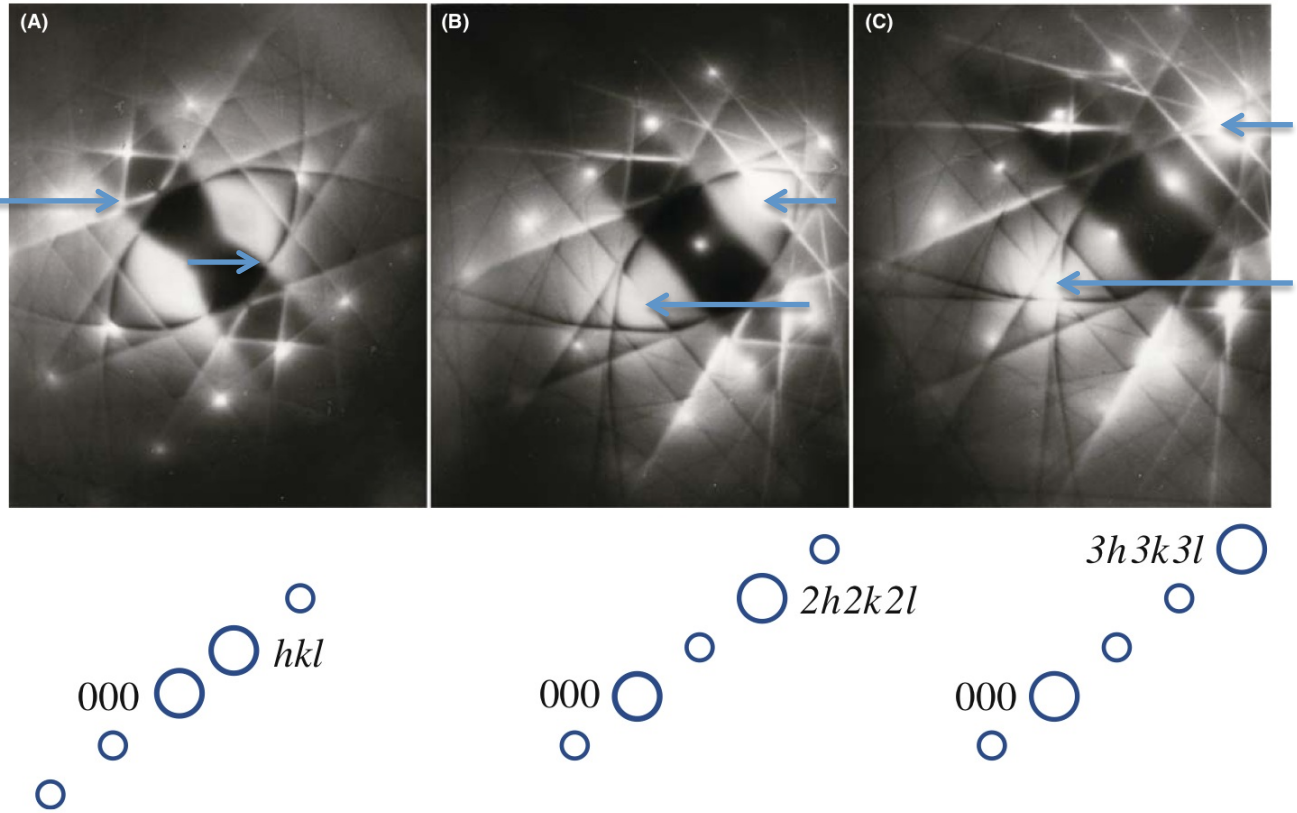

Two-beam DPs from pure Al, obtained under different tilting conditions. As shown schematically below each figure, in (A) the hkl spot is at the exact Bragg condition (the excess Kikuchi line goes through hkl). In (B) the 2h2k2l and in (C) the 3h3k3l spots, respectively, are strongly excited.

The position of the Kikuchi line pairs is very sensitive to specimen orientation. This is used to identify the excitation vector, in particular **s** = 0 when the diffracted beam coincides exactly with the excess Kikuchi line (and direct beam with the deficient line).

Kikuchi lines: “road maps” to reciprocal lattice

Kikuchi lines traverse reciprocal space, converging on zone axes

- use them to navigate reciprocal space as you tilt the specimen!

Examples: Si simulations using JEMS

Si [1 1 0]

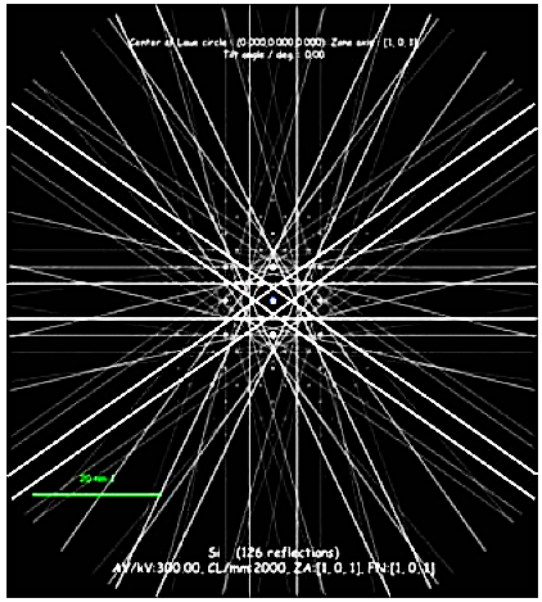

Si [1 1 0] tilted off zone axis

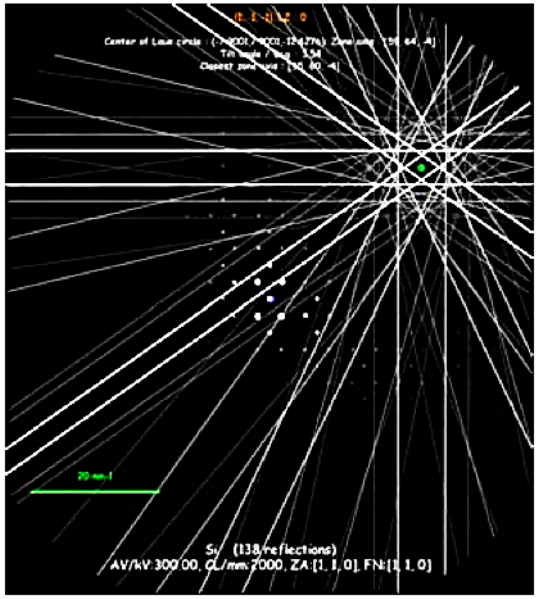

Si [2 2 3]

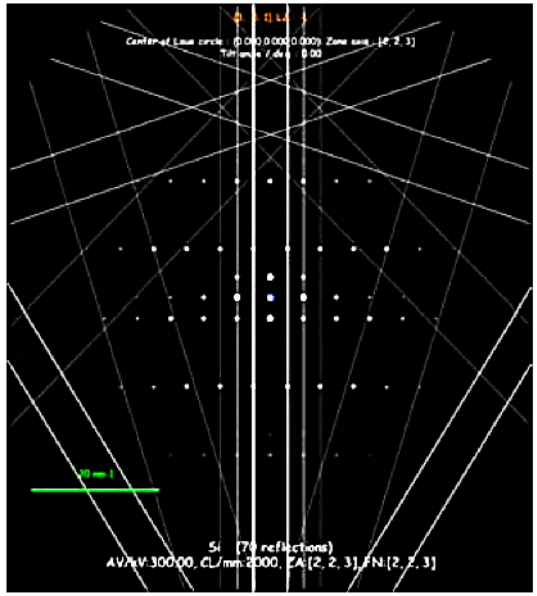

Kikuchi lines: “road maps” to reciprocal lattice

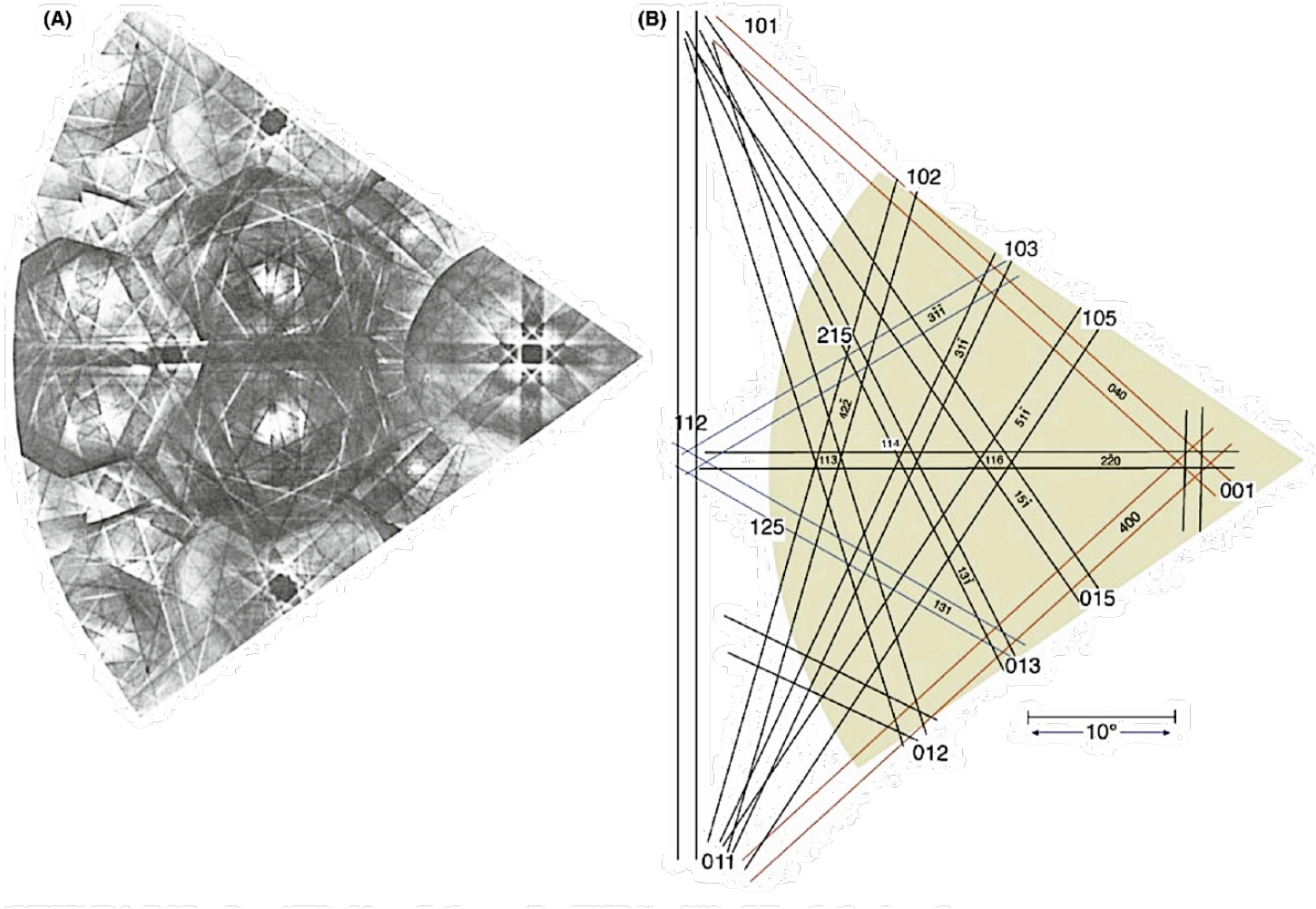

(A) Experimental Kikuchi map for fcc crystals and (B) indexed Kikuchi lines in the schematic map.

Recording and analyzing selected-area diffraction patterns

Recording SADPs

High symmetry

1. Orient your specimen by tilting to a **low index zone axis**:

    - focus the beam on specimen in image mode, select diffraction mode and use "Kikuchi" lines to navigate in reciprocal space
    - use contrast in image mode as multi-beam zone axis corresponds to strong diffraction contrast in the image

2. In image mode, insert chosen selected-area aperture

3. Focus the sample and the aperture border

3. Spread illumination fully (or near fully) overfocus to obtain parallel beam (not always necessary, depends on the number of lenses)

4. Select diffraction mode and focus diffraction spots using diffraction focus

5. Record :

    - using CCD camera: insert beam stopper to cut out central, bright beam to avoid detector saturation (unless you have *very* strong scattering to diffracted beams)
    - using plate negatives: consider using 2 exposures: one short to record structure near central, bright beam; one long (e.g. 60 s) to capture weak diffracted beams

Recording SADPs

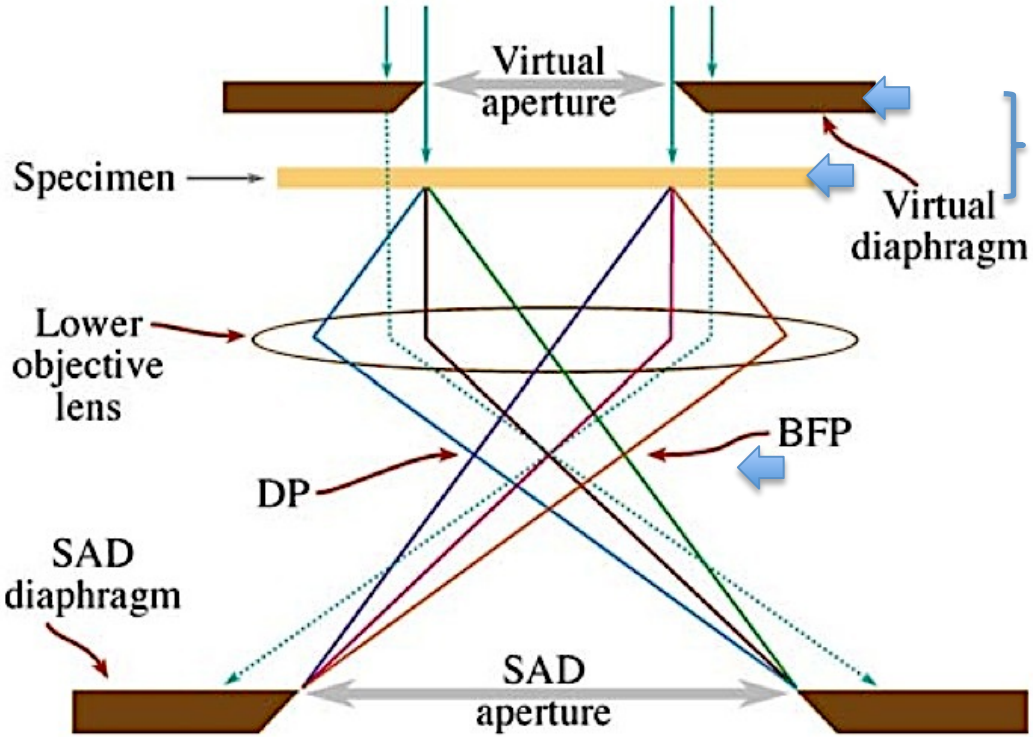

Ray diagram showing SADP formation: the insertion of an aperture in the image plane results in the creation of a virtual aperture in the plane of the specimen (shown here slightly above the specimen plane). Only electrons falling inside the dimensions of the virtual aperture at the entrance surface of the specimen will be allowed through into the imaging system to contribute to the SAD pattern. All other electrons (dotted lines) will hit the SAD diaphragm.

1. Focus both on the screen (specimen image and SAD aperture)
2. Make the beam parallel
3. Change to diffraction

3. Focus the diffraction spots at the BFP (back focal plane) on the screen

Recording media

image plates vs CCD camera

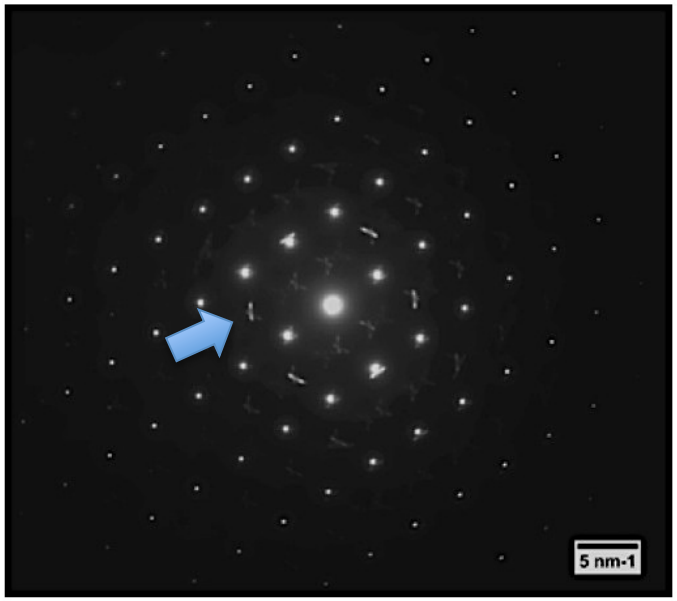

✔ no saturation damage
✔ high dynamic range and sensitivity
✔ linear dynamic range
✔ large field of view
✘ time consuming loading, scanning

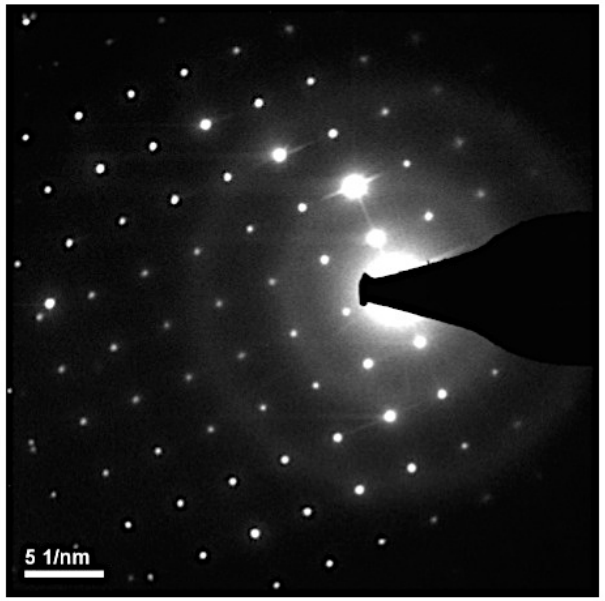

Not well oriented…

✔ immediate digital image
✔ linear dynamic range
✘ small field of view
✘ care to avoid oversaturatation
✘ reduced dynamic range

Analyzing the diffraction pattern

- **Spot pattern** – from single-crystals in the specimen
  - Major use:
    - The foil orientation can be determined;
    - Identification of phases;
    - The orientation relationship between structures can be determined.

- **Ring pattern** – from polycrystalline specimen
  - Major use:
    - Identification of the phases;
    - Analysis of texture.

Diffraction in electron microscope:

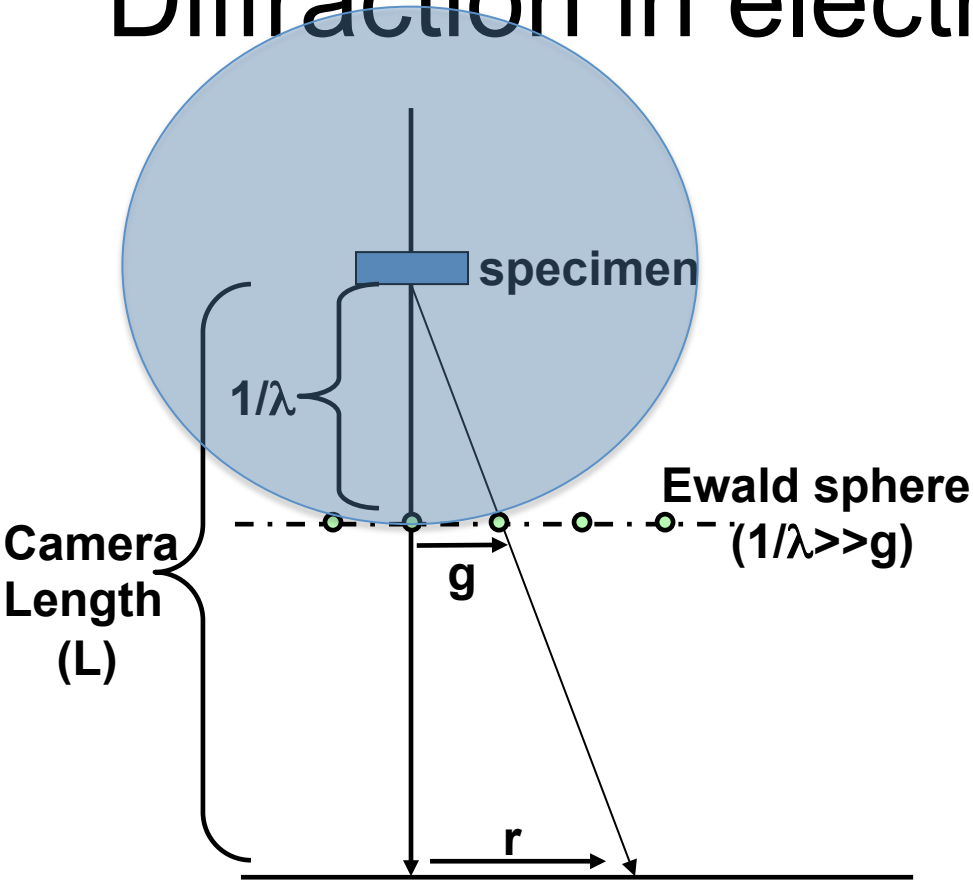

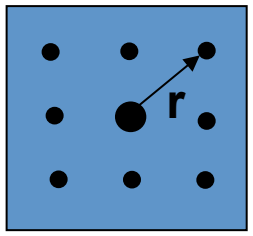

The single crystal electron diffraction pattern is a series of spots equivalent to a magnified view of a planar section through the reciprocal lattice normal to the incident beam.

Diffraction in electron microscope:

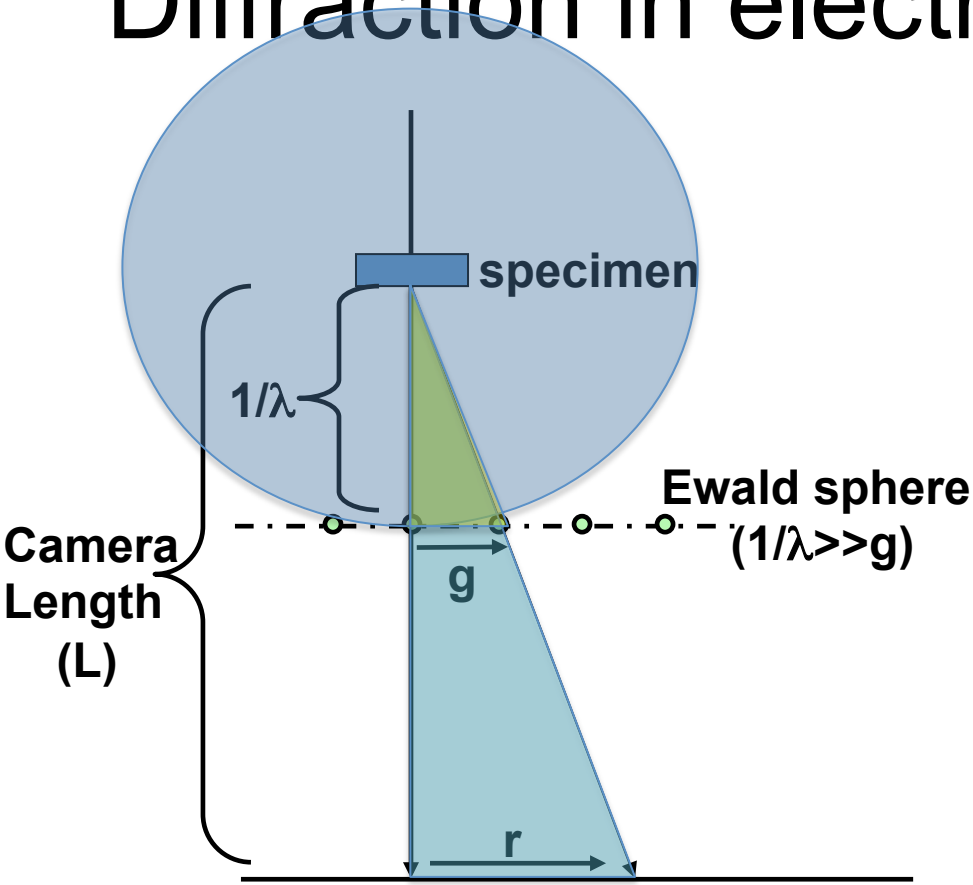

The single crystal electron diffraction pattern is a series of spots equivalent to a magnified view of a planar section through the reciprocal lattice normal to the incident beam.

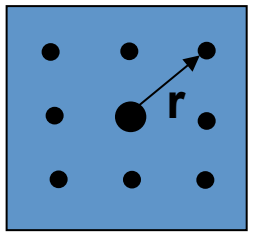

$$\frac{1\backslash\lambda}{L} = \frac{g}{r}$$

$$rd_{hkl} = L\lambda$$

$L\lambda$ - camera constant

Spot pattern

All diffraction spots are obtained from planes belonging to one zone.

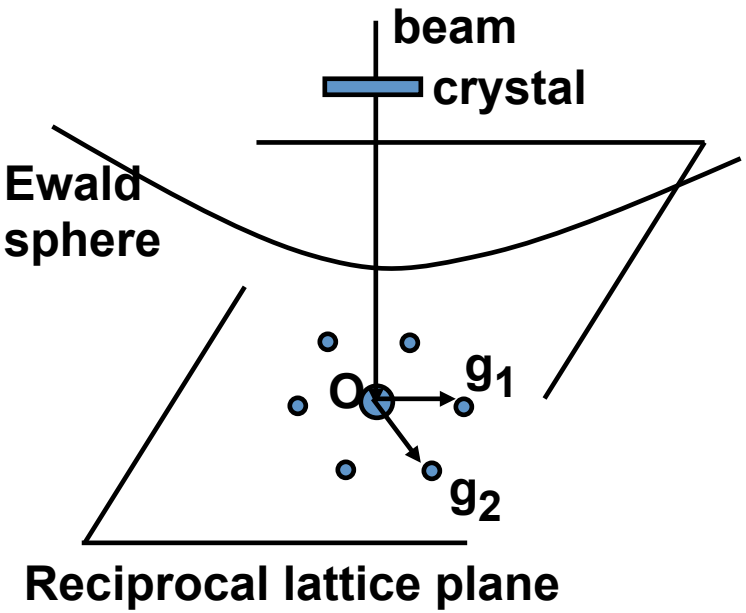

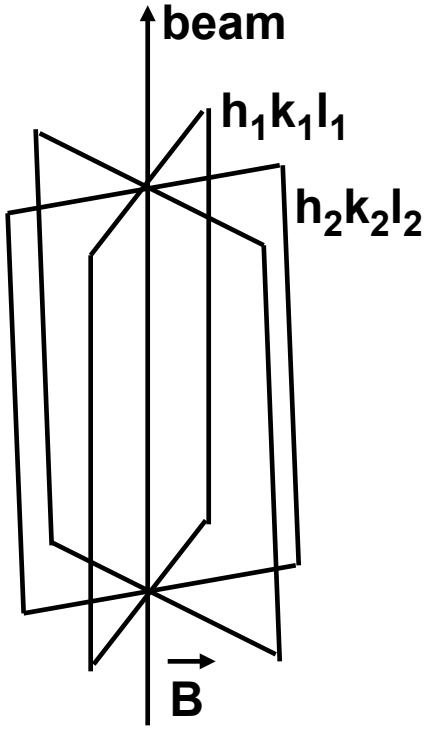

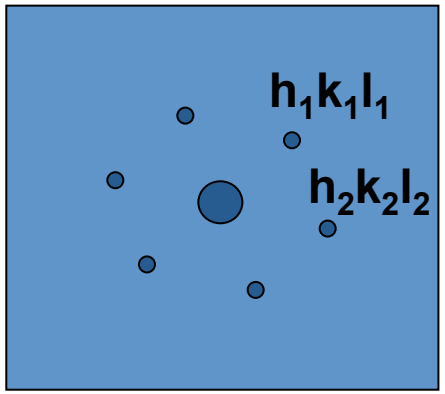

Real diffraction pattern:

Indexing single crystal pattern (spot pattern):

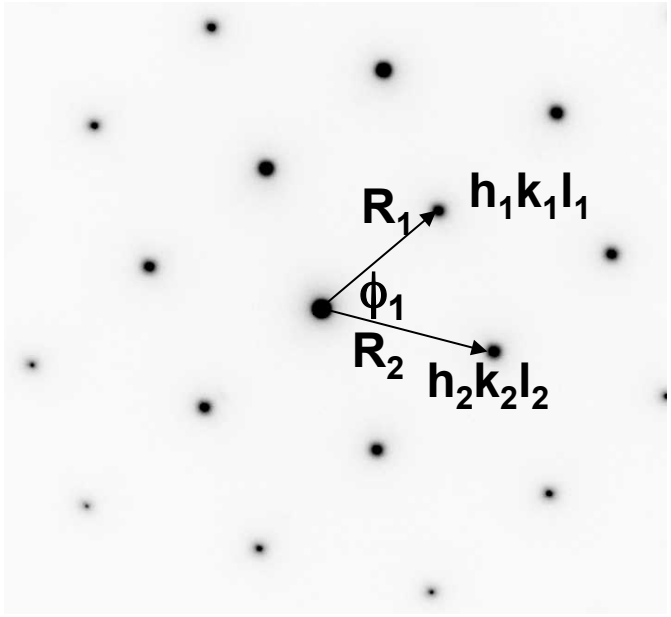

1) Choose the smallest independent R_1, R_2,
2) Measure distances R_1, R_2 and angle ϕ_1.
3) Calculate d_1,d_2 (using the rule $rd=L\lambda$).
4) Correlate the measured d-values with d_{hkl} taken from the list of standard interplanar distances for the given structure and ascribe $h_1k_1l_1$ and $h_2k_2l_2$ indices for the chosen spots.
5) Compare the measured angle ϕ_1 with the calculated angle.
6) Index the other spots by vector summation (sum the miller indexes).
7) Determine the zone axis of the pattern:

$$\mathbf{[uvw] = (h_1k_1l_1) \times (h_2k_2l_2)}$$

Indexing diffraction patterns

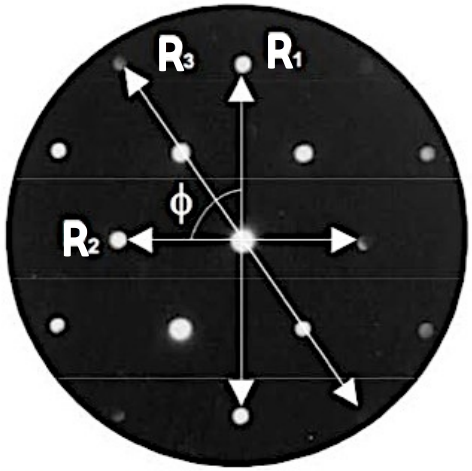

R_1 = 27,5 mm D_2 = 19,5 mm
D_3 = 33,5 mm

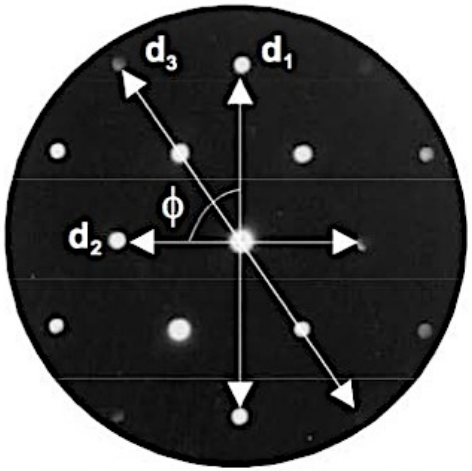

d_1 = 1,92 Å d_2 = 2,72 Å
d_3 = 1,58 Å

d_{hkl}	(hkl)
3,135	{111}
2,715	{020}
1,920	{022}
1,637	{113}
1,568	{222}
1,357	{004}
1,246	{313}
1,214	{024}

Indexing diffraction patterns

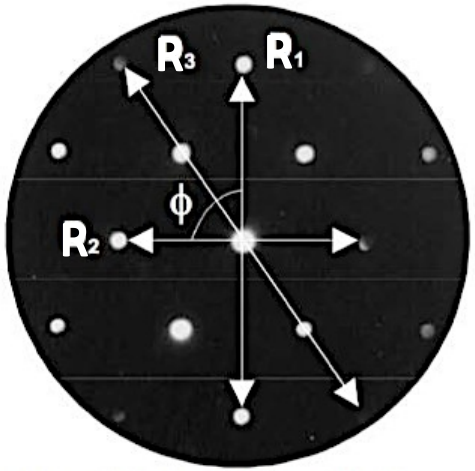

R_1 = 27,5 mm D_2 = 19,5 mm
D_3 = 33,5 mm

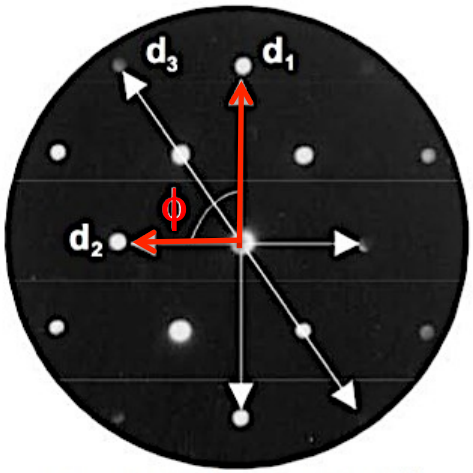

d_1 = 1,92 Å d_2 = 2,72 Å
d_3 = 1,58 Å

Check the angle ϕ between two reflections $h_1k_1l_1$ and $h_2k_2l_2$

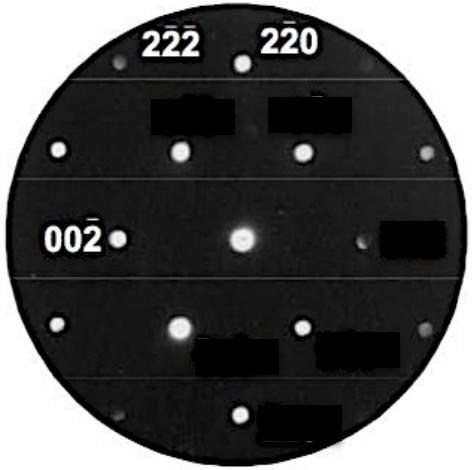

Indexing diffraction patterns

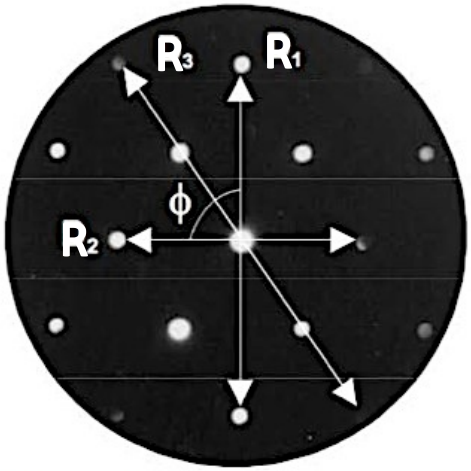

R_1 = 27,5 mm D_2 = 19,5 mm
D_3 = 33,5 mm

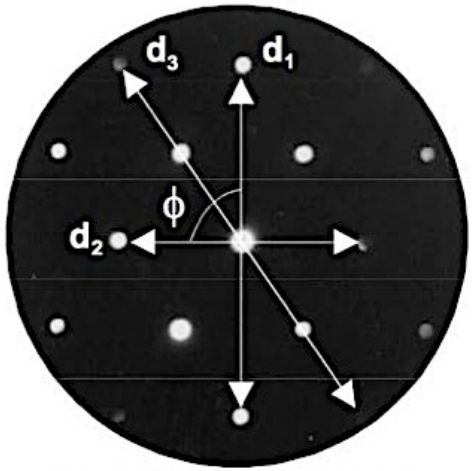

d_1 = 1,92 Å d_2 = 2,72 Å
d_3 = 1,58 Å

$h_3 = h_1 + h_2$
$k_3 = k_1 + k_2$
$l_3 = l_1 + L_2$

d_{hkl}	(hkl)
3,135	{111}
2,715	{020}
1,920	{022}
1,637	{113}
1,568	{222}
1,357	{004}
1,246	{313}
1,214	{024}

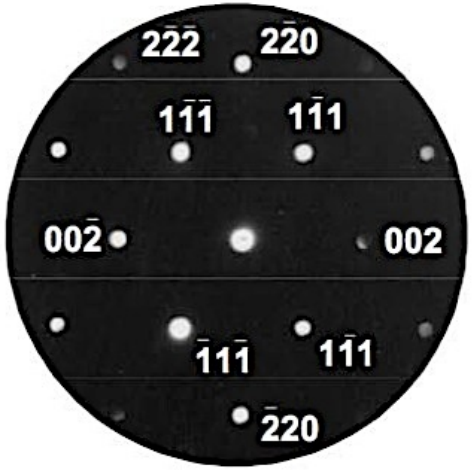

Indexing diffraction patterns

$$\mathbf{B} = \mathbf{g}_1 \times \mathbf{g}_2 = \begin{bmatrix} \mathbf{i}_1 & \mathbf{i}_2 & \mathbf{i}_3 \\ h_1 & k_1 & l_1 \\ h_2 & k_2 & l_2 \end{bmatrix}$$
$$= (k_1 l_2 - k_2 l_1, l_1 h_2 - l_2 h_1, h_1 k_2 - h_2 k_1)$$

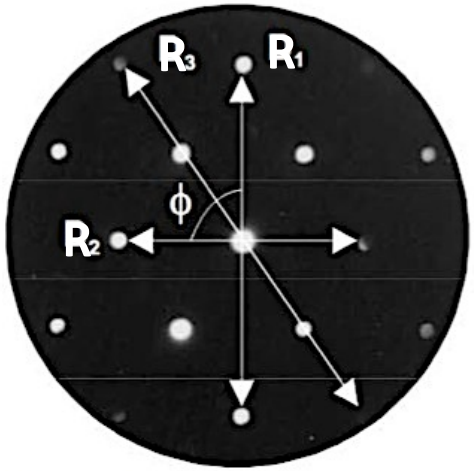

R_1 = 27,5 mm D_2 = 19,5 mm
D_3 = 33,5 mm

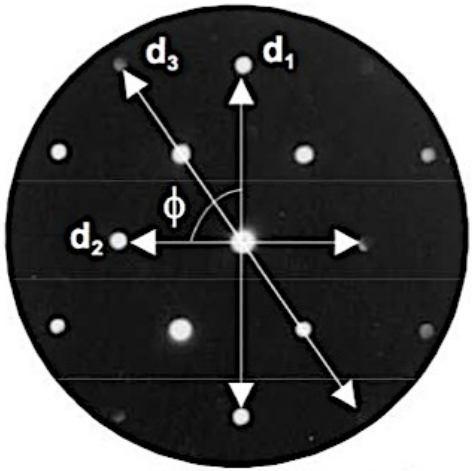

d_1 = 1,92 Å d_2 = 2,72 Å
d_3 = 1,58 Å

Cross product $h_1k_1l_1$ x $h_2k_2l_2$
▼
[uvw] // incident beam

$1\bar{1}\bar{1}$ x $\bar{1}1\bar{1}$ = [110]

Cross product between any two vectors according to the right-hand rule

Analyzing the diffraction pattern

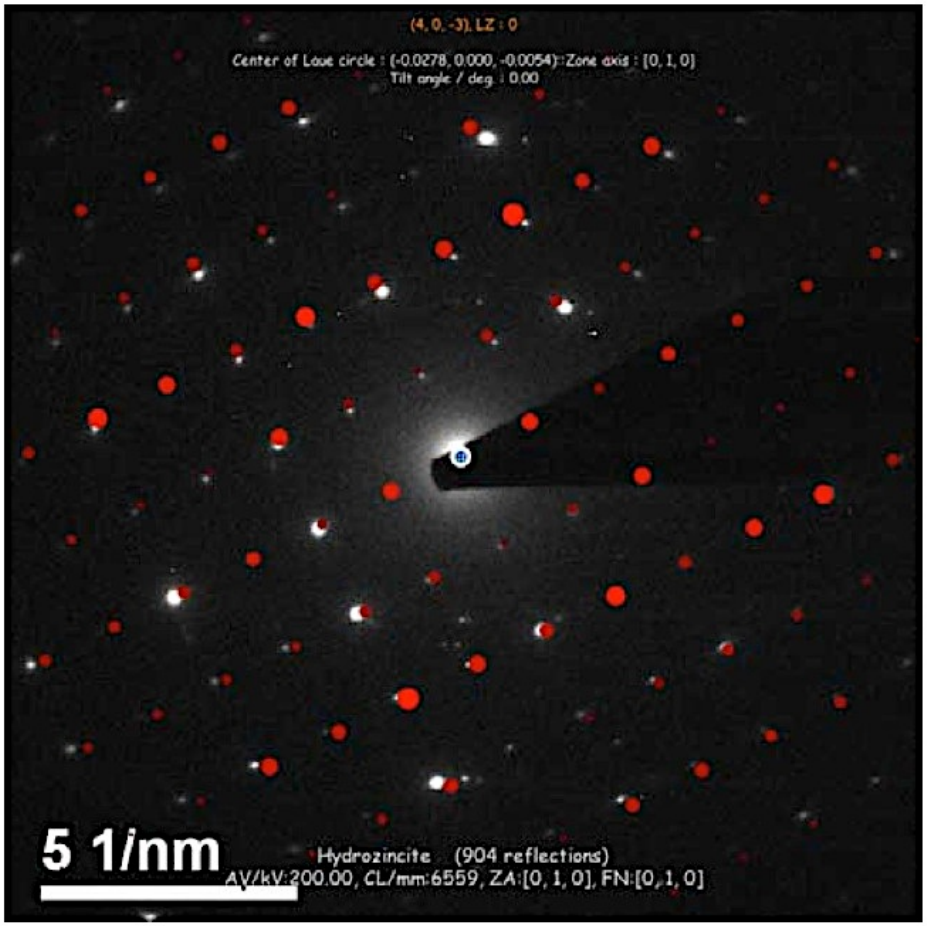

Calculate planes spacings for lower index reflections (measure across a number and average)

Measure angles between planes

Compare plane spacings e.g. with XRD data for expected crystals

Identify possible zone axes using Weiss Zone Law

Simulate patterns e.g. using JEMS; overlay simulation on recorded data

Ring pattern:

For polycrystalline material the reciprocal lattice becomes a series of concentric spheres

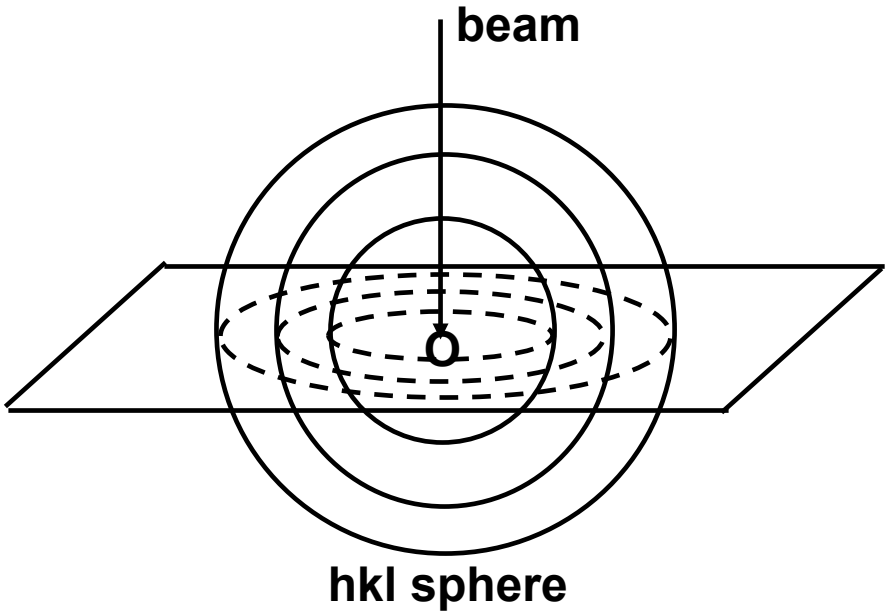

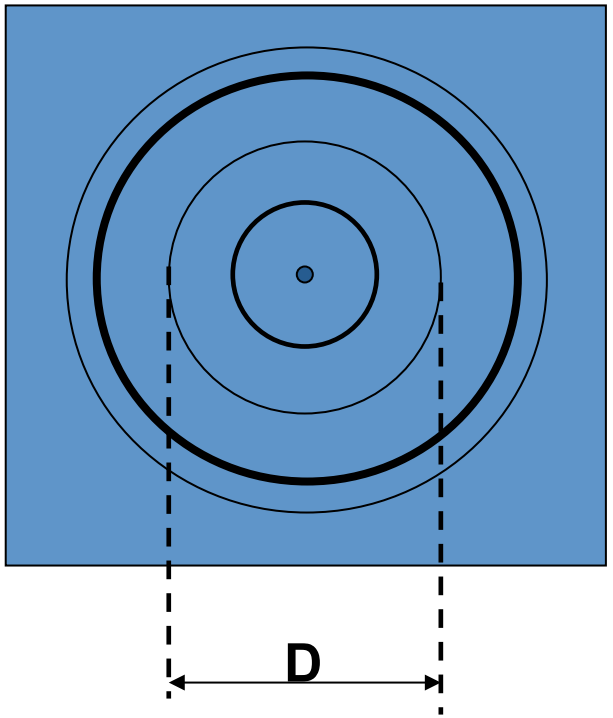

Steps for indexing ring patterns:

1) Measure ring diameters D_1, D_2, D_3 …….
2) Calculate d_{hkl} (using the expression: $rd_{hkl}=L\lambda$)
3) Use some structure database to index each ring.

Ring pattern:

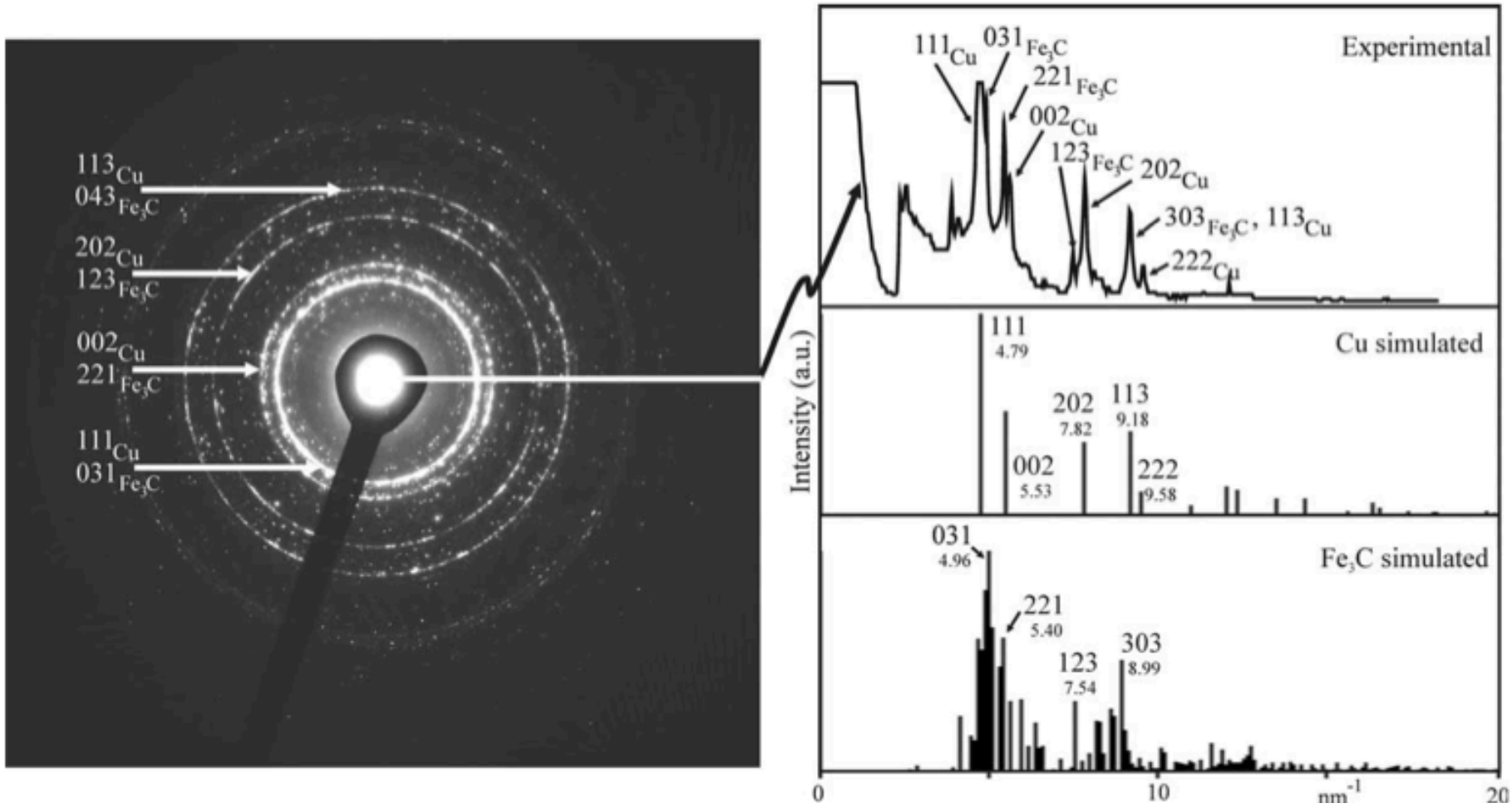

Compare with simulations
(take care with intensitities kinematical (XRD) vs dynamic)

Calibrating diffraction patterns

Plate negatives

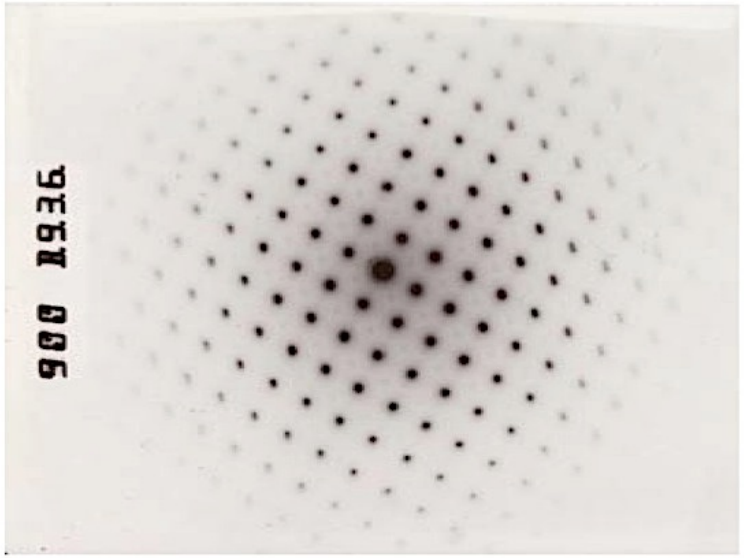

$\lambda L = d_{hkl} R_{hkl}$

λ: e^- wavelength (Å)
L: "camera length" (mm)
d_{hkl}: plane spacing (Å)
R_{hkl}: spot spacing on negative (mm)

CCD camera

Record SADP from a known standard - e.g. NiO_x ring pattern

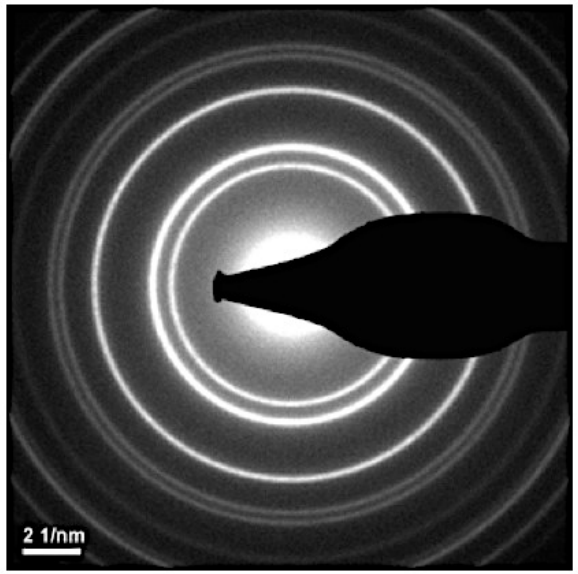

$(D/2)C = d_{hkl}^{-1}$

D: diameter of ring (pixels)
C: calibration (nm^{-1} per pixel)
d_{hkl}^{-1}: reciprocal plane spacing (nm^{-1})

Calibrating rotation

Required if relation between image and diffraction pattern is necessary

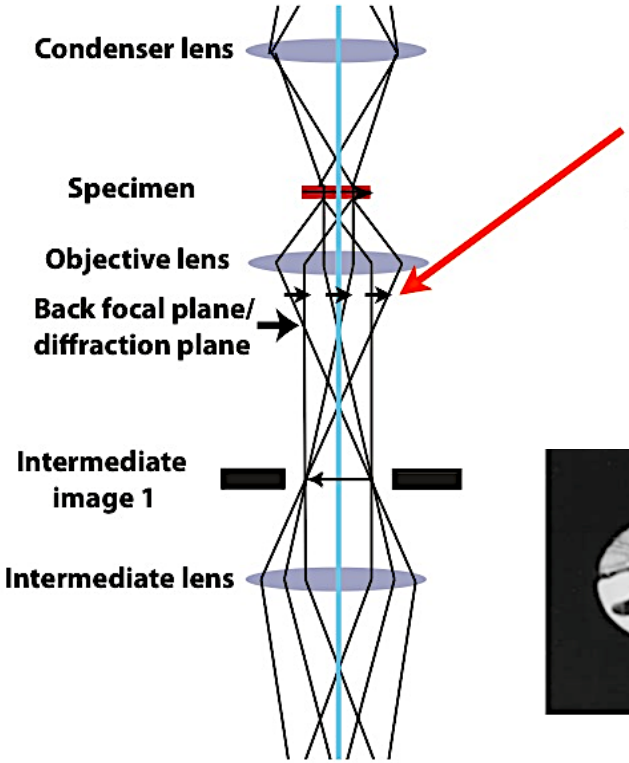

Use specimen with clear shape orientation

Defocus diffraction pattern (diffraction focus/ intermediate lens) to image pattern above BFP

Diffraction spots now discs; in each disc there is an image (BF in direct beam, DF in diffracted beams

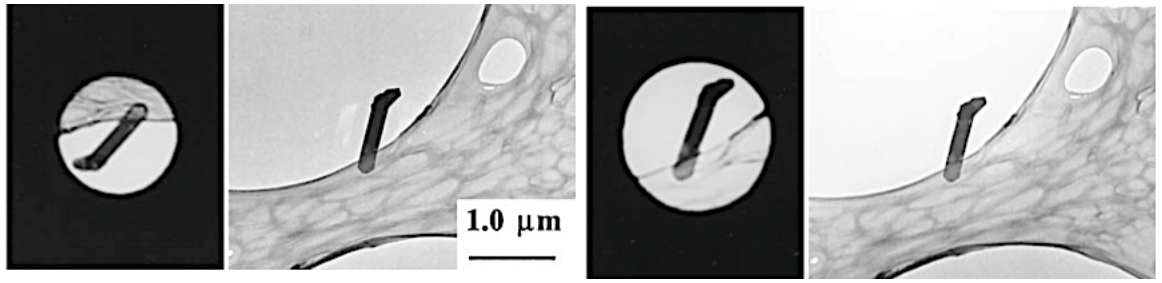

Defocused direct beam in a DP from α-MoO_3 compared with a BF image, showing how to determine if a 180° inversion exists or not. If the image of the specimen inside the expanded image of the beam is rotated with respect to the image on the screen, then a 180° inversion is required to determine the correct angle between directions in the DP and directions in the image (left). If no rotation occurs between the DP and BF image, no correction is necessary (right).

Disadvantages of conventional SADP

✖ Part of the symmetry information is lost
  - projection effect: 2-D information
  - intensities not kinematical: difficult to infer centering

✖ Dynamical intensity hard to interpret

✖ Poor measurement accuracy of lattice parameters (2-3%)

This problems can be overcome with:

- Higher order Laue zones: 3-D information
- Electron precession: “kinematical” zone axis patterns
- Convergent Beam Electron Diffraction (CBED): higher order symmetry, accurate lattice parameter measurement, interpretable dynamical intensity

Which allow:

- full symmetry/point group and space group determination;
- strain measurement;
- characterization of non-centrosymmetric crystals;
- thickness determination; ...

Non-linear dielectrics

Of the 32 crystal point groups, 21 are non-centrosymmetric *i.e.* crystals not having a center of symmetry.

Crystal class	Centro symmetric Point groups		Noncentrosymmetric Point groups					
			Polar		Non-polar			
Cubic	m3	m3m	none		432	$\bar{3}$ m	23	
Tetragonal	4 or m	4 or mmm	4	4mm	$\bar{4}$	$\bar{4}$ 2 m	22	
Orthorhombic	mmm		mm2		222			
Hexagonal	6 or m	6 or mmm	6	6mm	$\bar{6}$	$\bar{6}$2m	622	
Trigonal	$\bar{3}$	$\bar{3}$ m	3	3m	32			
Monoclinic	2 or m		2	m	none			
Triclinic	$\bar{1}$		1		none			
Total Number	11 groups		10 groups		11 groups			

The term centrosymmetric refers to a space group which contains an inversion center as one of its symmetry elements *i.e.* for every point (x, y, z) in the unit cell, there is an indistinguishable point (-x, -y, -z).

Non-linear dielectrics

Non-centrosymmetric point groups (except for group 432) are associated with the piezoelectricity *i.e.* upon application of an electric field, the crystals exhibit strain or upon application of an external stress, charges develop on the faces of the crystal resulting in an induced electric field.

Out of these 20 non-centrosymmetric point groups, 10 belong to polar crystals *i.e.* crystals which possess a unique polar axis, an axis showing different properties at the two ends: a **unique anisotropic axis**. These crystals can be spontaneously polarized and polarization can be compensated through external or internal conductivity or twinning or domain formation.

Spontaneous polarization depends upon the temperature. Consequently, if a change in temperature is imposed, an electric charge is developed on the faces of the crystal perpendicular to the polar axis. This is called pyroelectric effect. All 10 classes of polar crystals are pyroelectric.

In some of these polar non-centrosymmetric crystals, the polarization along the polar axis can be reversed by reversing the polarity of electric field. Such crystals are called ferroelectric i.e. these are spontaneously polarized materials with reversible polarization.

Hence, ferroelectric materials are simultaneously pyroelectric and piezoelectric. Similarly, all pyroelectric materials are by default piezoelectric but not all of them are ferroelectric.

Higher order Laue Zones (c)

"Multi-beam" conditions
[uvw] Zone Axis Pattern
(ZAP)

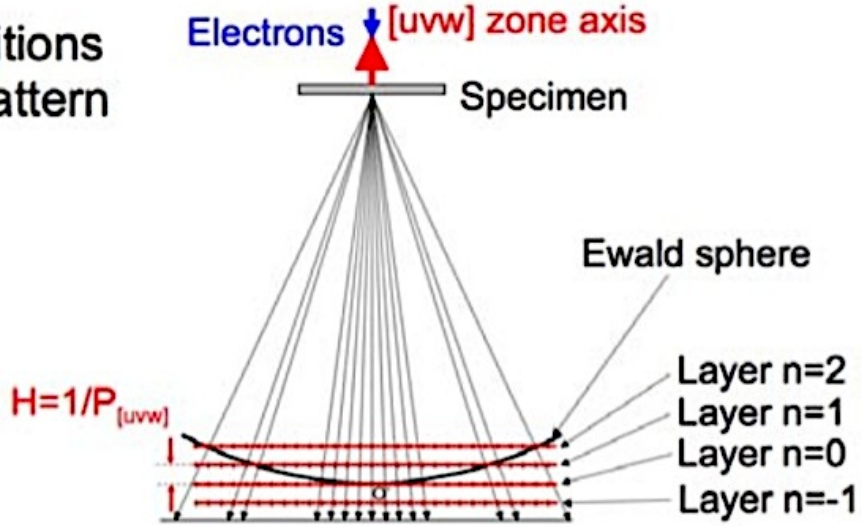

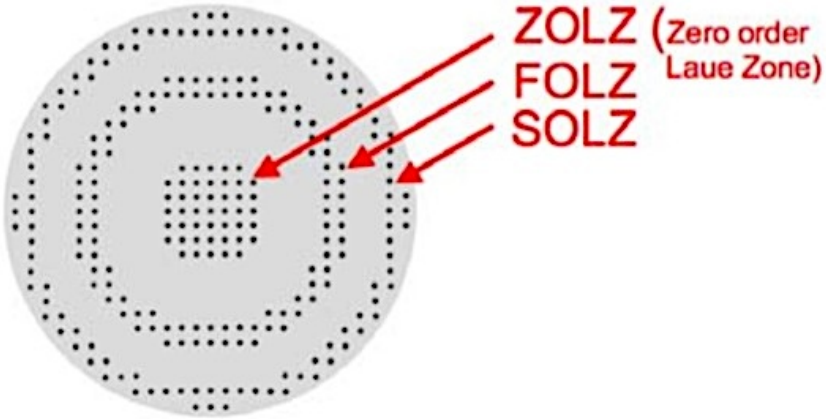

ZOLZ: hU + kV + lW = 0
FOLZ: hU + kV + lW = 1
SOLZ: hU + kV + lW = 2
...

→ Inclined planes: 3-D information

Higher order Laue Zones (HOLZ)

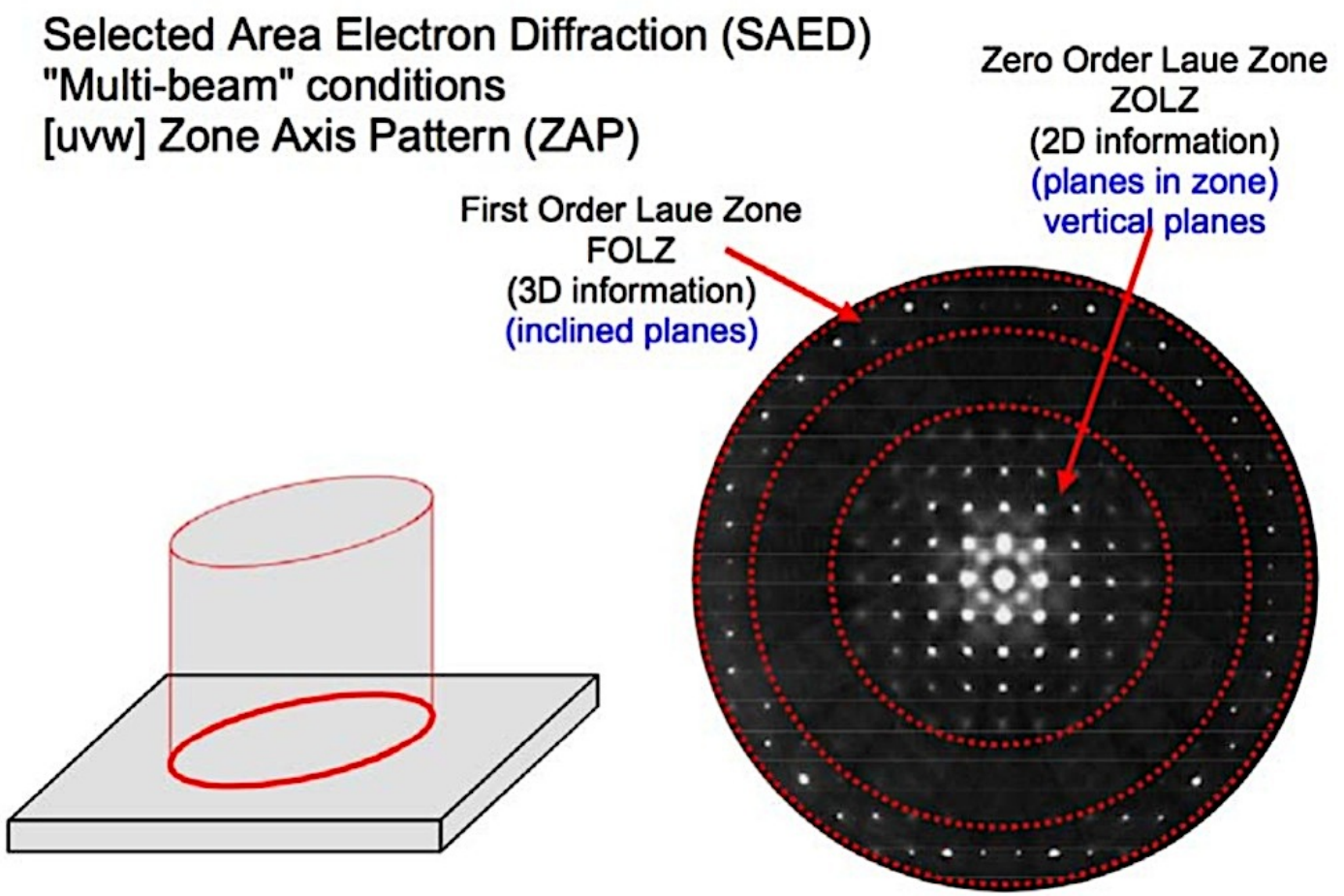

Precession diffraction

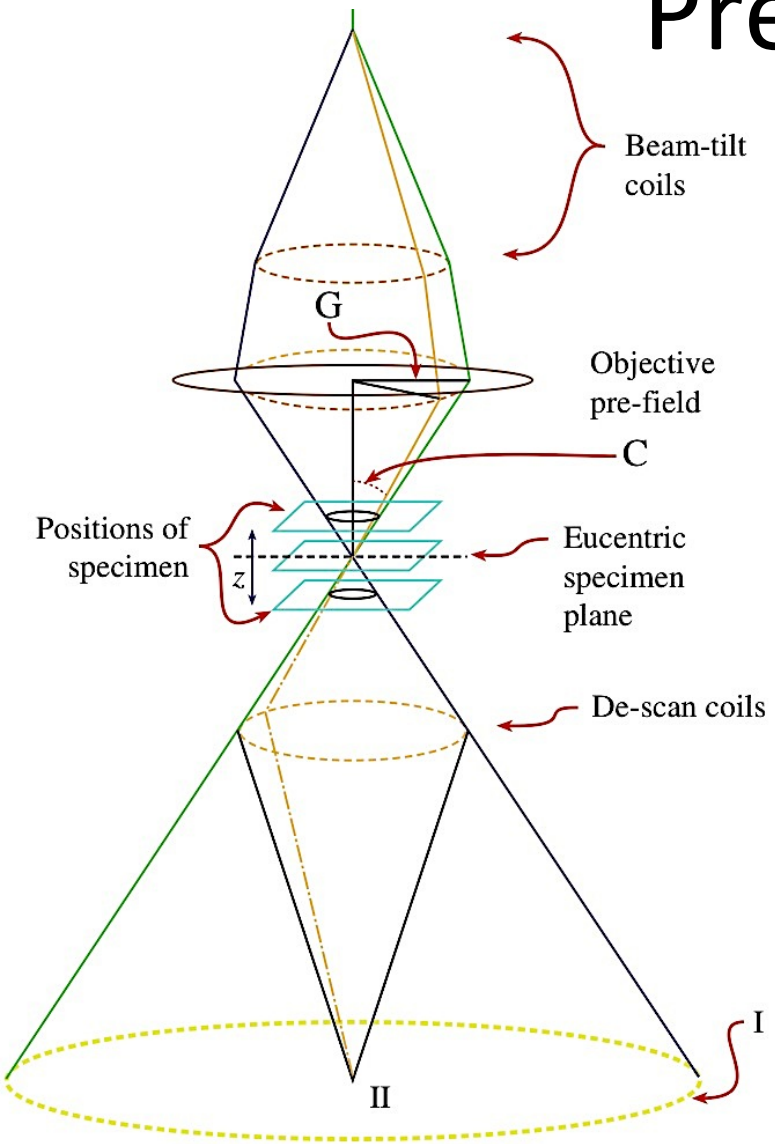

All the diffraction data correspond to a two-beam condition and show reduced dynamical diffraction effects because not many reflections are simultaneously excited off low-index zone-axis conditions.

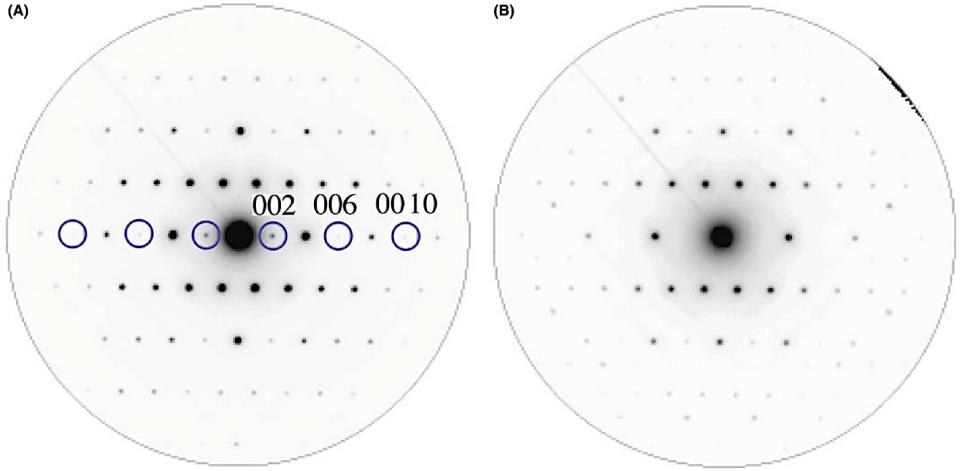

SAD Precession SAD

Double-deflection of the incident beam (either parallel (SAD) or convergent (CBED)):

- using the usual DF scan coils in a circular hollow cone (radius G and angle C) about a centered zone-axis direction and
- de-scan the beam onto the plane of the DP.

Precession diffraction

Because beam tilted off strong multi-beam axis, much less dynamical scattering

=> Multi-beam zone axis diffraction with "kinematical" intensity

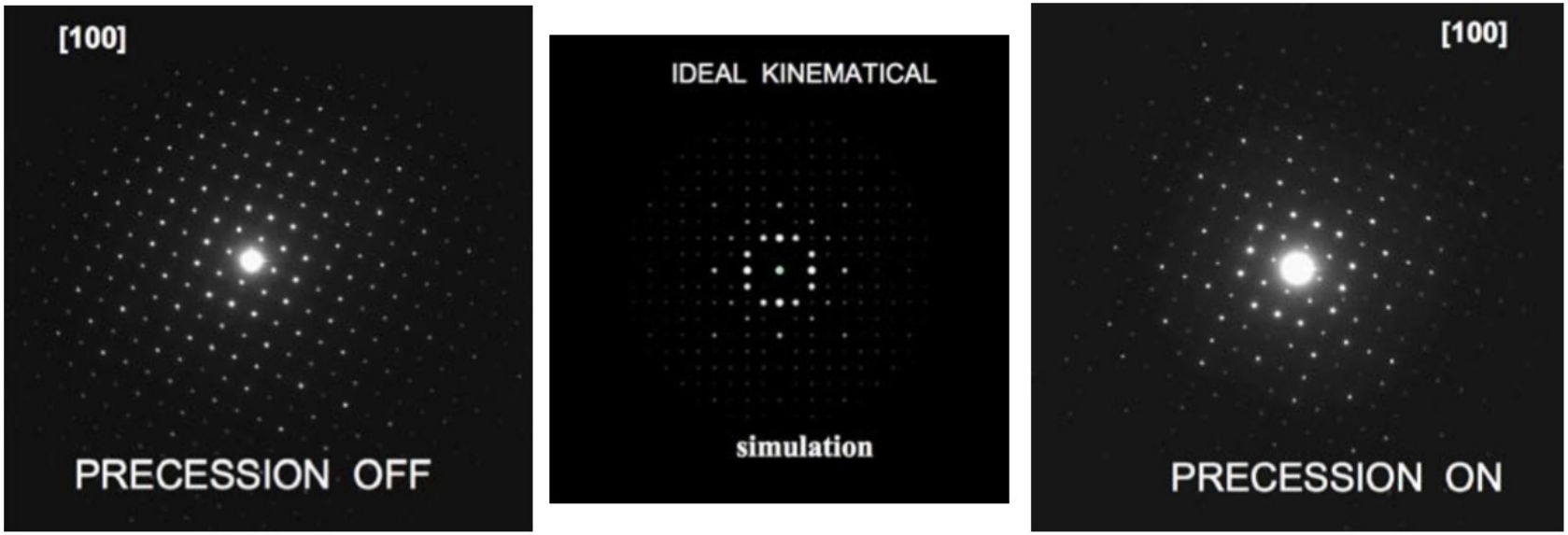

Precession pattern shows higher order symmetry lost in conventional SADP

Precession pattern also much less sensitive to specimen tilt

Images from www.nanomegas.com

Precession diffraction

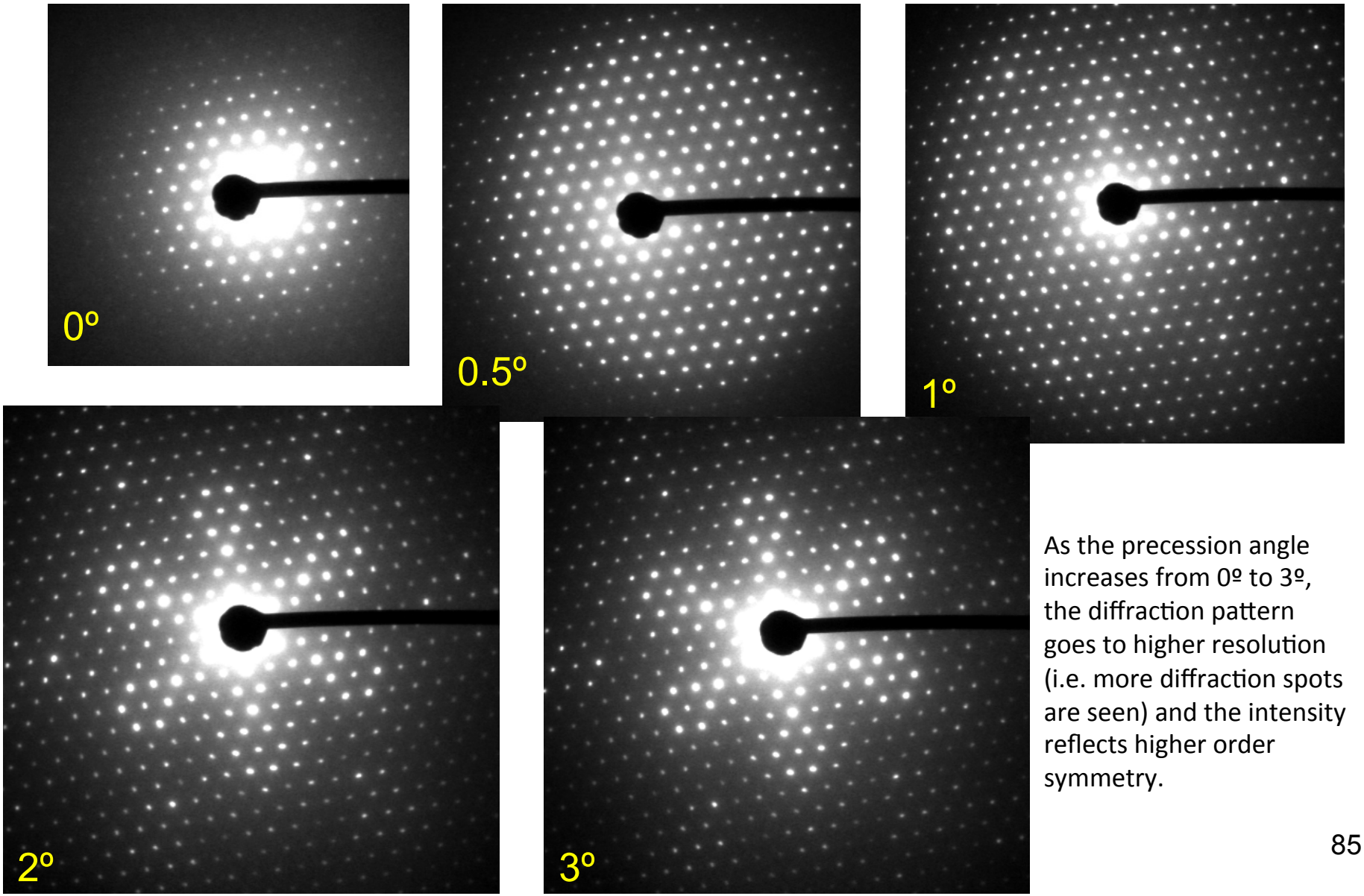

As the precession angle increases from 0º to 3º, the diffraction pattern goes to higher resolution (i.e. more diffraction spots are seen) and the intensity reflects higher order symmetry.

Convergent beam electron diffraction

Convergent beam electron diffraction

Instead of parallel illumination with selected-area aperture, CBED uses highly converged illumination to select a much smaller specimen region

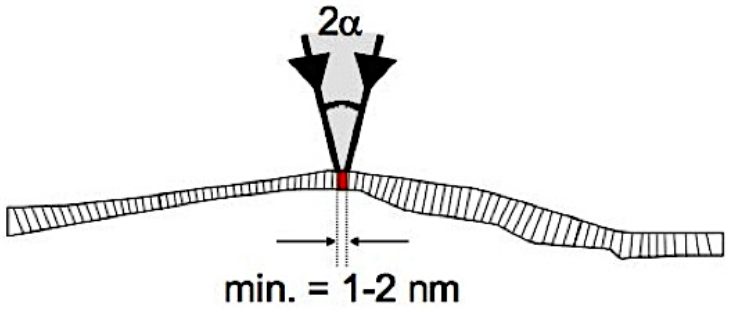

Small illuminated area =>
no thickness and orientation variations

There is dynamical scattering, but it is useful!

Can obtain disc and line patterns "packed" with information:

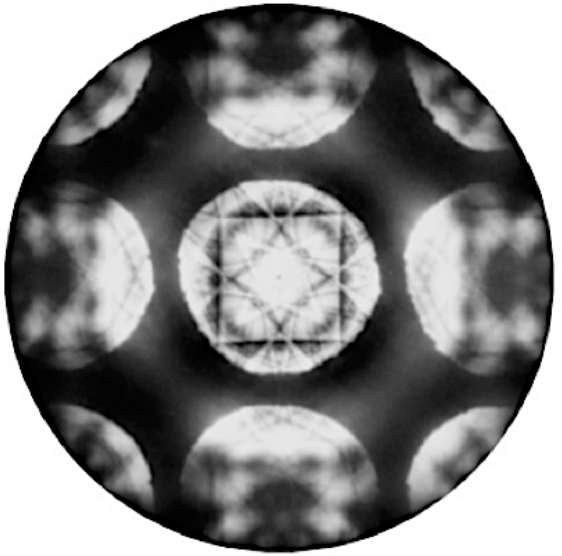

Introduction to lenses

http://micro.magnet.fsu.edu/primer

Ray diagrams (geometrical optics):

1. The optical axis contains the object focal point and the image focal point.
2. Rays going through the lens optical center (principal rays) are not deflected.
3. Parallel rays diverge from and converge to the focal points.
4. For identical optical media on both sides: $f_{object} = f_{image}$
5. Reversibility principle: swapping the object with the image results in a symmetrical ray diagram.

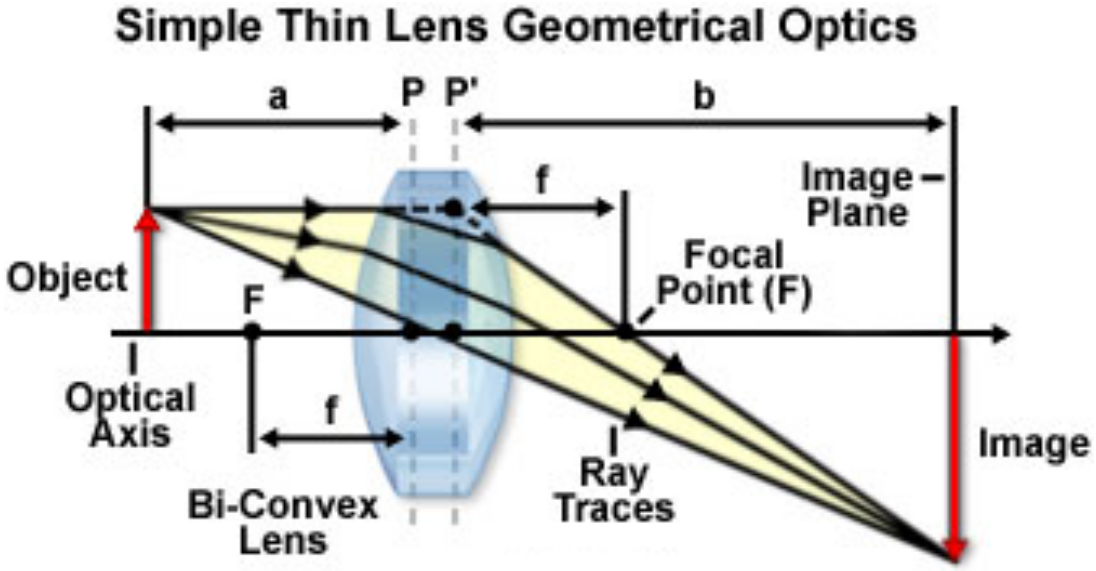

1/a + 1/b = 1/f

M = b/a

(magnification)

Convergent beam electron diffraction

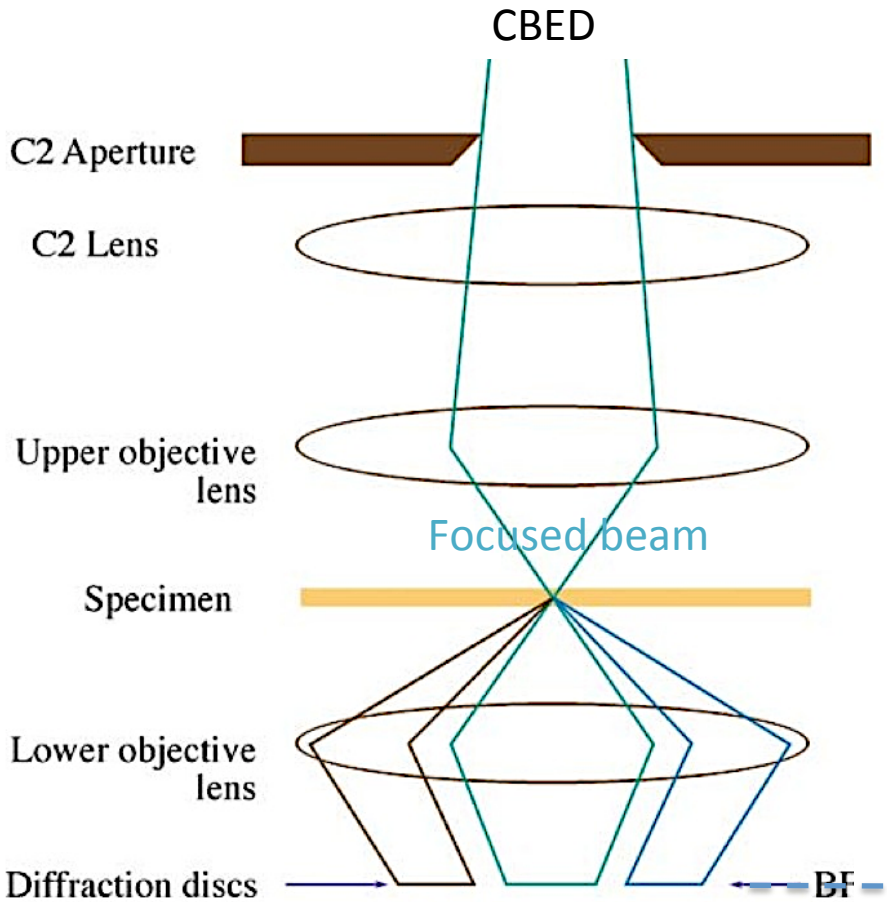

Ray diagram showing CBED pattern formation. If the c/o lens system focuses the beam at the specimen, the illuminated area is very small compared with parallel-beam SADP formation. A convergent beam at the specimen results in the formation of disks in the BFP of the objective lens.

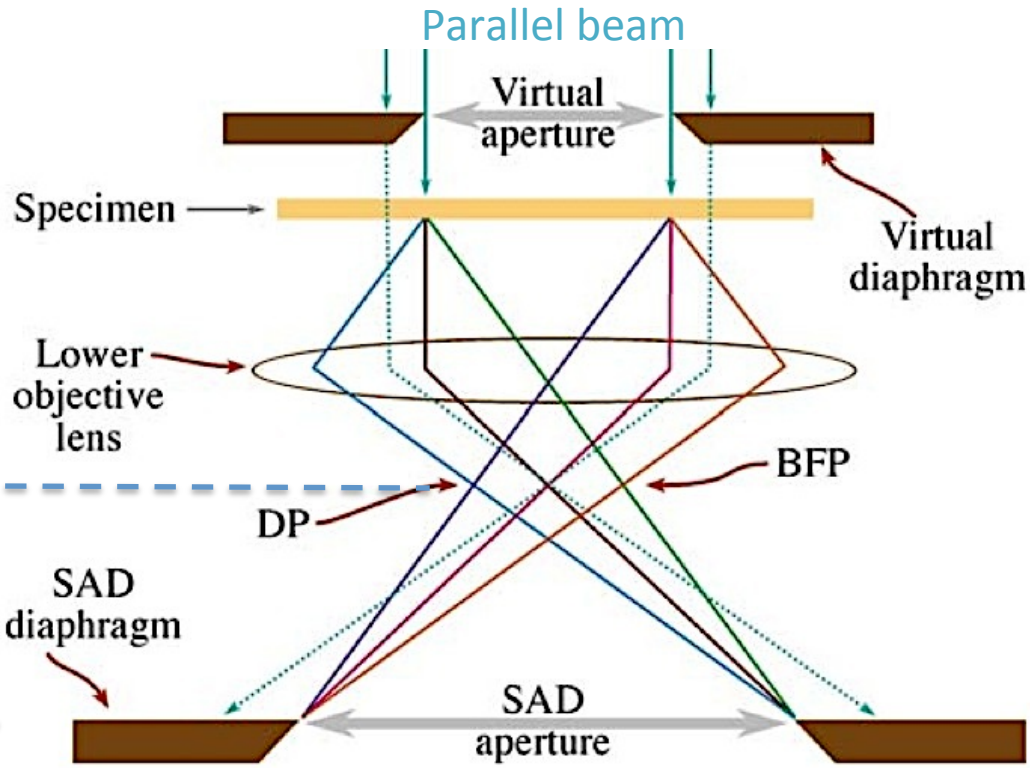

(Compare with SAD obtained with a parallel beam)

Convergent beam electron diffraction

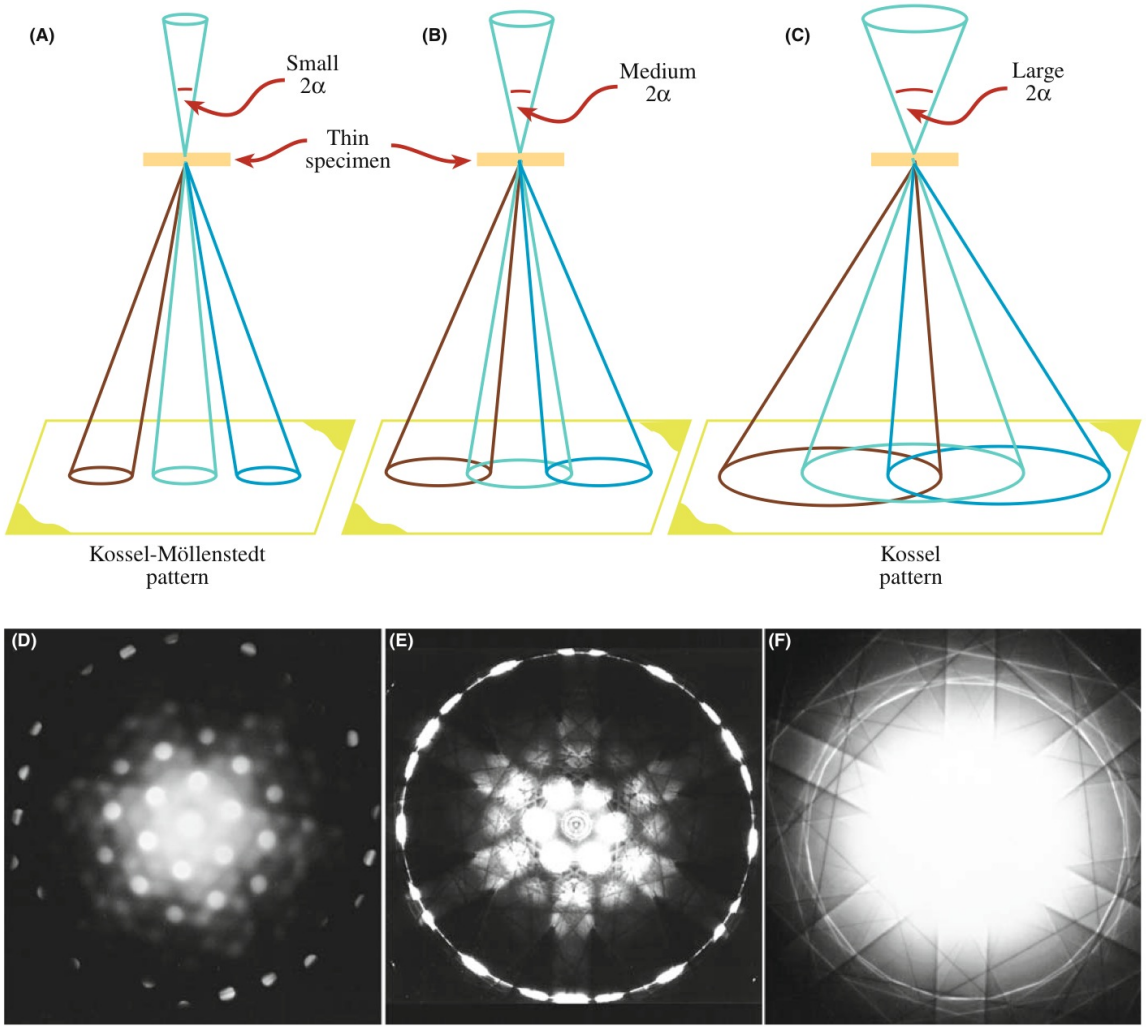

(A-C) Ray diagrams showing **how increasing the C2 aperture size** causes the CBED pattern to change from one in which individual disks are resolved (K-M pattern) to one in which all the disks overlap (Kossel pattern). (D–F) You can see what happens to experimental CBED patterns on the TEM screen as you select larger C2 apertures.

Convergent beam electron diffraction

CBED can be thought as means of magnifying the information within the spots in SAD

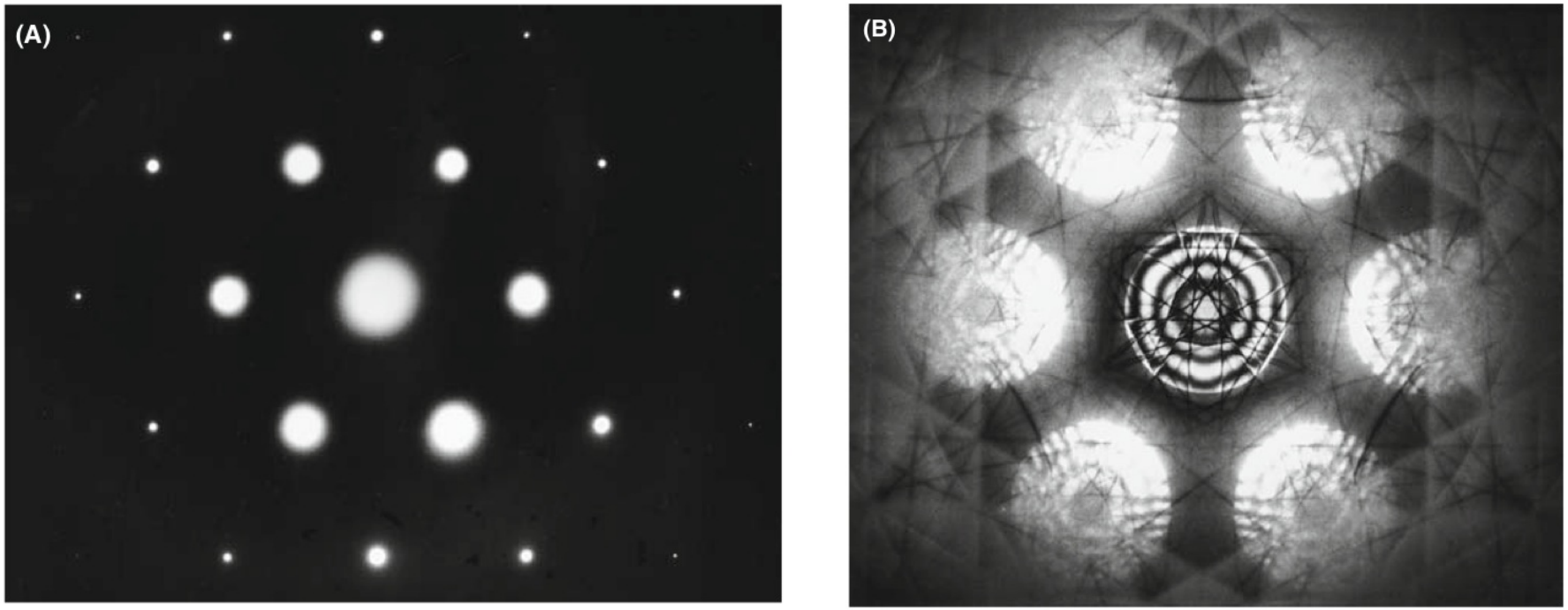

(A) SADP from [111] Si showing the first few orders of diffraction spots and no visible Kikuchi lines. (B) CBED pattern from [111] Si showing dynamical contrast within the disks as well as diffuse Kikuchi bands and sharp, deficient HOLZ lines.

Convergent beam electron diffraction

Kikuchi lines

The incident beam is not parallel to one direction, instead it forms a cone: So the Ewald sphere which is defined by the incident beam rotates around the reciprocal origin

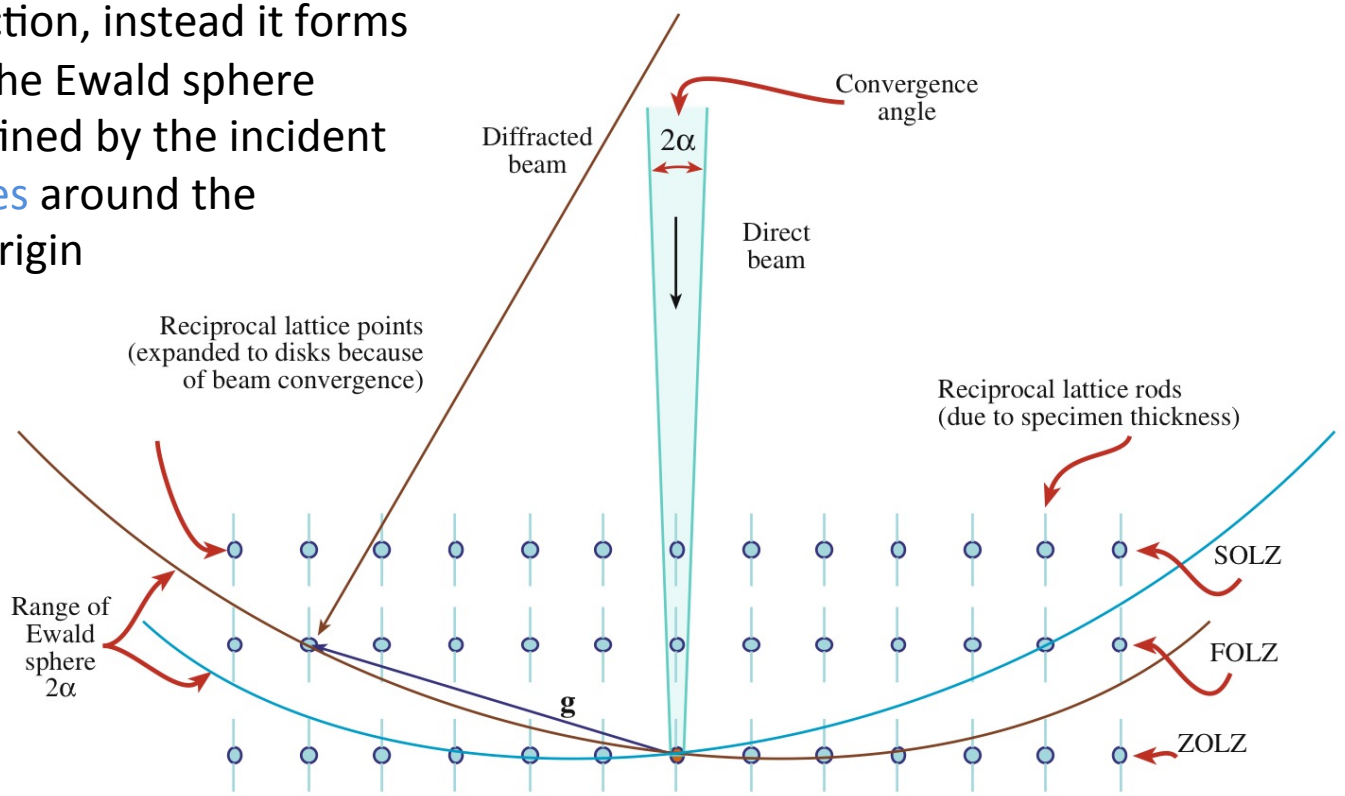

The Ewald sphere can intercept reciprocal-lattice points from planes not parallel to the electron beam whose g vectors are not normal to the beam. The sphere has an effective thickness of 2α because of beam convergence and so intercepts a range of these HOLZ reciprocal-lattice points.

Convergent beam electron diffraction

Kikuchi lines
(origin: Inelastic scattering)

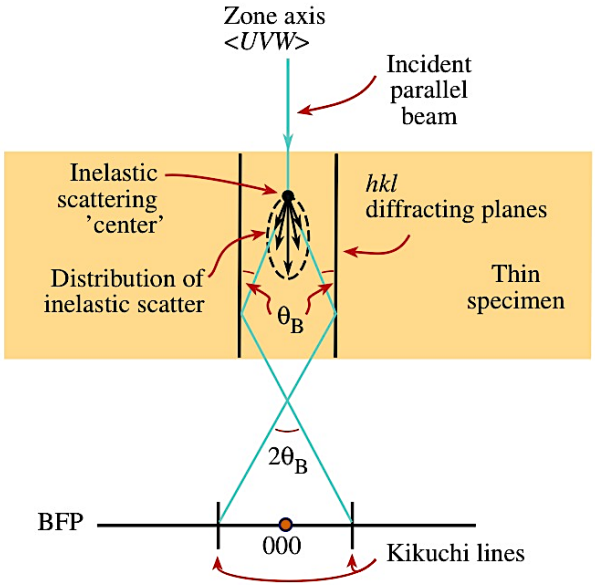

Bragg lines (sometimes called Kikuchi)
(only elastic scattering)

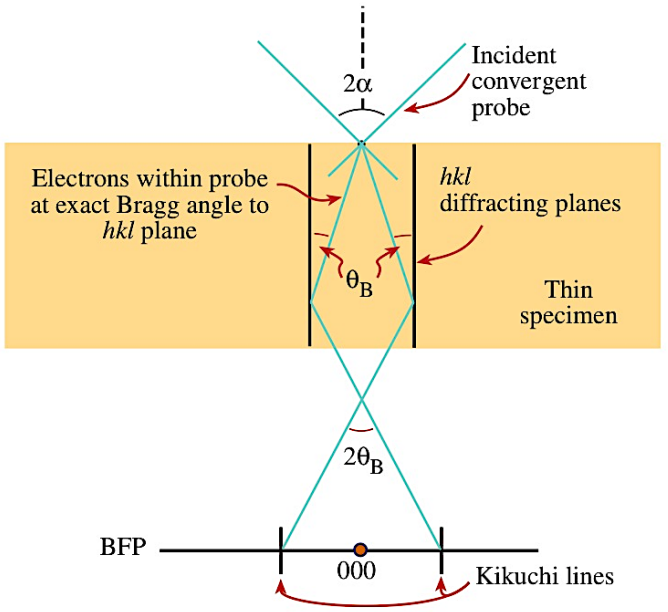

"Kikuchi" lines much less diffuse for CBED

=> use CBED to orient sample!

HOLZ lines in CBED

(the excess HOLZ lines lie in the middle of the HOLZ discs which are further away)

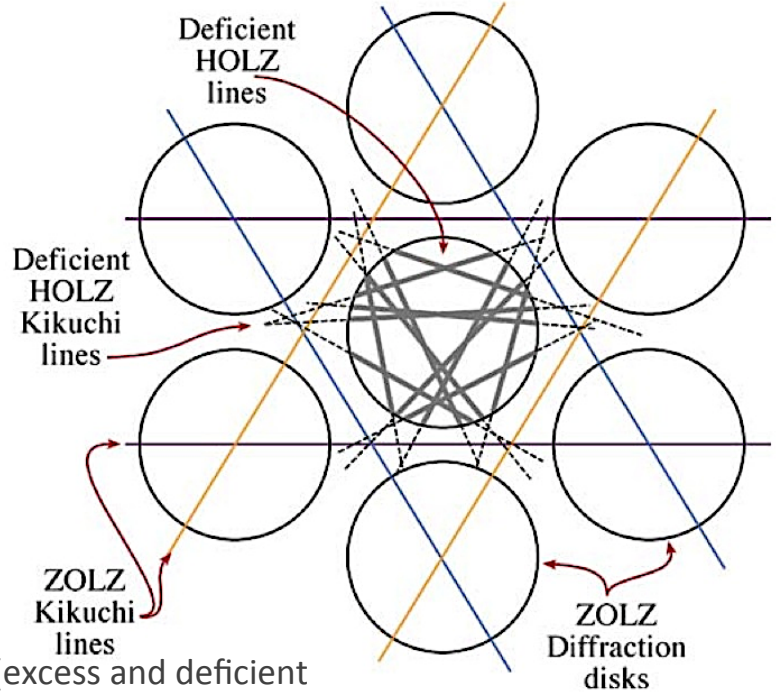

(excess and deficient and more diffuse)

The HOLZ lines arise when electrons within the cone of the incident probe are at the correct Bragg angle for diffraction by a HOLZ plane. Therefore, these electrons are diffracted out to very high angles compared with ZOLZ diffraction. The result of this scattering is a bright line through the HOLZ disk and a dark line across the 000 disk.

The relationship between Kikuchi lines and HOLZ lines is shown in this schematic of a <111> CBED pattern from a cubic crystal. The three principal pairs of 220 ZOLZ Kikuchi bands show sixfold symmetry (characteristic of the 2D 111 planes) and bisect the g vectors from 000 to the six 220 ZOLZ maxima. The inelastic deficient Kikuchi lines from the HOLZ planes are shown in the regions between the ZOLZ diffraction disks and the elastic deficient lines from the HOLZ planes are present within the 000 disk. In both cases, the HOLZ lines show threefold symmetry characteristic of looking down the <111> direction in a 3D crystal.

- The HOLZ lines contain 3D information that shows the true 3-D, threefold {111} symmetry of fcc structures, while the ZOLZ Kikuchi lines and spots show sixfold, 2D, {111} symmetry.
- The positions of Kikuchi HOLZ lines in the direct CBED beam are very sensitive to lattice parameters: used for lattice parameter determination with 0.1% accuracy and strain measurements.

Convergent beam electron diffraction

CBED as magnifying the information within the spots in the SAD

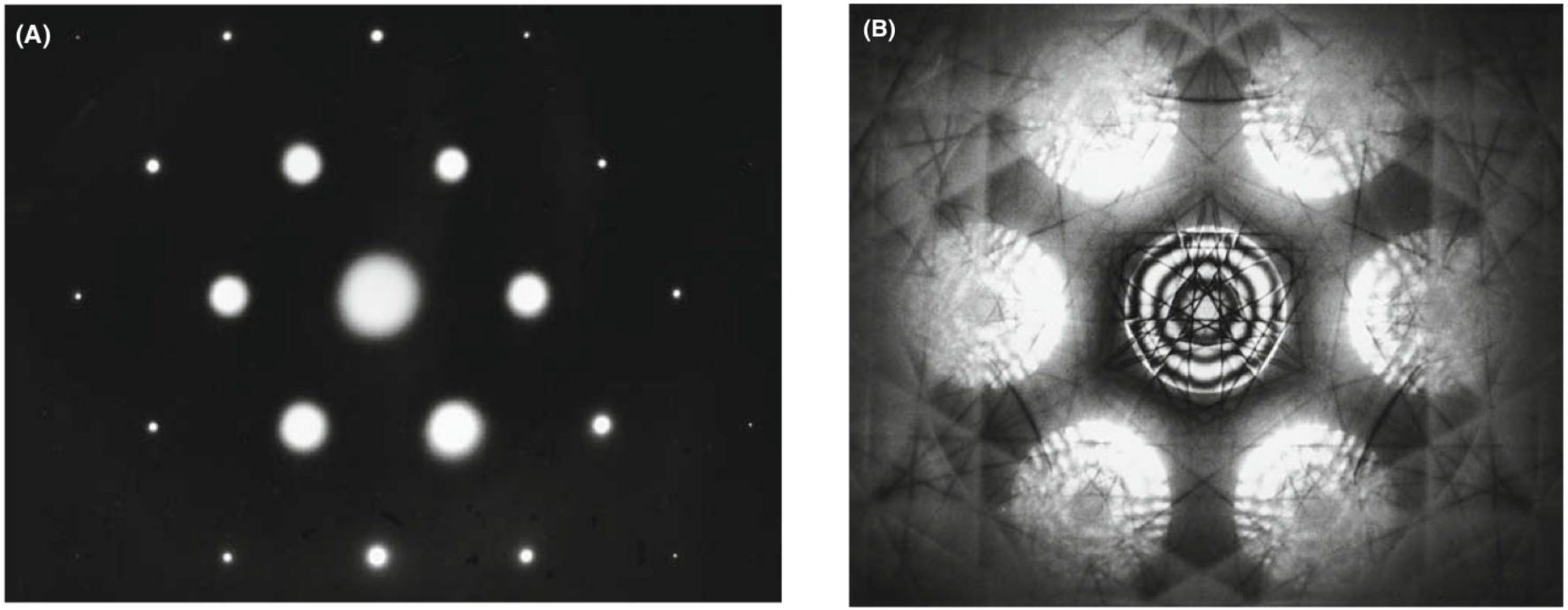

(A) SADP from [111] Si showing the first few orders of diffraction spots and no visible Kikuchi lines. (B) CBED pattern from [111] Si showing dynamical contrast within the disks as well as diffuse Kikuchi bands and sharp, deficient HOLZ lines.

HOLZ lines in CBED

Energy-filtered imaging mandatory for good quality CBED pattern
- e.g. Si [1 0 0] below taken with new JEOL 2200FS

Unfiltered

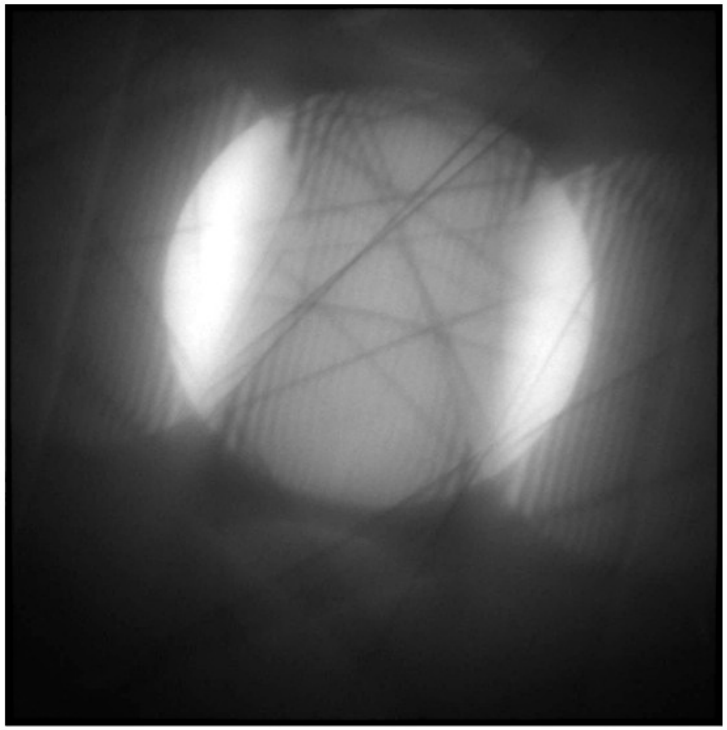

Filtered

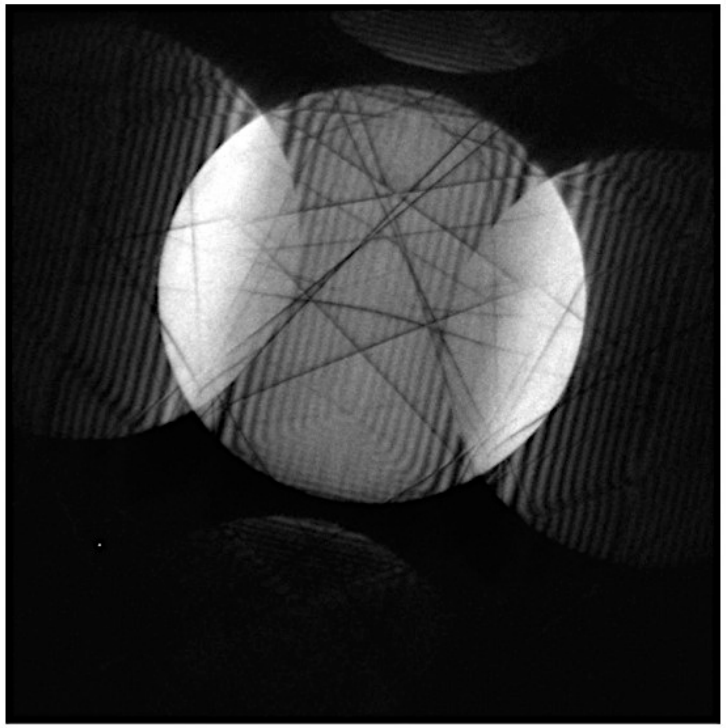

Images by Anas Mouti, CIME

Filtering electrons that have lost energy due to inelastic scattering!

Relevant software

JEMS
http://cimewww.epfl.ch/people/stadelmann/jemsWebSite/jems.html

Web-based Electron Microscopy APplication Software (WebEMAPS)
http://emaps.mrl.uiuc.edu/